

**ASSESSMENT OF NEARSHORE HYDRODYNAMIC PROCESS ALONG THE
COAST OF COX'S BAZAR**

SHARMIN AKHTAR



**DEPARTMENT OF WATER RESOURCES ENGINEERING
BANGLADESH UNIVERSITY OF ENGINEERING AND
TECHNOLOGY, DHAKA-1000**

APRIL 2015

**ASSESSMENT OF NEARSHORE HYDRODYNAMIC PROCESS ALONG THE
COAST OF COX'S BAZAR**

By

Sharmin Akhtar

(Roll No. 0412162078 P)

MASTER OF SCIENCE IN WATER RESOURCES ENGINEERING

DEPARTMENT OF WATER RESOURCES ENGINEERING

BANGLADESH UNIVERSITY OF ENGINEERING AND

TECHNOLOGY, DHAKA-1000

APRIL 2015

CERTIFICATE OF APPROVAL

The thesis titled “Assesment of Nearshore Hydrodynamic Process Along the Coast of Cox’s Bazar” submitted by Sharmin Akhtar, Roll No. 0412162078 P, Session: April/ 2012, has been accepted as satisfactory in partial fulfillment of the requirement for the degree of **Master of Science in Water Resources Engineering** on 26th, April 2015.

Dr. Umme Kulsum Navera
Professor
Department of WRE, BUET, Dhaka.
(Supervisor)

Chairman

Dr. Md. Sabbir Mostofa Khan
Professor and Head
Department of WRE, BUET, Dhaka.

Member (Ex-Officio)

Dr. Anika Yunus
Associate Professor
Department of WRE, BUET, Dhaka.

Member

Prof. Dr. M. R. Kabir
Pro-Vice Chancellor
University of Asia Pacific
House # 8/A, Road # 7, Dhanmondi,
Dhaka-1205, Bangladesh.

Member

DECLARATION

It is hereby declared that this thesis or any part of it has not been submitted elsewhere for the award of any degree or diploma.

Signature of the candidate

Sharmin akhtar

ACKNOWLEDGEMENT

I am grateful to Almighty Allah, Who has given me the strength and opportunity to do this research work.

I would like to express my deepest gratitude and sincere appreciation to my supervisor Dr. Umme Kulsum Navera, Professor, Department of Water Resources Engineering (WRE), Bangladesh University of Engineering Technology (BUET), Dhaka for providing her continuous supervision, cordial co-operation, valuable suggestion, support, guidance and encouragement during the thesis work. Her constructive comments, keen interest, and expertise helped me to better understand and enrich my knowledge to accomplish my thesis work seamlessly.

My sincere gratitude is also to the members of the Examination Committee Dr. Md. Sabbir Mostafa Khan, Professor and Head, Department of Water Resources Engineering (WRE), BUET, Dhaka, Dr. Anika Yunus, Assistant Professor, Department of Water Resources Engineering (WRE), BUET, Dhaka and Professor Dr. M. R. Kabir, Pro Vice-Chancellor, The University of Asia Pacific for their valuable comments and constructive suggestions regarding this study.

I would like to thanks those person who has been helped me for providing related necessary bathymetry data from BWDB, IWM and BMD to run the hydrodynamic model. I convey my gratitude to the persons and professionals helping me regarding this thesis work.

I also convey my deep appreciation to all of my family members, specially my mother Mahfuza Khatun, my elder brother Md. Naim Uddin, also my friends and all well-wishers for their co-operation and for supporting me to complete the M.Sc Engg.Degree.

ABSTRACT

The coastal area of Bangladesh is different from the rest of the country due to its unique geo-physical characteristics and vulnerability due to several natural disasters like erosion, cyclone, storm surges, tsunami, sea level rise, settlement and also various forms of pollution. These natural hazards are increasing with high frequency and intensity along the coast of Bangladesh and adversely affected lives and livelihoods in the coastal zone and slowed down the pace of social and economic developments in this region. Water movement in the coastal zone of Bangladesh is determined by the wave coming from the Bay of Bengal and other meteorological conditions.

A mathematical model study has been carried out to simulate the maximum wave height in the nearshore coastline of the Cox's Bazar area in Bangladesh. In this study a two dimensional hydrodynamic model DIVAST (Depth Integrated Velocity and Solute Transport) has been established based on different parameters like co-efficient of eddy viscosity, Manning roughness coefficient, advective and diffusion co-efficient etc. The DIVAST model is based on FORTRAN PROGRAMING and it has a number of modules for different purposes with different sets of equations.

The hydrodynamics of the selected area of the Bay of Bengal has been simulated by solving two-dimensional depth integrated momentum and continuity equations numerically with finite difference method. Consequently the respective velocity components in the x and y directions has been calculated across the selected coastal domain for real set of initial and boundary conditions. The hydrodynamic model has been set up at nearshore coastal water of Cox's Bazar in Bay of Bengal. The model output consists of wave height, wave direction, celerity, group velocity and water velocity at different grid point in the study area of Bay of Bengal. In this study, velocity profile has been observed and simulated for different wave angle from offshore area and also the nearshore wave climate has been developed. Simulated maximum wave height is verified at selected locations of coastal area with the measured field data, that is the maximum wave height along the coastal zone of Cox's Bazar coastline in Bangladesh. The output from the mathematical model DIVAST shown very good agreement with the measured data. These simulated results can be used for nearshore wave climate around the area. As a conclusion it can be said that the DIVAST model simulate reasonably sound output data for the selected domain of the nearshore zone of the Cox's Bazar area in Bangladesh.

TABLE OF CONTENTS

	Page No
ACKNOWLEDGEMENT	v
ABSTRACT	vi
TABLE OF CONTENTS	vii
LIST OF FIGURES	x
LIST OF TABLES	xvi
LIST OF NOTATIONS	xvii
LIST OF ABBREVIATIONS	xviii

CHAPTER 1

INTRODUCTION

1.1 General	1
1.2 Background of the study	2
1.3 Aim of the study	4
1.4 Objective of the study	4
1.5 Organization of the Contents	4

CHAPTER 2

LITERATURE REVIEW

2.1 General	6
2.2 Zoning of Coastal region of Bangladesh	6
2.3 Studies on the Bay of Bengal	9
2.4 Studies on Coastline (Hydrodynamics) in the World	15
2.5 Studies on Coastline (Hydrodynamics) By using Mathematical Modeling	19
2.6 Summary	22

CHAPTER 3

THEORY AND METHODOLOGY

3.1 General	23
3.2 Wave	23

3.3 Wave Mechanics	26
3.4 Theory of Wave	27
3.5 Nearshore Wave Climate	31
3.6 Wave-induced Longshore Currents.	32
3.7 Tides	33
3.8 Mathematical Modeling	34
3.8.1 Numerical Methods	35
3.8.2 Finite Difference Method	35
3.8.3 Concept of explicit and implicit schemes	37
3.8.4 Finite Difference Forms	38
3.8.5 Characteristics of Finite Different Schemes	38
3.9 DIVAST Model	40
3.10. Governing Equation of Model	41
3.11 Methodology	42
3.11.1 Data Collection	42
3.11.2 Bathymetry Data Organization for set up Model	43
3.11.3 Setting up Model with boundary Condition	45
3.11.4 Solution technique by Finite Difference Schemes	47
3.11.5 Model Input Data	51
3.11.6 Model Development stages	51
3.12 Summary	53

CHAPTER 4

RESULTS AND DISCUSSIONS

4.1 General	54
4.2 Study Area	54
4.3 Selection of Different Hydrodynamic Condition	56
4.4 Calibration	58
4.4.1 Calibration Results	60
4.5 Verification	61
4.5.1 Verification Results	62
4.6 Results	63
4.6.1 Wave Climate	93
4.7 Summary	95

CHAPTER 5

CONCLUSIONS AND RECOMEDATIONS

5.1 General	96
5.2 Conclusion	96
5.3 Recommendations for future study	98

REFERENCE	99
------------------	----

LIST OF FIGURES

Figure No	Title	Page No
Figure 2.1:	Coastal Zone of Bangladesh	7
Figure 3.1:	Definition sketch of free surface wave parameters for a linear Progressive	27
Figure 3.2:	Definition sketch for wave rays refracting over idealized plane parallel Bathymetry	31
Figure 3.3:	Long Shore Wave Induce Current	33
Figure 3.4:	Different types of tides that may occur at a coast	34
Figure 3.5:	Relation between partial differential equation, numerical scheme and finite difference equation	36
Figure 3.6:	Finite difference computational grid in (x,t) plane.	36
Figure 3.7:	Conceptual relationship between consistency, stability and convergency	39
Figure 3.8:	Defination sketch with notations and co-ordinates	41
Figure 3.9:	The satellite image for 2013	43
Figure 3.10:	The satellite image for 2013	44
Figure 3.11:	Computational space staggered grid system.	48
Figure 3.12:	Finite difference computational grid in (x,t) plane	49
Figure 3.13:	Schematic diagram of Model development stages	52
Figure 4.1:	(a) Study area in localation in Bangladesh (b) study area in Latitude & longitude (c) study area with Kilometers.	55
Figure 4.2:	The satellite image for 2013	58
Figure 4.3:	The maximum wave height for every month of the year 2011 Calibration at location point B4.	58
Figure 4.4:	The maximum wave height for every month of the year 2012 Calibration at location point B9.	62
Figure 4.5:	Velocity profile for incoming wave angle 230° with North	63
Figure 4.6:	Velocity profile for incoming wave angle 240° with North	64
Figure 4.7:	Velocity profile for incoming wave angle 250° with North	64
Figure 4.8:	Velocity profile for incoming wave angle 260° with North	65
Figure 4.9:	Velocity profile for incoming wave angle 270° with North	65
Figure 4.10:	Velocity profile for incoming wave angle 280° with North	66
Figure 4.11:	Velocity profile for incoming wave angle 290° with North	66
Figure 4.12:	Velocity profile for incoming wave angle 230° with North	67

Figure 4.13:	Velocity profile for incoming wave angle 240° with North	67
Figure 4.14:	Velocity profile for incoming wave angle 250° with North	68
Figure 4.15:	Velocity profile for incoming wave angle 260° with North	68
Figure 4.16:	Velocity profile for incoming wave angle 270° with North	69
Figure 4.17:	Velocity profile for incoming wave angle 280° with North.	69
Figure 4.18:	Velocity profile for incoming wave angle 270° with North	70
Figure 4.19:	Study area with section A-A	71
Figure 4.20:	Celerity (C) for incoming wave angle 230°with north for section A-A	72
Figure 4.21:	Group velocity (Cg) for incoming wave angle 230° with north for section A-A	72
Figure 4.22:	Celerity (C) for incoming wave angle 240° with north for section A-A	73
Figure 4.23:	Group velocity (Cg) for incoming wave angle 240° with north for section A-A	73
Figure 4.24:	Celerity (C) for incoming wave angle 250° with north for section A-A	74
Figure 4.25:	Group velocity (Cg) for incoming wave angle 250° with north for section A-A	74
Figure 4.26:	Celerity (C) for incoming wave angle 260° with north for section A-A	75
Figure 4.27:	Group velocity (Cg) for incoming wave angle 260° with north for section A-A	75
Figure 4.28:	Celerity (C) for incoming wave angle 270° with north for section A-A	76
Figure 4.29:	Group velocity (Cg) for incoming wave angle 270° with north for section A-A	76
Figure 4.30:	Celerity (C) for incoming wave angle 280° with north for section A-A	77
Figure 4.31:	Group velocity (Cg) for incoming wave angle 280° with north for section A-A	77
Figure 4.32:	Celerity (C) for incoming wave angle 290° with north for section A-A	78
Figure 4.33:	Group velocity (Cg) for incoming wave angle 290° with north for section A-A	78
Figure 4.34:	Celerity (C) for incoming wave angle 230°with north for section A-A	79
Figure 4.35:	Group velocity (Cg) for incoming wave angle 230° with north for section A-A	79
Figure 4.36:	Celerity (C) for incoming wave angle 240° with north for section A-A	80
Figure 4.37:	Group velocity (Cg) for incoming wave angle 240° with north for section A-A	80

Figure 4.38: Celerity (C) for incoming wave angle 250° with north for section A-A	81
Figure 4.39: Group velocity (Cg) for incoming wave angle 250° with north for section A-A	81
Figure 4.40: Celerity (C) for incoming wave angle 260° with north for section A-A	82
Figure 4.41: Group velocity (Cg) for incoming wave angle 260° with north for section A-A	82
Figure 4.42: Celerity (C) for incoming wave angle 270° with north for section A-A	83
Figure 4.43: Group velocity (Cg) for incoming wave angle 270° with north for section A-A	83
Figure 4.44: Celerity (C) for incoming wave angle 280° with north for section A-A	84
Figure 4.45: Group velocity (Cg) for incoming wave angle 280° with north for section A-A	84
Figure 4.46: Celerity (C) for incoming wave angle 290° with north for section A-A	85
Figure 4.47: Group velocity (Cg) for incoming wave angle 290° with north for section A-A	85
Figure 4.48: Wave Height for incoming wave angle 230° with north for section A-A	86
Figure 4.49: Wave Height for incoming wave angle 240° with north for section A-A	86
Figure 4.50: Wave Height for incoming wave angle 250° with north for section A-A	87
Figure 4.51: Wave Height for incoming wave angle 260° with north for section A-A	87
Figure 4.52: Wave Height for incoming wave angle 270° with north for section A-A	88
Figure 4.53: Wave Height for incoming wave angle 280° with north for section A-A	88
Figure 4.54: Wave Height for incoming wave angle 290° with north for section A-A	89
Figure 4.55: Wave Height for incoming wave angle 230° with north for section A-A	89
Figure 4.56: Wave Height for incoming wave angle 240° with north for section A-A	90
Figure 4.57: Wave Height for incoming wave angle 250° with north for section A-A	90
Figure 4.58: Wave Height for incoming wave angle 260° with north for section A-A	91
Figure 4.59: Wave Height for incoming wave angle 270° with north for section A-A	91
Figure 4.60: Wave Height for incoming wave angle 280° with north for section A-A	92
Figure 4.61: Wave Height for incoming wave angle 290° with north for section A-A	92
Figure 4.62: Wave Climate profile for incoming wave angle 230° with north	93
Figure 4.63: Wave Climate profile for incoming wave angle 270° with north	94
Figure 4.64: Wave Climate profile for incoming wave angle 230° with north	94
Figure 4.65: Wave Climate profile for incoming wave angle 270° with north	95

LIST OF TABLES

Table No	Title	Page No
Table 3.1:	Input Parameters used for calibration of Model	46
Table 4.1:	The total condition for run the program for case 1	57
Table 4.2:	The total condition for run the program for case 2	57
Table 4.3:	The maximum wave height for Year 2011	59
Table 4.4:	The maximum wave height for Year 2012	61

LIST OF NOTATIONS

η	Sea surface Elevation (m)
C	Celerity
C_g	Group velocity
U	Velocity in x direction
V	Velocity in y direction
H	Total depth of flow
β	Momentum correction factor for non-uniform vertical velocity profile
f	Coriolis parameter
g	Gravitational acceleration
P_a	Atmospheric pressure
τ_{xw}	Surface wind shear stress component in x direction
τ_{yw}	Surface wind shear stress component in y direction
τ_{xb}	Bed shear stress component in x direction
τ_{yb}	Bed shear stress component in y direction
ϵ	Depth-averaged eddy viscosity
C	Chezy's roughness coefficient
P_a	Air density
W_s	Wind speed
R_e	Renolds number

LIST OF ABBREVIATIONS

ADI	Alternating Direction implicit
BMD	Bangladesh Metrological Department
BTM	Bangladesh Transverse Mercator
BUET	Bangladesh University of Engineering and Technology
BWDB	Bangladesh Water Development Board
CZPo	Coastal Zone Policy
DIVAST	Depth Integrated Velocity and Solute Transport
FTCS	Forward Time Central Space
GMB	Ganges-Brahmaputra-Meghna
GoB	Government of Bangladesh
IWM	Institute of Water Modelling
MSL	Mean sea level
SLR	Sea level rise
UTM	Universal Tranverse Mercator

CHAPTER 1

INTRODUCTION

1.1 General

Earth's coastline has evolved with the change in coastal dynamics, habitat and the supply of sediment from the continental interior. The morphology of coastal zone is evolved with changing the boundary conditions of coastal processes such that wind circulation, wave, tides and the storage of sediment on beaches [Syvitski et al., 2005, Kamphuis, 2012]. Coasts are dynamic systems, undergoing adjustments of morphodynamics form and process at different time and space scales in response to geomorphological and oceanographical factors [Nicholls, 2007]. It combines processes that such as bottom shear stress, wave impact, energy dissipation, erosion, accretion and transport of sediment with difficult combinations of inputs such as water levels, waves, tides, current and wind [Kamphuis, 2012]. Coastal zones are interfaces of land and ocean balancing geosphere, atmosphere and biosphere [Enemark, 2007]. About two-thirds of the world's population lives near the coast [Inman et al., 1973, Weide et al. 1993,]. The coastal zone is composed of the coastal plain the continental shelf and the water that covers the shelf. It also includes other major features such as large bays, estuaries lagoons, coastal dune fields, river estuaries and deltas [Inman et al. 1973, Crossland et al., 2005, Fedra, et al., 1988].

Bangladesh is located at the head of the Bay of Bengal [Chowdhury, 2009]. According to 2001 population census, Bangladesh has a population of about 13 crore living on 147,570 square kilometer of land. The Ganges, the Brahmaputra and the Meghna that constitute one of the largest river systems in the world drain through the Bangladesh into the Bay of Bengal. The coast of Bangladesh is known as a zone of vulnerabilities as well as opportunities. It is prone to natural disasters like cyclone, storm surge and flood. The combination of natural and man-made hazards, such as erosion, high arsenic content in ground water, water logging, earthquake, water and soil salinity, various forms of pollution, risks from climate change, etc, have adversely affected lives and livelihoods in the coastal zone and slowed down the pace of social and economic developments in this region [CZPo, 2005].

The coastline of Bangladesh is around 734 km which involves coast and island boundaries. Nearly 33% of people, which is about one-third of the total population of Bangladesh lives near the coast [Rahman et al, 2010]. The country has three (3) distinct coastal regions—

namely, western, central and eastern coastal zone. The western part is known as the Ganges tidal plain, comprises the semi active delta and is criss-crossed by numerous channels and inlets [Sarwar et al., 2005]. Central coastal zone is distributaries channel with Ganges, Brahmaputra and Meghna (GBM system). The eastern coastal zone is covered by hilly area and sandy beaches [Barua et al., 1995]. The coastal zone of Bangladesh is often perceived as a zone of multiple vulnerabilities [CDS, 2006,]. Which areas are affected by natural hazards like cyclones, coastal flooding, tidal surges, salinity and the like phenomenon

[Rahman et al., 2010].

1.2 Background of the study

There are many problems arising in Coastal zones. Disasters like cyclone, tide storm, drainage congestion, land erosion and drought that take toll on life and property and depletion of natural resource. In the coastal zone, agriculture continues to be a major source of employment, which is seasonal in nature. So reducing these disasters there has been a growing public concern with an increased awareness of different impacts on nearshore of coastal zone. Nearshore Hydrodynamic model has been used to calculate near-shore wave conditions based on offshore wave data. This work will be provided a framework in which a developer or contractor could quickly estimate near-shore wave conditions for a small section of coastline, using existing offshore wave data and without running complicated global wave models.

Numerous numbers of mathematical models have been developed to study different coastal processes of different coast throughout the world like: Flow and Water Quality Modeling in coastal and inland Waters (Falconer, 1992); Modeling of morphological changes due to coastal structures (Leonet'yev, 1999); Nonlinear propagation of unidirectional wave field over varying topography (Girard et al., 1999); Estimation of 3-D current fields near the Rhine outflow from HF radar surface current data (Valk, 1999); Some observations of wave current interaction (Wolf, 1999); Wave deformation and vortex generation in water wave propagation over a submerge dyke (Huang, 1999); Application of 2D Mathematical Model for Verification of Water Velocity at Coastal Area of Bangladesh (Hossain, 2012); Mathematical Modelling Of Wave-Induced Nearshore Circulation (Yoo et al., 1986); Numerical Modelling of Nearshore Circulation (Ebersole, 1980); A Method of Numerical Analysis of Wave Propagation-Application to Wave Diffraction and refraction (Ito et al.

1972).

A number of modeling studies of the Bay of Bengal have also been carried out to assess various impacts like: A storm surge inundation model of the northern Bay of Bengal using publicly available data (Lewis et al., 2013); Deep Water Wave Hindcasting, Wave Refraction Modeling, and Wind and Wave Induced Motions in the East Ganges-Brahmaputra Delta Coast (Barua et al., 1995); Biological aspects of the coastal and marine environment of Bangladesh (Hossain, 2001); Longshore Transport Based on Directional Waves Along North Tamilnadu Coast, India (Jena et al., 2001); Successful Integrated coastal Zone Management (ICZM) Program model of a Developing Country (Xiamen, China) – Implementation in Bangladesh Perspective (Islam et al., 2009).

The numerical model DIVAST (Depth-Integrated Velocities and Solute Transport) is a robust and reliable numerical model for solving the two-dimensional depth-integrated equations by using a uniform rectangular mesh grid (Falconer, 1992). Two-dimensional depth integrated numerical models are more widely used at present time because three-dimensional hydrodynamic numerical models are sensitive and not always successful which implies a relatively large cost-benefit ratio (Kevin and Daniel, 2004). The numerical DIVAST model simulates two dimensional distributions of currents, water surface elevations and various water quality parameters within a modeling domain as function of time, taking into account the hydraulic characteristics governed by the bed topography and the boundary condition.

In this study, DIVAST model is used in Bay of Bengal. The bathymetry of Bay of Bengal has been set up based on data of Cox's bazar of Bay of Bengal. The bathymetry data has been collected from Institute of Water Modelling (IWM). The bathymetry data has been collected two steps: primary data and secondary data. The secondary data has been collected in Bangladesh Traverse Mercator (BTM) co-ordinate system. The data has been transformed to Universal Transverse Mercator (UTM) co-ordinate system and finally to corresponding latitude-longitude for setting up the bathymetry of bay of Bengal. The study describes the calibration and verification of DIVAST model output maximum wave height against the measured maximum wave height some location of Bay of Bengal. The velocity, celerity, group velocity also determined by this model some specific point of bay of Bengal.

1.3 Aim of the study

The velocity data is very important to analyze the hydrodynamics parameters at near shore coastal water. Model simulations are generally undertaken for several waves. Using high resolution numerical models covering a part of Bay of Bengal is a rather new scientific approach for this area. A number of modeling studies have been carried out for coastal zone of Bangladesh with varying degree of success and limitations during last several decades.

In this thesis work, a mathematical model study has been carried out in the coastal zone of Bangladesh using FORTRAN-V language. Aim of this study is to set up a hydrodynamic model at near shore coastal water of Cox's Bazar and to assess the nearshore wave climate due to change in wave direction. It is important to mention that monitoring and forecasting of tidal currents are necessary for assessing the value of nearshore wave height, wave celerity and wave angle from deep water wave condition. Thus such monitoring and forecasting of velocities and directional movements of flows are very much important and essential for designing and planning purposes, e.g. construction of coastal structures such as embankments, barrages, erosion protection works, tidal sluices, regulators, cross dams, closures to connect coastal islands, jetties, sea ports, offshore platforms, enhancement of land reclamation, oil rigs, sea bed condition, for placement of pipelines, etc.

1.4 Objectives of the study

Based on the background overall objectives of this proposed study would be:

1. To set up a hydrodynamic model at nearshore coastal water of Cox's Bazar.
2. To assess the value of nearshore wave height, wave celerity and wave angle from deep water wave condition.
3. To assess the nearshore wave climate due to change in wave direction

1.5 Organization Contents of the Thesis

This thesis paper has six chapters in it. The contents of each chapter have been summarized briefly as follows:

Chapter-1 of the study gives a brief description of the coastal zone of Bangladesh, background of the study. It also includes the main objectives of the study and the

organization of the contents.

Chapter -2 gives short accounts of the previous studies and literature review available for the study regarding the Bay of Bengal as well as some other bays in the world. It also gives brief ideas about some prominent mathematical models in the world related with the processes of coasts, estuaries and rivers.

Chapter-3 explains the concept of wave and wave theory. Brief discussion about the different methods of solving partial differential equations (analytical and numerical) solutions are illustrated thereof.

This chapter also deals with the alternating direction implicit (ADI) method and shows the gradual steps of solving the governing hydrodynamic equations such as continuity equation and momentum equations in x and y directions and its solution techniques. It also describes the DIVAST model, bathymetry setup and development of model.

Chapter - 4 describes the results and discussions with interpretation, calibration and validation of model with the maximum wave height of different locations throughout the coast of Bangladesh showing the matching of measured maximum wave height with output maximum wave height.

Chapter-5 study contains the conclusions of the study and also recommendations for further study.

CHAPTER 2

LITERATURE REVIEW

2.1 General

The coastal region of Bangladesh is marked by morphologically dynamic river network, sandy beaches and estuarine system. The Bay of Bengal is the major coastline of Bangladesh, Cox's Bazar is a part of it. The hydrodynamic parameters are varying distinctly from season to season. Many coastal processes, modeling studies have been carried out worldwide and also in Bangladesh to assess the impacts of different coastal processes, natural hazard etc. Many numerical modeling studies have been carried out on the coastal area of Bangladesh as well as different coastal areas in the World to understand the impact of various events like: Generation of waves, waves induce generation circulations, climate change induced SLR, storm -surge, tide –surge interaction etc. Some of them are cited in the following sections. Several different coastal processes studies regarding coastal zone of Bangladesh as well as of the world are reviewed in this chapter.

2.2 Zoning of Coastal region of Bangladesh

Bangladesh is a flood plain delta, sloping gently from the north to the south and meets the Bay of Bengal at the southern end [Hossain, 2012]. The coastline of Bangladesh is 710 kilometres long and runs parallel to the Bay of Bengal [CZPo, 2005, Islam et al., 2009]. 19 districts out of 64 are in the coastal zone covering a total of 147 upazillas of the country (Figure 2.1). Out of these 19 districts, only 12 districts meet the sea or lower estuary directly [Hossain, 2012].

The zone is divided into exposed and interior coast according to the position of land. The Upazillas that face the coast or river estuary are treated as exposed coastal zone. Total number of upazillas that fall on exposed coastal zone 48 in 12 districts. A total of 99 upazillas that are located behind the exposed coast are treated as interior coast. The exposed coast embraces the sea directly and is affected by different coastal hazards like cyclone, storm surge, salinity intrusion, tidal level variation, erosion, accretion, sea level rise due to tidal wave and current etc [Hossain, 2012].

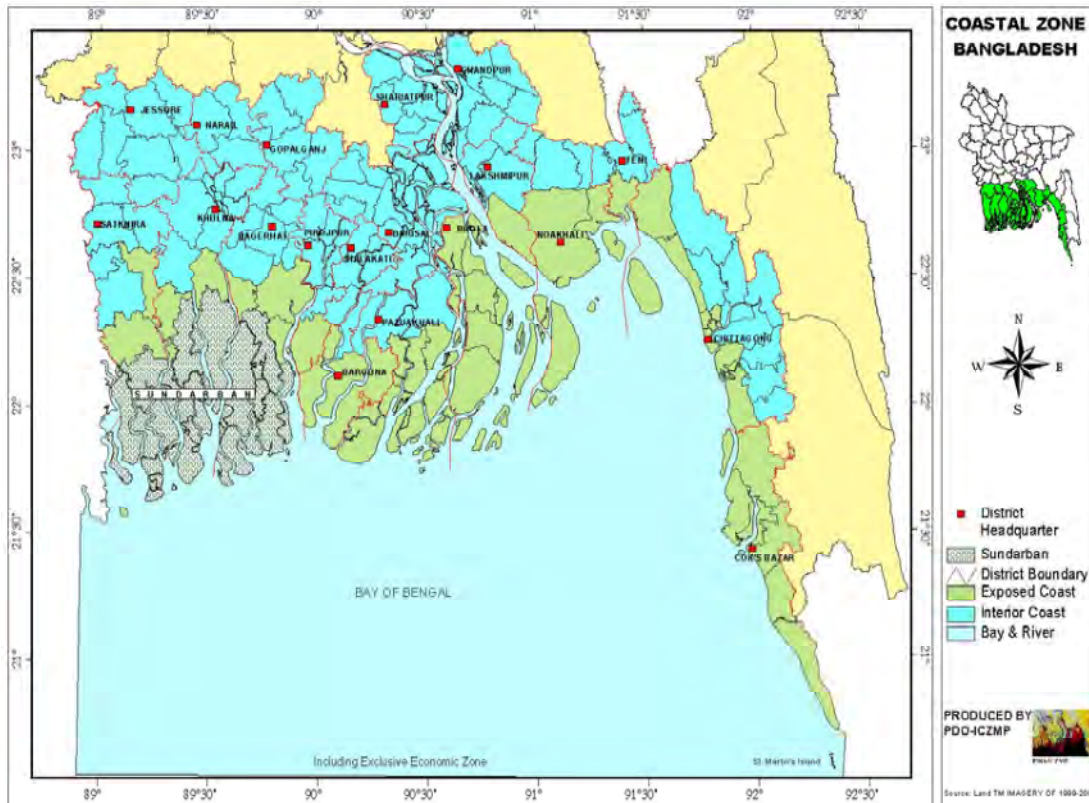


Figure 2.1: Coastal Zone of Bangladesh (Source: Islam, 2004)

The southern part of Bangladesh falls under coastal zone that receives discharge of numerous rivers, including Ganges-Brahmaputra –Meghna (GMB) river system, creating one of the most productive ecosystems of the world. Except Chittagong – Cox’s Bazar, other parts of the coastal zone are plain land with extensive river networks and accreted land, which is known as char land in Bangladesh. India is at the west of the zone whereas Myanmar is at the east coast [Hossain, 2012].

Western coastal zone

The western coastal zone is covered with sundarbans mangrove forest, covering greater Khulna and part of Patuakhali district. Because of presence of mangrove forest, the zone is relatively stable in terms of soil erosion. Mangrove swamps, tidal flats, natural levees and tidal creeks are characteristics of the zone.

Mangroves of the area support feeding and breeding grounds for fish and shrimps species, enriching the area in fisheries bio-diversity. The area lies at 0.9 to 2.1 metre above mean sea level .Soil characteristics of the western coastal zone are silty loams or alluvium. Mangrove dominated coastal areas have developed on soil formations of recent origin consisting of alluvium washed down from the Himalayas. The zone also has tourist attraction in the Sundarbans [Hossain, 2012].

Central coastal zone

Central coastal zone extends from Feni river estuary to the eastern corner of the Sundarbans, covering Noakhali, Barisal, Bhola and Patuakhali districts. The zone receives a large volume of discharge from the Ganges-Bhrahmaputra-meghna river system, forming high volume of silty deposition. More than 70% of the sediment load of the region is silt; with an additional 10% sand. Because of the sediment discharge and strong current, the morphology of the zone is very dynamic and thus erosion and accretion rates in the area are very high. Numerous islands are located in the area including the country's only island district Bhola. Many islands have been formed in last few years in the area by the process of land accretion. At the same time many have been eroded or disappeared. Kuakata, an attractive sandy beach is located at the zone under Khepupara upazilla of Patuakhali district [Hossain, 2012].

Eastern coastal zone

The eastern coastal zone starts from the Feni river estuary to Bodormokam, the southern tip of mainland. This zone is very narrow. A series of small hills are run parallel to this zone. Karnafuly, Sangu and Matamuhury rivers fall into the Bay of Bengal in this area. The Naf river falls to the Bay of Bengal dividing Bangladesh from Myanmar. Soil characteristics of the eastern coastal zone are dominated by submerged sands and mudflats. The submerged sand of the zone has formed a long sandy beach of 145 km from Cox's Bazar towards Teknaf. Two of the country's most important sandy beaches from tourist's perspective, namely Patenga and Cox's Bazar are located in this coastal zone. Fish farming, fishing in the bay, salt production and tourism are main economic activities of the zone [Hossain, 2012].

Island

About 60 islands are identified in the coastal zone, most of the islands are located in the central zone, because of the dynamic river flow of the Ganges-Brahmaputra-Meghna river system. Hatia, Sandwip and Maishkhali are three upazillas and Bhola an administrative district are four bigger islands in the zone. Saint Martin is the only coral island of the country located in Bay of Bengal, about 9.8 km to the southeastern side of mainland. The island has an area of 7.5 sq km and situated under Teknaf thana of Cox's Bazar district. A total number of 177 char lands are also identified in the coastal zone [Hossain, 2012].

The Bay of Bengal

The coastal zones along the Chittagong and Cox's Bazar shorelines are wave dominated sandy beaches, strong windbreaks with hill forests in the eastern coast of the Bay of Bengal [Rahman, 2010]. The Bay of Bengal is the major coastline of Bangladesh represents the margin of a deltaic plain where enormous quantities of sediments are discharged at the river mouth, which is subjected to comparatively high tidal and wave energies [Herbich et al., 1990].

The Bay of Bengal forms the northeastern part of the Indian Ocean [Mahodadhi, 2013,]. It is located between latitudes 5°N and 22°N and longitudes 80°E and 100°E at the northern arm of the Indian ocean [Banglapedia]. The Cox's Bazar coastal plain is located at the south-eastern corner of Bangladesh [Noda, 1974]. The coast of Cox's Bazar is 250 km long and sediments are fine seaward and westward with the thickest accumulation of mud near the submarine canyon. The shallow part (less than 20m) of the continental shelf off the coast of Chittagong and Teknaf is covered by sand and the intertidal areas show well-developed sandy beaches [Banglapedia]. The role of wind and wave induced motion which result is effect on sediment distribution and shaping of nearshore morphology [Herbich, 1990]

2.3 Studies on the Bay of Bengal

Lewis et al. (2013) studied that a computationally inexpensive inundation model has been developed from freely available data sources for the northern Bay of Bengal region to estimate flood risk from storm surges. The change in atmospheric pressure and extreme wind stress creates storm surge raises the water level temporarily which producing the storm tide.

The suitability of publicly available data for inundation models therefore needs to be assessed for the management of coastal inundation risks. The main aim of this paper is to develop a LISFLOOD-FP inundation model of the northern Bay of Bengal based on only freely available data sources, and test the model against maximum water level observations taken during the 2007 “ Sidr” even using parameters from two cyclone databases (IBTrACs and UNISYS). Validation showed inundation prediction accuracy with a root mean squared error (RMSE) on predicted water level of ~ 2 m. The suitability of SRTM data for use in dynamic coastal inundation models is unknown due to resolution accuracy and vegetation effects within the SRTM data. Better SRTM processing techniques may improve inundation model performance, and future work should also seek to improve storm tide uncertainties in this region.

Barua et al. (1995) studied that the majority of the coastline of Bangladesh represents the margin of a deltaic plain which is located at the head of the Bay of Bengal. The deltaic plain is formed by the Ganges-Brahmaputra river system which is ranked as the number one sediment carrier in the world. This paper is presented in three sections. First is an analysis of the wind field from which wave hindcasts are derived. Secondly, we have used a finite element refraction model developed by Coastal Science & Engineering to see the convergence and divergence of wave energies. This section also contains computations of wave refraction by tidal currents. The third section deals with some estimates on wind and wave induced transport and provides a qualitative analysis of the morphological consequences resulting from them. Hindcasted wind waves under gale force conditions occur about 7 times per year and wave divergence over the the subaqueous delta due to the refracting effect on the eastern Bengal shelf. The effect of tidal currents on wave refraction show that flood currents deflect waves more to the east while ebb currents deflect them more to the west. This may induce a counterclockwise sediment transport gyre around the Bengal shelf at the mouth of the Ganges-Brahmaputra rivers. The near bed orbital velocities obtained from refraction modeling and indicating that waves play an important role in the redistribution of river borne sediments.

Hossain (2001) studied that Bangladesh is a vast delta bounded by the Bay of Bengal on its southern limit. The landmass is mostly flood plain in origin, with most of the territory only a few meters above sea level except a portion of hilly lands in the north and south.

The coastal zone of Bangladesh enjoys a tropical maritime climate, which is more or less similar to that country's climate. The entire coastal zone is prone to violent storms and tropical cyclones during pre-monsoon and post-monsoon seasons. Sometimes cyclones associated with tidal waves cause great loss of lives and property. The topography of the coastal zone and the tidal patterns of the Bay of Bengal play an important role in the economy of the area. Tidal behavior varies along the coast in terms of magnitude but not of pattern. The variation in such a short coastline might be attributed to the shallowness of the Bay and varying topography of coastal waters. The tidal range at the head of the Bay of Bengal is strong, ranging from 1.3m at neap tide to about 4.83m at spring tide near Sagardip. Similarly, 4.27m neap tides and 6.10m spring tides are observed in the Sandwip area (Satalkhal). This range is reduced toward the south along the eastern shore of the Bay of Bengal. At Sadarghat, Chittagong, monthly mean tidal range varies from 1.48 to 4.90m with a 24 year average of 3.84 m.

Jena et al. (2001) studied that India has a long coastline of about 7000 km bounded by the Bay of Bengal on the east, the Indian Ocean on the south, and the Arabian Sea on the west. The factual assessment on sediment transport along Nagapattinam-Poompuhar coastline is vital since it adjoins the sheltered Palk Bay. The Nagapattinam-Poompuhar coastline consists of long, narrow and low sandy beaches. The nearshore bathymetry is relatively steep, straight and parallel to the coast. The tides in this region are semi diurnal with an average spring range of 0.67 m and neap range of 0.19 m. Based upon oceanographic climate, three distinct seasons are recognised: i) the southwest monsoon (June to September), ii) the northeast monsoon (October to January) and iii) the fair weather period (February to May). Extreme wave conditions occur during severe tropical cyclones which are frequent in the Bay of Bengal during the northeast monsoon. Based on the analysis of these wave data, the predominant wave characteristics were established for each month. The significant wave heights persisted between 0.5-1 m during March to October, and 1-1.5 m from November to February. Highest significant wave height of 2.1 m was recorded in November during the period of one year measurement. The zero crossing wave period predominantly varied 3-8 s in November and December and 3-5 s during the rest of the year. The wave direction (with respect north) mostly prevailed between 60'-120' during November to February, and 90'-120' during the rest of the year. Directional waves were measured off Nagapattinam coastline for one year to estimate the longshore sediment

transport rate. It shows that the transport rate is relatively high about $0.1 \times 10^6 \text{ m}^3/\text{month}$ in November and December and is low showing less than $0.03 \times 10^6 \text{ m}^3/\text{month}$ in March, April and July. Though the annual gross transport is found to be $0.6 \times 10^6 \text{ m}^3/\text{year}$, the annual net transport is very low showing less than $0.006 \times 10^6 \text{ m}^3/\text{year}$ (towards north), indicating the coastline tends to be a nodal drift regime. The temporary rise in wave activities during the cyclonic days often increases the southerly drift, which partly gets deposited in the Palk Bay and causes deficit for the northerly drift.

Lewis et al. (2014) studied that coastal flood risk from tropical cyclone storm surge is high in the northern Bay of Bengal and projected to increase with sea level rise. Accurate estimates of storm surge magnitude and frequency are essential to coastal flood risk studies. Several hydrodynamic models have been developed to simulate storm surges in the region. One successful example is predictive skill is the IIT-D (Indian Institute of Technology-Delhi) storm surge model has been used as a part of the Bangladesh early warning and credited with reducing loss of life in the 2007 cyclone Sidr flooding event especially when compared to a similar cyclone event in 1991. In the Bay of Bengal, extreme water levels are derived from numerical storm surge models based on an idealized cyclone event; however, uncertainty within such calculations for this region is poorly understood, especially when propagated through to the flood hazard. There has been used the IBTrACs data set to estimate natural variability for “1 in 50 year” recurrence interval cyclone events. Each idealised cyclone is then used to force a storm surge model to give predicted peak water levels along the northern Bay of Bengal coast. The descriptive parameters of 18 cyclone events (between 1990 and 2008) appear to show no statistically significant variation (at the 5 % level) due to landfall location, which allows us to pool characteristics for the entire Bay of Bengal. Using the variability estimates for a 1-in-50-year cyclone event making landfall at the 2007 Sidr location, cyclone central pressure drop uncertainty had the greatest effect upon simulated storm surge magnitude. Storm surge hazard uncertainty due to cyclone parameter variability was found to be comparable to the inundation difference simulated when the peak surge coincided with either a mean spring high or low water. In this research indicates the importance of improving extreme water level estimates along the Bay of Bengal coastline for robust flood hazard management decisions in the Bay of Bengal.

Islam et al. (2009) studied that Bangladesh has been 710 km long coast to the Bay of

Bengal which contains several ecosystems that have important conservation values. As a zone of vulnerabilities as well as opportunities this coast prone to natural disasters like cyclone, storm surge and flood. This paper represents the overall current situation of two Integrated Coastal Zone Management (ICZM) programs- one is as a successful model like Xiamen ICZM program in China and another is as a developing project like ICZM program in Bangladesh. Integrated Coastal Zone Management (ICZM) activity policy has eight objectives to address the vulnerabilities and opportunities of the coastal areas. In these areas environmental friendly industrial activities and other sustainable use of natural resources have been addressed very carefully and lawfully. Implementing ICZM is a costly project and the Xiamen ICZM program consists of the cost of regulatory development. In Bangladesh the Government and local Government Institutions, all concerned Agencies, NGOs, private sector and the civil society will put their efforts for the development of the coastal zone. There is a brief consideration of the progress of the management for ICZM of Bangladesh and how this project might be more effective and beneficial for Bangladesh .

Komol (2011) set up a two dimensional hydrodynamic Depth Integrated Velocity and Solute Transport Model (DIVAST) for Bay of Bengal for simulation of tidal level at selected coastal area of Bangladesh. The bathymetry of the Bay of Bengal has been generated based on the data of Meghna Estuary Study (MES) phase I and phase II. the simulated tidal levels of the bay of bengal model have been calibrated and verified with the observed tidal levels of tidal gauge stations located at Daulatkhan, Tazumuddin, Hatiya, Sandwip, Feni river, Rangadia and Hiron point locations .

Sayma and Salehin (2012) assessed salinity constraints to different water uses in coastal area of Bangladesh. It was an attempt to delineate the salinity related problems on multi-purpose uses of water and assess better water management options in a small scale water resources subproject in south-west coastal region of Bangladesh .

Sarwar (2005) studied on the Impacts of sea level rise on the coastal zone of Bangladesh. The study revealed that a one meter sea level rise will affect the vast coastal area and flood plain zone of Bangladesh. Both livelihood options of coastal communities and the natural environment of the coastal zone will be affected by the anticipated sea level rise. It will also affect national and food security of the country .

Ayub et al. (2007) set up a Depth Integrated Two-Dimensional Numerical Model to study the sediment dynamics within the Meghna Estuary by. Both cohesive and noncohesive

sediment transport formulation were used to estimate the total sediment transport. An interactive morphological computation was used here to verify the bed level changes over 2 years. Sediment transport of both monsoon and dry seasons were modeled. Land reclamation dams were tested by the model and found to be effective in enhancing the accretion in its vicinity .

CZPo (2005) studied that the Ganges, the Brahmaputra and the Meghna that constitute one of the largest river systems in the world drain through the Bangladesh into the Bay of Bengal. The coast of Bangladesh is known as a zone of vulnerabilities as well as opportunities. It is prone to natural disasters like cyclone, storm surge and flood. The combination of natural and man-made hazards, such as erosion, high arsenic content in ground water, water logging, earthquake, water and soil salinity, various forms of pollution, risks from climate change, etc, have adversely affected lives and livelihoods in the coastal zone and slowed down the pace of social and economic developments in this region. Increasing population, competition for limited resources, natural and man-made hazards, lack of economic opportunities, important ecological hot spots, etc, calls for distinctive coastal management. Three indicators have been considered for determining the landward boundaries of the coastal zone of Bangladesh. These are: influence of tidal waters, salinity intrusion and cyclones/storm surges. 19 districts of the country are being affected directly or indirectly by some of these phenomena. The districts are considered including all upazilas/thanas. A total of 48 upazilas/thanas are considered as ‘exposed’ directly to vulnerabilities from natural disasters. The exclusive economic zone (EEZ) is regarded as the seaward coastal zone. The Government has made the coastal zone policy statements in relation to development objectives. These policies provide general guidance so that the coastal people can pursue their livelihoods under secured conditions in a sustainable manner without impairing the integrity of the natural environment.

Jackobsen et al (2002) studied that the coast of Bangladesh is exposed to extreme meteorological and hydrological conditions. Occasional cyclone surges in combination with high tides have had devastating effects on the southern part of Bangladesh. The Meghna Estuary is a ‘coastal plain estuary ’ on the Bangladeshi coastline in the Bay of Bengal, which is part of the Indian Ocean. The ultimate aim of the MES (Meghna Estuary Study II) was to increase the physical safety and social security of the inhabitant in the coastal area and to promote sustainable development. Bathymetrically, the estuary can be

considered as a sudden dramatic widening of the Meghna River, which is shallow and followed by a deep, wide opening towards the Bay of Bengal. The long and shallow continental shelf and the shape of the Bangladeshi coastline strongly amplify the tidal and cyclone surges. A numerical model covering the northern half of the Bay of Bengal including the Meghna Estuary was set up with the objective to increase our understanding of the hydrographic features and morphological dynamics in the Estuary, especially in the case where man-made physical interventions are constructed. The simulations revealed a counter-clockwise residual circulation with a northward net flow in the Sandwip Channel of $10\,000\text{ m}^3/\text{s}$ during the dry season and $15\,000\text{ m}^3/\text{s}$ during the wet season. The residual flow is forced by tides together with the bathymetry. The residual circulation to some extent traps the river water inside the Meghna Estuary and is one of the reasons for the relatively low salinity in the estuary even during the dry season. It is also believed to be important for the morphological development. Finally, a suggested intervention north of Sandwip shows to stop the residual circulation in the Estuary, for which reason it was advised not to construct such an intervention without further detailed investigations.

Jain et al. (2010) studied that coastal regions of the east coast of India are very vulnerable to severe flooding due to storm surges associated with intense tropical cyclones originating in the Bay of Bengal. Wind is the main generating mechanism of storm surges, and a rise sea level. The tides augment the storm surges and resulting water levels enhanced significantly. The head Bay region which covers part of West Bengal is more prone to high water elevation due to the presence of the Ganges-Brahmaputra-Meghna deltaic river system, a high tidal range and shallow waters. The main objective of this study was to present the total water level (TWL) for each coastal district of the maritime states along the coast of India. A database of cyclonic tracks and intensity information is prepared from various available sources for maritime states along the east coast of India. Frequency of occurrence relationship is obtained using 117 years of data for all the major historical storms that struck different segments of the coast. The total water level is computed based on a linear Combination of surge, tide, and wave set up along the coast. So an assessment of cyclone risk and vulnerability was evolved which is an important component of the information used to create sustainable local-level development action plans for preparedness and mitigation.

2.4 Studies on Coastline Hydrodynamics around the World

Falnes (2007) Studied, comparing ocean-wave energy with its origin, wind energy, the former is more persistent and spatially concentrated. The global power potential represented by waves that hit all coasts worldwide, has been estimated to be in the order of 1TW (1 terawatt $\frac{1}{4}$ 1012W). If wave energy is harvested on open oceans, energy that is otherwise lost in friction and wave breaking, may be utilised. The term wind sea is used for waves that are actively growing due to forcing from local

wind. These waves travel in or close to the local wind direction. Many different types of wave-energy converters, of various categories, have been proposed. It is useful to think of primary conversion of wave energy by an oscillating system as a wave-interference phenomenon. Corresponding to optimum wave interference, there is an upper bound to the amount of energy that can be extracted from a wave by means of a particular oscillating system. Swell is the term used to describe long-period waves that have moved out from the storm area where they were generated. Swells in deep water will, typically, have wavelengths of 100–500m whilst wind seas may range from a few metres to 500m depending on the wind speed. Taking physical limitations into account, another upper bound, for the ratio of extracted energy to the volume of the immersed oscillating system, has been derived. Finally, the significance of the two different upper bounds is discussed.

Folley (2009) studied that analysis of the nearshore wave energy resource. When wave energy began to be taken seriously as a potential source of renewable energy, the majority of wave energy converters (WEC's) have been conceived as offshore devices, where the highest wave energy densities was found. The gross nearshore wave energy resource is significantly smaller than the gross offshore wave energy resource implying that the deployment of wave energy converters in the nearshore is unlikely to be economic. Calculation of a site's potential using the exploitable wave energy resource is considered superior because it accounts for the directional distribution of the incident waves and the wave energy plant rating that limits the power capture in highly energetic sea-states. A third-generation spectral wave model is used to model the wave transformation from deep water to a nearshore site in a water depth of 10 m. It is shown that energy losses result in a reduction of less than 10% of the net incident wave power. A significant proportion of the wave energy resource can arrive at an offshore site during storms making it largely unexploitable. Natural filtering of storm waves by depth-limited wave breaking means that

this accounts for a much smaller proportion of the nearshore wave energy resource.

Wolf (2009) studied that about the Tides, Storm surges, Wind waves, Coastal flooding, Wave–current interaction. Coastal flooding is generally caused by a combination of high water levels, which may be caused by tides and storm surges, together with waves, which can lead to overtopping of coastal defences and inundation of low-lying areas. Wind waves and elevated water levels together can cause flooding in low-lying coastal areas, where the water level may be a combination of mean sea level, tides and surges generated by storm events. In areas with a wide continental shelf a travelling external surge may combine with the locally generated surge and waves and there can be significant interaction between the propagation of the tide and surge. Wave height at the coast is controlled largely by water depth. The storm surge is the meteorologically driven component of water level driven by synoptic variations of atmospheric pressure and wind. If the storm surge is combined with tide, the combined water level may be known as the ‘storm tide’ or sometimes the ‘still water level’ since changes occur over periods of hours to days, compared to typical wave periods of 1–20 s. The principles of wave and surge generation by wind are universal, although the impacts vary in different geographical locations. For both it is necessary to have a good wind forecast model of as high resolution as possible and this can be used to run separate wave and surge forecasts. These processes are well understood and accurately predicted by models, assuming good bathymetry and wind forcing is available. Other interactions between surges and waves include the processes of surface wind-stress and bottom friction as well as depth and current refraction of waves by surge water levels and currents, and some of the details of these processes are still not well understood. The recent coastal flooding in Myanmar (May 2008) in the Irrawaddy River Delta is an example of the severity of such events, with a surge of over 3 m exacerbated by heavy precipitation. In this paper review the existing capability for combined modelling of tides, surges and waves, their interactions and the development of coupled models.

Hiles (2007) studied that a Computational models for wave climate assessment in support of the wave energy industry. This thesis identifies, and where necessary develops, appropriate methods and procedures for using nearshore wave modelling software to provide critical wave climate data to the wave energy industry. The nearshore computational wave modelling packages SWAN and REF/DIF were employed to estimate wave conditions near-shore. These models calculate wave conditions based on the offshore

wave boundary conditions, local bathymetry and optionally, other physical input parameters. Wave boundary conditions were sourced from the Wave WatchIII offshore computational wave model operated by the National Oceanographic and Atmospheric Administration. SWAN and REF/DIF was used in a complementary fashion, where SWAN was used at an intermediary between the global-scale offshore models and the detailed, small scale computations of REF/DIF. The most promising areas for wave energy development are located near-shore, in less than 150m of water. Using SWAN to model most of Vancouver Island's West Coast (out to the edge of the continental shelf), the sensitivity of wave estimates to various modelling parameters was explored. Computations were made on an unstructured grid which allowed the grid resolution to vary throughout the domain. A study of grid resolution showed that a resolution close to that of the source bathymetry was the most appropriate. Further studies found that wave estimates were very sensitive to the local wind conditions and wave boundary conditions, but not very sensitive to currents or water level variations.

Noda (1974) studied that the phenomenon of wave-induced nearshore circulation. The most visually evident characteristic of nearshore circulation patterns is the phenomenon of rip currents. The driving mechanism for circulation patterns in the nearshore region was assumed to be due to a longshore variation in the radiation stress field. Herein is presented a theoretical analysis of nearshore wave induced circulation patterns produced by the interaction of incoming waves and local bottom topography. This interaction results in a spatial variation of wave characteristics that produces a possible driving mechanism for nearshore circulation patterns. Both normal and oblique wave incidence are considered with the imposed beach profiles developed from an examination of prototype data. The analytical model results are compared with field measurements and yield optimistic results.

Wolf et al. (1999) observed wave-current interaction both coastal and offshore. Wave-current interactions can occur over a wide range of both wave and current conditions. The important effect of surface waves on the generation of wind driven surge currents is omitted, as is wave-generated mean flow. Two aspects was highlighted: (i). the effect of waves on enhancing the bottom friction experienced by tidal currents, and (ii). the effect of tidal currents on the propagation of surface waves. The main energy in the coastal region is due to tides, surges, and wind waves. Interactions occur between these different 'waves' because the tides and surges change the mean water depth and current field experienced by

the waves. The surge and tidal currents appear to the wind waves as quasi-steady over measurement periods of 10–20 min. Using data collected during the SCAWVEX Project, the effect of depth and current changes particularly tidal on waves and the effect of waves on tidal currents were examined. The possible interaction mechanisms between waves, tides and surges were reviewed. These include the effective surface wind stress, bottom friction, depth and current refraction and modulation of the absolute and relative wave period. Waves and currents should always be measured simultaneously since the correct determination of either in shallow water requires knowledge of the other. Since the algorithms are quite complex and may depend on a good ‘first guess’, the future probably lies in combining remote sensing plus modelling together with ground truth ‘in situ’ data.

Ozyurt et al. (2010) studied on impacts of sea-level rise to coastal zone management. The prediction of future characteristics of coastal areas is a major concern at national and local levels due to the vast land and sea resources that are available ecologically, physically, and socioeconomically. Integration of climate change impacts on coastal areas, especially impacts of sea-level rise, with coastal zone management practices was performed through coastal vulnerability assessments. Out of the types of vulnerability assessments, a proposed model demonstrated that relative vulnerability of different coastal environments to sea level rise may be quantified using basic information that includes coastal geomorphology, rate of sea-level rise, and past shoreline evolution for the National Assessment of Coastal Vulnerability to Sea-Level Rise for U.S. Coasts. The vulnerability cannot be directly equated with particular physical effects. Thus, using this concept as a starting point, a coastal vulnerability matrix and a coastal vulnerability index that use indicators of impacts of sea-level rise are developed. Using available regional data, each parameter is assigned a vulnerability rank of very low to very high (1–5) within the developed coastal vulnerability matrix to calculate impact subindices and the overall vulnerability index. The developed methodology and Thieler and Hammar-Klose the proposed methodology were applied to the Go˘ksu Delta, Turkey. It is seen that the Go˘ksu Delta shows moderate to high vulnerability to sea level rise. The outputs of the two models indicate that although both models assign similar levels of vulnerability for the overall region, which is in agreement with common the literature, the results differ significantly when in various parts of the region is concerned. Overall, the proposed Thieler and Hammar-Klose method assigns higher vulnerability ranges than does the developed coastal vulnerability index sea-level

rise (CVISLR) model. A histogram of physical parameters and human influence parameters enables decision makers to determine the controllable values using the developed model.

2.5 Studies on Coastline Hydrodynamics By using Mathematical Modeling

Hossain (2012) studied verification of water velocity at coastal area of Bangladesh by using mathematical model. This study was based upon an analysis of tidal velocity in different location. The hydrodynamics of the selected area of Bay of Bengal is simulated by solving two-dimensional depth integrated continuity and momentum equations numerically with finite difference (ADI-Scheme) method. Consequently the water elevation η and the respective velocity components U, V in the x and y directions are calculated across the selected locations. Simulated velocity has been verified at selected locations of coastal area with the measured field data and compared with the other study carried out in the coastal region. The model was calibrated and verified with the measured data at six locations such as: Noakhali –Urirchar Channel, Sandwip-Zahajerchar Channel, Hatia-Noakhali Channel, Sandwip-Sitakundu Channel, Sandwip-Urirchar Channel and Shahbazpur-Monpura Channel of the Bay of Bengal. Outcome of this work shows a good agreement between the measured and model simulated velocities of nearshore areas of the Bay of Bengal.

Yoo et al. (1986) studied on a mathematical modeling of wave –induced nearshore circulation. Wave-induced nearshore circulations are the result of complex processes driven by gravity water waves. When waves approach either the shoreline or man- made coastal structures, processes of shoaling, refraction, diffraction, dissipation and wave current interaction occur. In this paper a mathematical model for describing wave climates and wave-induced nearshore circulations. The Model accounts for current-depth refraction, diffraction, wave –induced currents, set-up and set-down, mixing processes and bottom friction effects on both waves and currents. The importance of including processes such as advection, flooding and current interaction in coastal models was demonstrated by comparing the numerical results without each process to the results from the complete scheme.

Ebersole et al. (1980) studied that nearshore circulation of fundamental importance and transport of nearshore contaminants as well as littoral materials. In this study a non linear numerical model is presented based on a leapfrog finite difference scheme which includes

time dependency and eddy viscosity term. The numerical model is formulated using the usual time-averaged (over one wave period) and depth –averaged conservation equations of mass and momentum, in terms of the mean horizontal and vertical velocities (u, v) and the mean free surface displacement η . The longshore current over a prismatic beach profile including an offshore bar was showing of the effects of the bar on velocity profile. Model was accurately predicted currents and wave transformations in the nearshore zone and necessary step in attempting to predict actual changes to coastline. From the results shown here it appears that the inclusion of the convective acceleration terms and lateral mixing terms in the horizontal momentum equations had important effects which must be included in models used to predict nearshore circulation. The terms become especially significant in attempts to model circulation over irregular bottom topographies which include bars and channel.

Ito et al. (1972) studied on a method of numerical analysis of wave propagation. The method was presented to obtain numerically wave patterns in the region of arbitrary shape. The principle is to solve the linearized wave equations under given boundary conditions from a certain initial state. In this paper two application of numerical analysis was presented in the fundamental fashion. The first application method was related to wave diffraction. The distribution of wave height along a semi-infinite breakwater and a detached breakwater was calculated and compared with that obtained from the conventional analytic solutions to confirm the validity of numerical method. The second application was to wave refraction. In particular, this method of numerical analysis is applicable to the analysis of wave propagation in the region of ray intersections which was indicated by the conventional geo-optic wave refraction theory. The application to the region of variable water depth, the correction factor of shoaling has been introduced. The shoaling factor for basic wave equation is a function of phase velocity instead of the group velocity in the conventional relation. This value of correction factor varies from 1 in deep water to 0.707 in the region of long waves, when the deep water was taken as reference.

Lee et al. (1992) studied on evaluation of models on wave –current interactions. Five contemporary numerical models on wave-current interactions were evaluated in a two – dimensional domain through mutual comparisons, in this paper. The bases of evaluation were mathematical exactness, degree of computational difficulty and practical applicability in term of the abilities of handling shoaling, refraction, diffraction, reflection and wave

current interaction. On the five wave models, four were selected from existing literature and one was developed by the authors. The evaluation was limited in that the bench mark cases were restricted to those with either theoretical solution or accepted hydraulic model results. The main differences among the 5 models were their governing wave equations and the associated numerical methods. They include two hyperbolic types, two elliptic types and one parabolic type. The current model was governed by the depth integrated momentum and continuity equations. The current condition was given as input rather than coupled with the circulation model. Within this context, the performance of each model was evaluated and comparisons were given in matrix. The selection of model for application depends upon the intended purpose.

Nielsen (1983) studied that nearshore wave height variation due to refraction shoaling and friction. Wave that propagate over a sloping bed was changed their height and direction. Explicit wave formulae derived from the dispersion relation for linear wave were used to find an analytical solution to the problem of wave height variation on a simple topography i.e topographies with incrementally constant slope and straight parallel contours. The solution accounts for shoaling, refraction and frictional dissipation and could be sufficiently accurate for practical purposes considering the simplifying assumption that were necessary for treatment of this problem by any method. The solution was simple enough to be handled on a personal calculator and has the advantage over numerical solutions that it could be solved for other parameters, for example to give friction factors from observed wave height data.

2.5 Summary

A brief description of various earlier studies in the Bay of Bengal has been presented in this chapter. In addition a few coastlines (hydrodynamics) and few numerical model research studies have also been mentioned here. It was found that several studies had been carried out on the coastal area of world to understand the wave nearshore circulation, nearshore wave height variation, wave-current interactions. As coastal area of Bangladesh is low lying and exposed to the sea. They are more vulnerable to wave induced velocity action that causes more erosion and accretion than that of other land areas. That is why the main focus of the study to assess the value of nearshore wave height, wave celerity and wave angle from deep water wave condition by using DIVAST numerical model at several locations in the coastal zone of Cox,s Bazar of Bay of Bengal of Bangladesh.

CHAPTER 3

THEORY AND METHODOLOGY

3.1 General

The prediction technique of flow velocity of wave and water level through numerical equations are illustrated in this chapter. A-2 dimensional numerical hydrodynamic model has been set up using the bathymetry of Bay of Bengal. This model has been based on the FORTRAN program. Numerical model has a number of modules for different purposes and each module deals with different sets of equations. In this study hydrodynamic module of the Numerical model has been used to simulate hydrodynamics parameters in the nearshore coast of Cox's Bazar of the Bay of Bengal. Concept of wave and wave theory, different methods of solving partial differential equations (analytical and numerical) are illustrated thereof. The gradual steps of solving the governing hydrodynamic equations and its solution techniques through ADI (alternating direction implicit) method have been discussed here. A short description of Numerical model, bathymetry generation, development of Bay of Bengal model with the governing equations of hydrodynamic module of Numerical model and key stages of model development have been illustrated in the following section.

3.2 Wave

Nearshore hydrodynamics is the study of liquids in motion. It describes the characteristics of wave, tide, pressure etc. The ability to accurately predict wave process from deep to shallow water is vital to an understanding of coastal processes. Wave propagates towards the shore, a combination of shoaling, refraction and diffraction processes effect and modify the deep water wave [Wei et al., 1995].

Wave action is a major factor of hydrodynamics in coastal engineering design [Holmes,2001]. Waves determine the composition and geometry of beaches. Since waves interact with human-made shore structures or offshore structures, safe design of these structures depends to a large extent on the selected wave characteristics. The structural stability criteria are often stated in terms of extreme environmental conditions (wave heights, periods, water levels, astronomical tides, storm surges, tsunamis, and winds). Waves in the ocean constantly change and are irregular in shape, particularly when under

the influence of wind; such waves are called seas. When waves are no longer under the influence of wind and are out of the generating area, they are referred to as swells [Herbich,1990].

The phenomenon of wave-induced nearshore circulation is one of the key processes to the ultimate understanding of coastal zone dynamics. The nearshore circulation patterns are the phenomenon of rip currents [Noda, 1974]. Waves in the ocean constantly change and are irregular in shape, particularly when under the influence of wind [Herbich,1990]. Waves on the surface of a natural body of open water are the result of disturbing forces that create a deformation, which is restored to equilibrium by, gravitational and surface tension forces. Surface waves are characterized by their height, length, and the water depth over which they are traveling [Meadows et al., 2003].

The ability to accurately predict wave transformation from deep to shallow water is a vital to an understanding of coastal processes [Wei et al., 1995]. When waves approach from deepwater to shallow water the processes of shoaling, refraction, diffraction, dissipation and wave current interaction occur [Ebersole et al.,1980, Nwogu, 1993]. The wave fields were highly variable with up to 3 orders of magnitude difference in energy scale in individual cases. The model accounts for shoaling, refraction, generation by wind, whitecapping, triad and quadruplet wave-wave interactions, and bottom and depth-induced wave breaking [Ris et al.,1999]. Wind waves and elevated water levels together can cause flooding in low-lying coastal areas, where the water level may be a combination of mean sea level, tides and surges generated by storm events. Waves and storm surges are caused by storm events with high winds blowing over the adjacent sea [Wolf, 2009].The nearshore currents are modified by bottom friction and mixing processes, particularly in the surf zone [Yoo et al., 1986]. Waves impinging on beaches induce mean flows, such as long shore and rip current [Ebersole et al., 1980].

Wave model applicability depends not only on the size of the area of the model but also the dominant physical processes affecting wave evolution in that area, including those defined in :

1. Wave generation by wind: the development of surface gravity waves caused by the transfer of energy from wind to the ocean surface;
2. Shoaling: an effect whereby wavelength decreases and wave height increases due to a decrease in water depth (as described by the dispersion relationship);

3. Refraction: a turning of wave fronts toward shallower water due to phase speed dependence on water depth. In shallow water, refraction tends to line up wave fronts so that they parallel bathymetric contours;
4. Diffraction: a process which spreads wave energy laterally, orthogonal to the propagation direction, that occurs when waves encounter obstacles whose radius of curvature is comparable to the wavelength of the incident waves;
5. Reflection: a change in direction of a wave front resulting from a collision with a solid obstacle;
6. Bottom friction: a mechanism that transfers energy and momentum from the orbital motion of the water particles to a turbulent boundary layer at the sea bottom;
7. Energy dissipation due to wave breaking: a loss of wave energy due to the turbulent mixing which occurs when wave steepness surpasses a critical level causing water to spill off the top of a wave crest;
8. Wave-wave interactions: (triad) two propagating waves exchange energy with a third wave, (quadruplet) four propagating waves exchange energy with one-another;
9. Wave-current interactions: encompasses changes in wave amplitude due to shoaling (caused by current related change in propagation speed), change in frequency due to the Doppler effect and change in direction due to current induced refraction.

Accommodating all of these processes into a single wave model is difficult. Different governing equations and numerical schemes lend themselves to modelling different physical processes and no single model adequately incorporates all of the effects listed above. Offshore, the dominant physical processes are wave generation by wind, quadruplet wave-wave interactions and a wind induced wave breaking called white-capping. Near-shore, the dominant physical processes are refraction, bottom friction, depth induced breaking, triad wave-wave interactions, current-wave interactions and, in very shallow waters, diffraction and reflection. Most wave models target a specific region (e.g offshore, near-shore, enclosed harbours) and incorporate only the physical processes important in that region [Hiles, 2007].

3.3 Wave Mechanics

Waves on the surface of a natural body of open water are the result of disturbing forces that create deformation, which is restored to equilibrium by, gravitational and surface tension forces. Surface waves are characterized by their height, length, and the water depth over which they are traveling. Figure 3. 1 shows a two-dimensional sketch of a sinusoidal surface wave propagating in the x direction. The wave height H , is the vertical distance between its crest and leading trough. Wavelength, L , is the horizontal distance between any two corresponding points on successive waves and wave period is the time required for two successive crests or troughs to pass a given point. The celerity of a wave C , is the speed of propagation of the waveform (phase speed), defined as $C = L/T$.

Most ocean waves are progressive; their waveform appears to travel at celerity C relative to a background. Standing waves, their waveforms remains stationary relative to a background, occur from the interaction of progressive waves traveling in opposite directions and are often observed near reflective coastal features. Progressive deep ocean waves are oscillatory meaning that the water particles making up the wave do not exhibit a net motion in the direction of wave propagation. However, waves entering shallow-water begin to show a net displacement of water in the direction of propagation and are classified as translational. The equilibrium position used to reference surface wave motion, (Still Water Level SWL) is $z = 0$ and the bottom is located at $z = -d$ (Figure 3.1).

The free surface water elevation, h , for a natural water wave propagating over an irregular, permeable bottom may appear quite complex. However, by assuming that, viscous effects are negligible (concentrated near the bottom), flow is irrotational and incompressible, and wave height is small compared to wavelength, a remarkably simple solution can be obtained for the surface wave boundary value problem. This simplification, referred to as linear, small-amplitude wave theory, is extremely accurate and easy to use in many coastal engineering applications. Furthermore, the linear nature of this formulation allows for the free surface to be represented by superposition of sinusoids of different amplitudes and frequencies, which facilitates the application of Fourier decomposition and associated analysis techniques [Meadows et al., 2003].

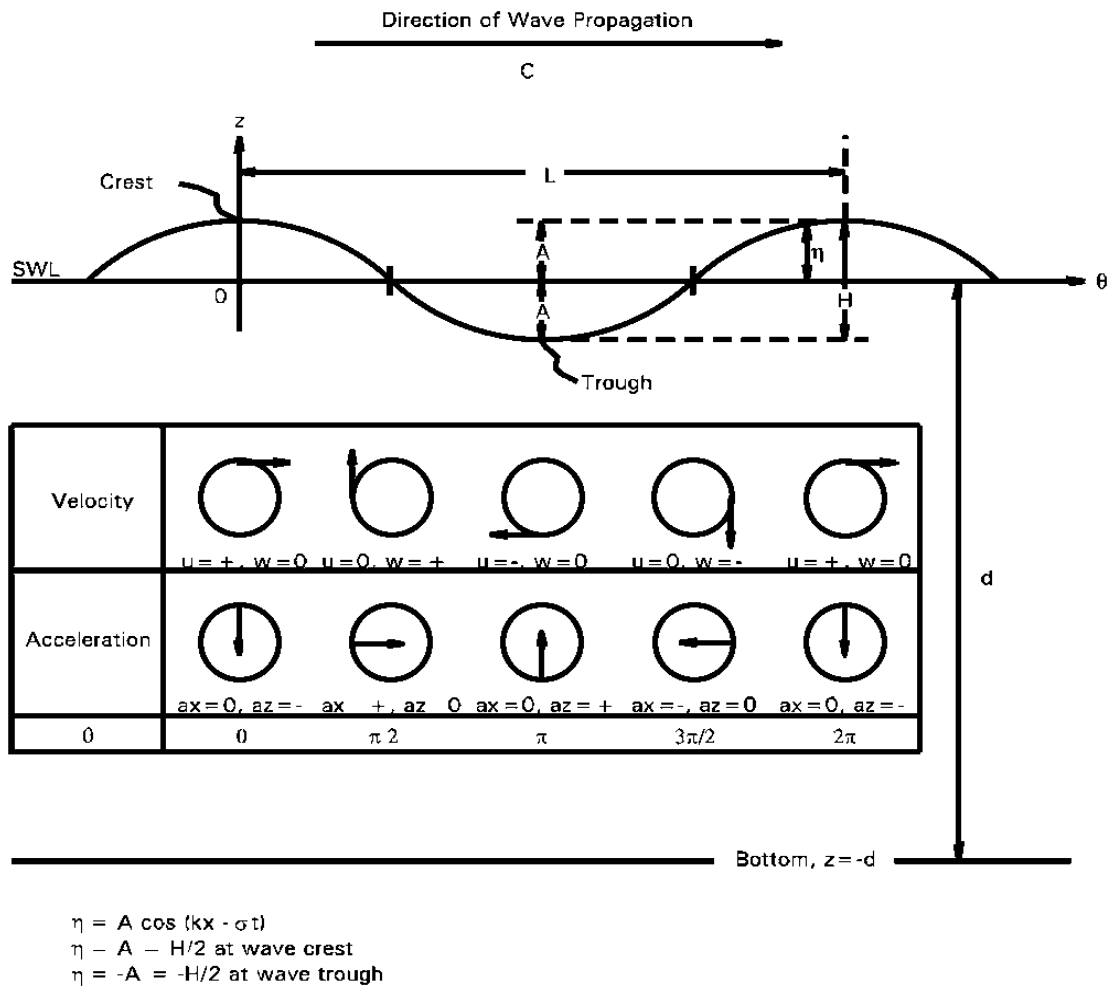


Figure 3.1: Definition sketch of free surface wave parameters for a linear progressive
[source: Meadows et al., 2003]

3.4 Theory of Wave

Progressive, Small-Amplitude Waves — Properties

The equation for the free surface displacement of a progressive wave is

$$\eta = A \cos(kx - \sigma t) \quad 3.1$$

Where,

amplitude, $A = H/2$

wave number, $k = 2\pi/L$

wave frequency, $\sigma = 2\pi/T$

The expression relating individual wave properties and water depth, d , to the propagation behavior of these waves is the dispersion relation,

$$\sigma = gk \tanh kd, \quad 3.2$$

where g is the acceleration of gravity.

From Eq. (3.2) and the definition of celerity (C) it can be shown that

$$C = \sigma/k = gT/2\pi * (\tanh kd) \quad 3.3$$

and

$$L = gT^2/2\pi * (\tanh kd) \quad 3.4$$

The hyperbolic function ($\tanh kd$) approaches useful simplifying limits of 1 for large values of kd (deep water) and kd for small values of kd (shallow water). Applying these limits to Eqs. (3.3) and (3.4) results in expressions for deep water of

$$C_o = gT/2\pi = 5.12T \quad (\text{English units, ft/s}) \quad \text{or}$$

$$C_o = 1.56T \quad (\text{SI units, m/s}) \quad \text{and}$$

$$L_o = gT^2/2\pi = 5.12T^2 \quad (\text{English units, ft}). \quad 3.5$$

or

$$L_o = 1.56T^2 \quad (\text{SI units, m}).$$

A similar application for shallow water results in

$$C = (gd)^{1/2} \quad 3.6$$

which shows that wave speed in shallow water is dependent only on water depth. The normal limits for deep and shallow water are $kd > \pi$ and $kd < \pi/10$ ($d/L > 1/2$ and $d/L < 1/20$) respectively, although modification of these limits may be justified for specific applications. The region between these two limits ($\pi/10 < kd < \pi$) is defined as intermediate depth water and requires use of the full Eqs. (3.3) and (3.4).

Some useful functions for calculating wave properties at any water depth, from deep water wave properties, are

$$C/C_0 = L/L_0 = \tanh(2\pi d/L) \quad 3.7$$

Values of d/L can be calculated as a function of d/L_0 by successive approximations using

$$d/L \tanh(2\pi d/L) = d/L_0 \quad 3.8$$

The term d/L has been tabulated as a function of d/L_0 and is presented, along with many other useful functions of d/L .

Particle Motions

The horizontal component of particle velocity beneath a wave is

$$u = \left(\frac{H}{2}\right) \times \sigma \times \left[\frac{\cosh k(d+z)}{\sinh kd}\right] \times \cos(kx - \sigma t) \quad 3.9$$

and

The vertical particle velocity is

$$v = \left(\frac{H}{2}\right) \times \sigma \times \left[\frac{\sinh k(d+z)}{\sinh kd}\right] \times \sin(kx - \sigma t) \quad 3.10$$

It can be seen from Eqs. (3.9) and (3.10) that the horizontal and vertical particle velocities are 90° out of phase at any position along the wave profile. Extreme values of horizontal velocity occur in the crest (+, in the direction of wave propagation) and trough (–, in the direction opposite to the direction of wave propagation) while extreme vertical velocities occur mid-way between the crest and trough, where water displacement is zero. The u and v velocity components are at a minimum at the bottom and both increase as distance upward in the water column increases. Maximum vertical accelerations correspond to maximum in horizontal velocity and maximum horizontal accelerations correspond to maximum in vertical velocity [Meadows et al., 2003].

Wave Shoaling

Waves entering shallow water conserve period and, with the exception of minor losses, up to breaking, conserve energy. However, wave celerity decreases as a function of depth and correspondingly wavelength shortens. Therefore, the easiest conservative quantity to follow is the energy flux, which remains constant as a wave shoals. Equating energy flux in deep water (H_0, C_0) to energy flux at any shallow water location (H_x, C_x) results in the general shoaling relation

$$\frac{H_x}{H_0} = \sqrt{\left(\frac{1}{2n} * \frac{C^0}{C_x}\right)} \quad 3.11$$

Wave Refraction

It can be shown that a deep water wave approaching a coast at an angle α_0 and passing over a coastal bathymetry characterized by straight, parallel contours refracts according to Snell's law:

$$\frac{\sin \alpha_0}{C_0} = \frac{\sin \alpha}{C} \quad 3.12$$

Since waves in shallow water slow down as depth decreases, application of Snell's law to a plane parallel bathymetry indicates that wave crests tend to turn to align with the bathymetric contours. Unfortunately, most offshore bathymetry is both irregular and variable along a coast and the applicable refraction techniques involve a non-linear partial differential equation, which can be solved approximately by various computer techniques [Meadows et al., 2003].

Considering two or more wave rays propagating shoreward over plane parallel bathymetry, Figure 3.2, it is possible to have the rays either converge or diverge. Under these conditions, the energy per unit area may increase (convergence) or decrease (divergence) as a function of the perpendicular distance of separation between wave rays b_0 and b_x . Using the geometric relationships shown in Fig. 3.3.2, Eq. (3.3.11) is modified to account for convergence and divergence of wave rays as

$$\frac{H_x}{H_0} = \sqrt{\left(\frac{1}{2n} * \frac{C^0}{C_x}\right) * \left(\frac{b_0}{b_{xx}}\right)} \quad 3.13$$

also written as

$$H_n = H_0 K_s K_R \quad 3.14$$

where K_s = the shoaling coefficient

K_R = the refraction coefficient.

This expression is equally valid between any two points along a wave ray in shallow water.

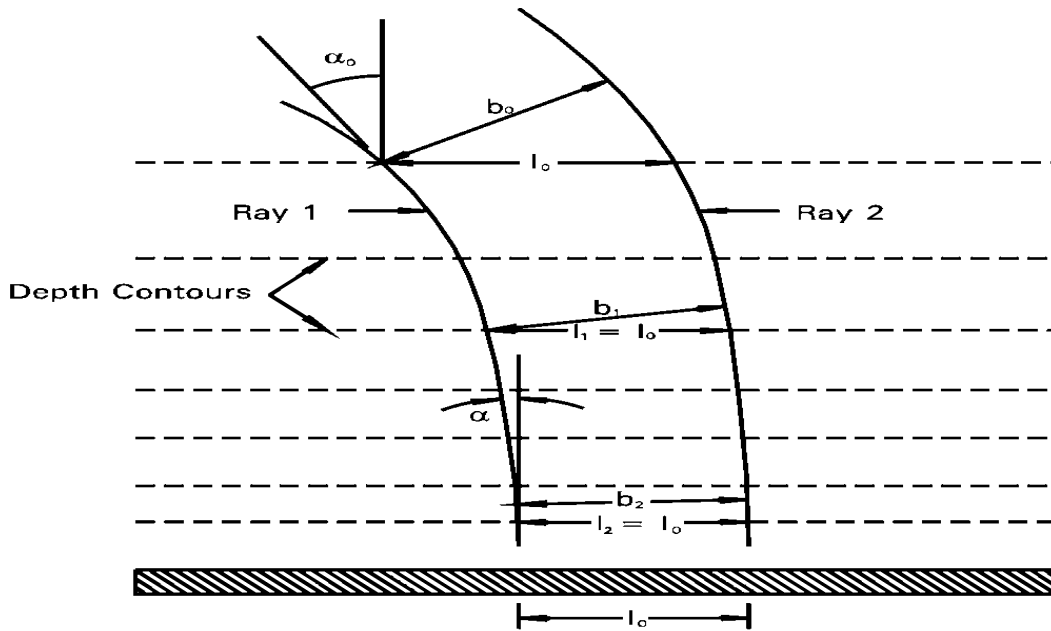


Figure 3.2: Definition sketch for wave rays refracting over idealized plane parallel bathymetry [source: Meadows et al., 2003].

Wave Breaking

Waves propagating into shallow water tend to experience an increase in wave height to a point of instability at which the wave breaks, dissipating energy in the form of turbulence and work done on the bottom. Breaking waves are classified as: spilling breakers generally associated with low sloping bottoms and a gradual dissipation of energy; plunging breakers generally associated with steeper sloping bottoms and a rapid, often spectacular, “explosive” dissipation of energy; and surging breakers generally associated with very steep bottoms and a rapid narrow region of energy dissipation. A widely used classic criteria (McCowan, 1894) applied to shoaling waves relates breaker height H_b to depth of breaking d_b through the relation

$$H_b = 0.78 d_b \quad 3.15$$

3.5 Nearshore Wave Climate

Nearshore wave climate will be assessed based on the change in wave height due to change in different deep water wave angle.

If wave reflection occurs this can be taken into account by applying a reflection coefficient which will depend on the properties of the reflecting boundary. The direction of the

reflected waves is given by “the angle of incidence equals the angle of reflection”. Note that reflections will produce a complex wave pattern in the form of “standing waves”. Knowing the offshore wave climate, in terms of HS, TZ and θ_0 , the products of the coefficients can be applied to each component of the wave climate to give the wave conditions at a shallow water location – but note that wave directions may change significantly [Holmes, 2001].

As mentioned previously, if wave measurements were available in a location in shallow water the inverse of the above transformation would have to be applied to give deep water wave conditions which could then be retransformed to the specific site for design [Holmes, 2001].

3.6 Wave-induced Longshore Currents.

In the full momentum equations for wave motion in shallow water there are six mechanisms involved:

1. Radiation Stresses
2. Pressure gradients due to mean water level variations – the latter termed wave set-up and set-down.
3. Mean bottom friction due to currents and waves.
4. Lateral mixing due to turbulence and the horizontal shear of currents.
5. The inertia of the water column – because it experiences accelerations.
6. Interactions between the waves and the currents.

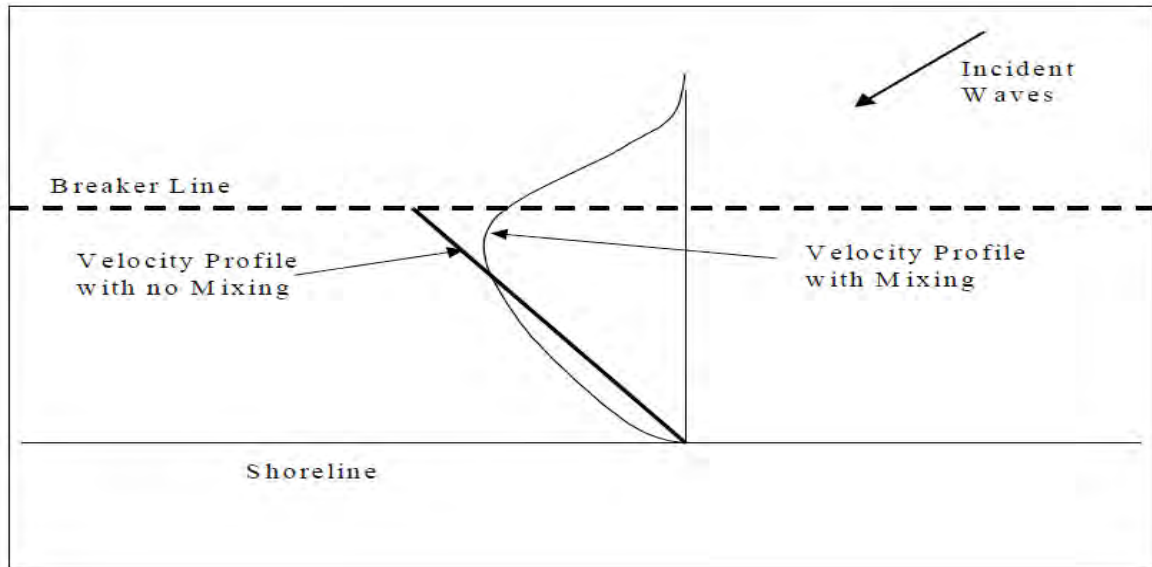


Figure 3.3: Long Shore Wave Induce Current [source: Holmes, 2001].

Waves arriving at the coastline at any angle other than zero will generate these currents but any variations in the height of breaking waves in the longshore direction will also generate currents.

Ignoring the mixing processes due to turbulent flow and the shear stresses that this generates, an estimate of the lonshore wave-induced velocity at the breaker line is given by:

$$V = (5\pi/16 fc) \gamma(gh_b)^{1/2} s. \sin \theta_b \quad 3.16$$

3.7 Tides

Tides are periodic variations in mean sea level caused by gravitational attraction between the earth, moon and sun and by the centrifugal force balance of the three-body earth, moon, sun system. Although complicated, the resultant upward or downward variation in mean sea level at a point on the earth's surface can be predicted quite accurately. Tide tables for the coastlines of the United States can be obtained for the U.S. Department of Commerce, National Ocean Service, Rockville, MD. Tides tend to follow a lunar (moon) cycle and thus show a recurrence pattern of approximately 1 month. During this one month cycle there will be two periods of maximum high and low water level variation, called spring tides and two periods of minimum high and low water level variation, called neap tides (figure 3.4).

Figure 3.4 also illustrates the different types of tides that may occur at the coast. These tides may be: diurnal, high and low tide occur once daily; semi-diurnal, high and low tides occur twice daily; or mixed, two highly unequal high and low tides occur daily. Diurnal tides occur on a lunar period of 24.84 hours and semi-diurnal tides occur on a half lunar period of 12.42 hours. Therefore, the time of occurrence of each successive high of low tide advances approximately 50 (diurnal) or 25 (semidiurnal) minutes.

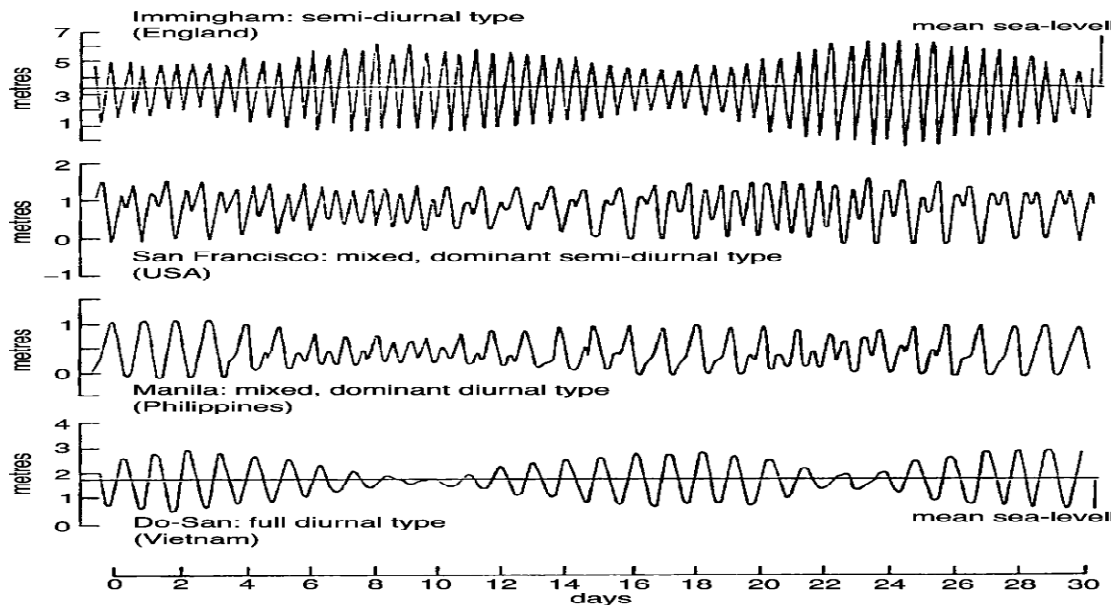


Figure 3.4: Different types of tides that may occur at a coast[source: Meadows et al.,2003].

3.8 Mathematical Modeling

A natural phenomenon can be represented through mathematical formulation considering all parameters involved with that particular phenomenon [Hossain, 2012]. A mathematical model is description of a system using mathematical concepts and language. The process of developing a mathematical model is termed mathematical modeling. It is a method of simulating real-life situations with mathematical equations to forecast their future behavior. Modeling gives a possibility to formulate hypotheses and to receive new knowledge about the object which was unavailable before. Mathematical modeling gives a possibility to avoid too great expenses, which are needed for direct study.

3.8.1 Numerical Methods

Most differential equations in Water resources Engineering cannot be solved analytically without simplification. Analytical treatment of the differential equations often with certain simplification is mainly meant to obtain qualitative insight into the characteristics of the solutions. For quantitative information, numerically solving the differential equations, with the modern digital computer is a powerful method. The exact or analytical solutions of the differential equations are usually continuous functions in the time-space domain. When the differential equations are solved numerically, the solutions are obtained at a finite number of grid points or nodes in time-space domain [Hossain, 2012, Halim et al., 1995]. This is done by replacing the differential equations by the difference equations (e.g. $\partial U/\partial t \rightarrow \Delta U/\Delta t$).

Computer-based numerical methods are now a days practically the major tools for solving surface and subsurface flow and contaminant transport forecasting problems as encountered in practice. In recent years, parallel to the advance in computer technology, much effort has been devoted to the development of the methodology and technique for numerical simulation of partial differential equations, which govern the flow of water in the open channel of various types. There are several numerical methods available for the solution of differential equations. The methods can be classified in to the following three categories.

1. Finite difference method
2. Finite element method
3. Method of characteristics

In this study finite difference method has been used to solve the hydrodynamic equations. Different aspects of this method have been illustrated in the following sections.

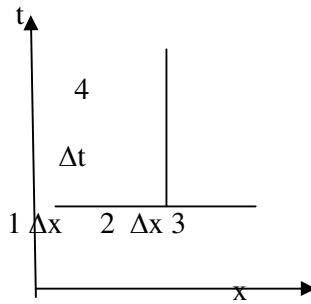
3.8.2 Finite Difference Method

The finite difference method is a numerical technique of solving the differential equations in which the derivatives are replaced by finite difference quotients so that the governing differential equations are converted into a set of algebraic finite difference equations. These later equations are solved numerically, usually on a digital computer.

Differential equation:
equation

$$\frac{\partial f}{\partial t} + \frac{\partial f}{\partial x} = 0$$

Numerical Scheme:



Finite difference

$$\frac{f_4 - f_2}{\Delta t} + \frac{f_3 - f_1}{2\Delta x}$$

derivatives

discretization with nodal points

finite difference quotients

Figure 3.5: Relation between partial differential equation, numerical scheme and finite difference equation

The governing equations are solved at a finite number of grid points within the considered domain. Suppose, the differential equations to be solved involved two independent variables x and t , then an (x,t) diagram (figure.3.5) constitutes the solution domain and the dependent variables can be defined at any point on the (x,t) plane within the end boundaries. As it is impossible to obtain solutions for the dependent variables at all points on the (x,t) diagram, the numerical solutions are obtained only at some fixed grid points, the choice of which depends on the features of the problem and the finite difference scheme to be used.

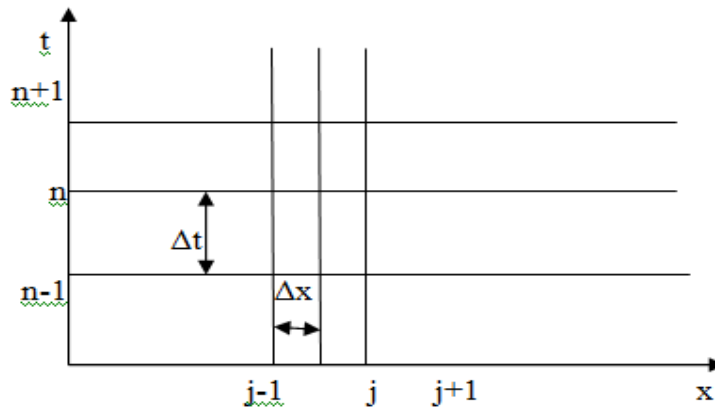


Figure 3.6: Finite difference computational grid in (x,t) plane.

The computational grid may be uniform in space (along the x-axis) in which case there are $(j-1)$ equal space intervals Δx . If the grid is not uniform, space intervals Δx are of variable length. In general the discretization along x-axis may be described as a set of points $x_j = j\Delta x, j=1,2,3,\dots,j; \Delta x_j = x_{j+1} - x_j$. In the same way the discretization in time is defined by a set of points $t_n = n\Delta t, n=1,2,3,\dots,N; \Delta t_n = t_{n+1} - t_n$. The computational grid in the (x,t) plane is then defined by the set $\{(x_j, t_n); j=1,2,3,\dots,j; n=1,2,3,\dots,N\}$. A non uniform computational grid is convenient when one wishes to refine the representation of the phenomena of interest in certain parts of the domain where the flow parameters and / or channel geometry vary more widely.

3.8.3 Concept of explicit and implicit schemes:

In a fixed grid finite difference method the Δx and Δt values are fixed to have a rectangular grid in the (x,t) plane as shown in figure 3.6. there are two basic types of fixed grid finite difference schemes explicit schemes and implicit schemes. Explicit schemes are those in which the value of a variable at any point at the advance time level $(n+1)$ is computed explicitly from known values at a few adjacent points at the time level n and independently of the other points at the times level $n+1$. Thus, the equations are arranged to solve for one point at a time and the unknown value is expressed directly in terms of known values.

For stability, the step sizes Δx and Δt of an explicit scheme must be so chosen that the Courant-Friedrichs-Lewy condition (shortly Courant number) is satisfied throughout the computation space which in turn puts a limit on the size of the time step Δt . The FTCS (forward time central space) scheme, the modified Lax scheme and the leap-frog scheme are three examples of the explicit finite difference schemes.

An implicit scheme, on the other hand, solves for a group of points at the advance time level $(n+1)$ which include the unknown values at the time level $(n+1)$ and the known values at the time level n . Thus, in this scheme the unknown values at the unknown time level occur implicitly in the finite difference form. The method most commonly employed is to solve for entire row, i.e. for all the grid points at the time level $(n+1)$ through the use of simultaneous equations containing the unknowns. This entails a more complicated computer program than the explicit method, but it allows one to use a longer time step than the explicit method without any stability problem. The Crank-Nicholson scheme and the Peaceman scheme are two examples of the implicit finite difference schemes.

Equation:

$$\text{Explicit Scheme: } \frac{\partial f}{\partial x} = \frac{f_{j+1}^n - f_{j-1}^n}{2\Delta x} \quad 3.17$$

$$\text{Implicit Scheme: } \frac{\partial f}{\partial x} = \frac{f_{j+1}^n - f_{j+1}^{n+1} + f_{j-1}^n - f_{j-1}^{n+1}}{2\Delta x} \quad 3.18$$

In general, the implicit method is more difficult to handle and it requires more computational efforts especially when a system of equations is solved or nonlinear equations are solved. However, it is sometimes more practical to choose an implicit method, especially when different time scales are present in a system of equations. Usually the largest time scale determines the behavior of the system whereas the smallest time scale determines the time-step restriction due to stability condition.

3.8.4 Finite Difference Forms

Another important difference between the finite difference schemes is the way they translate the derivatives into the finite difference quotients. The well-known finite difference forms are

- (i) Forward Difference
- (ii) Backward difference, and
- (iii) Central difference

The difference between the difference equation and the original differential equation is called the truncation error or order of approximation.

3.8.4 Characteristics of Finite Different Schemes

Some characteristics are important in solving the finite difference equations such as consistency, stability, convergency and accuracy. A finite difference scheme is said to be consistent or compatible when the truncation error tends to vanish and the solutions to the finite difference equations approach the solution to the differential equations as the computational mesh is refined (i. e. $\Delta x \rightarrow 0$ and $\Delta t \rightarrow 0$). Otherwise, it is inconsistent or incompatible.

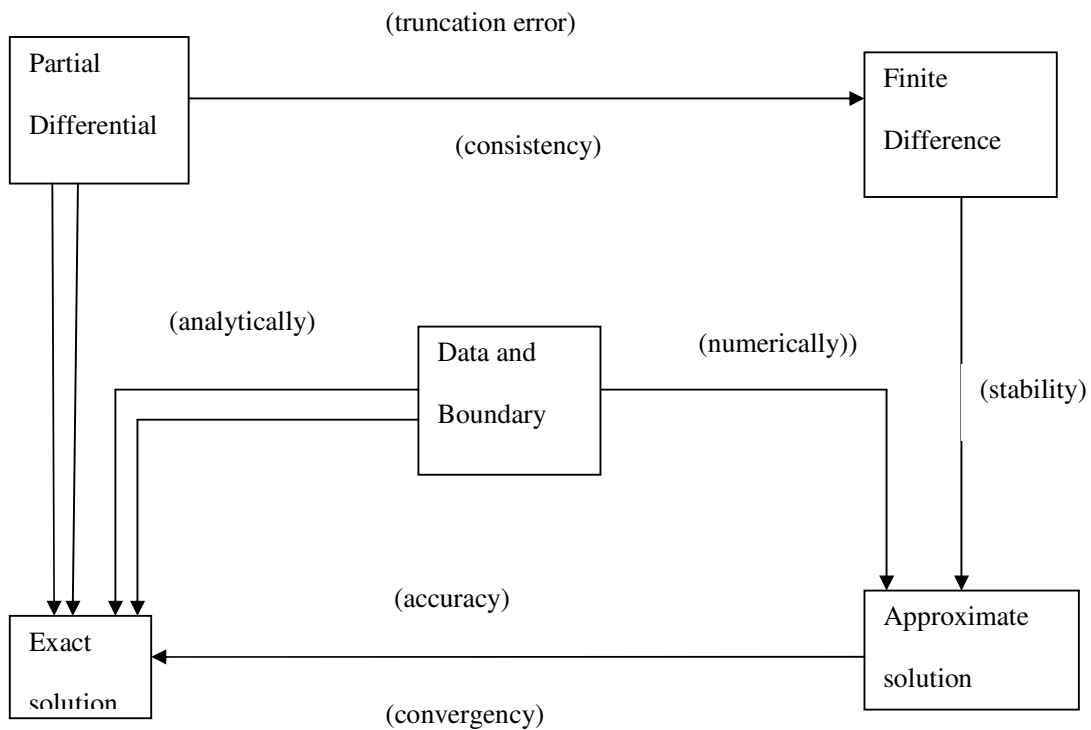


Figure 3.7: Conceptual relationship between consistency, stability and convergency

Stability:

The stability of a finite difference method concerns the amplification errors. These errors may be introduced by inaccurate initial and /or boundary conditions or due to rounding up errors. Stability is tested by asking if a particular part of the solution is likely to amplify without limit until destroys the calculation.

Convergency:

If the discrete (i.e. numerical) solutions to the governing differential equations approach the exact (i.e. analytical) solutions to the same equations as the computational mesh is refined, i.e. as $\Delta x \rightarrow 0$ and $\Delta t \rightarrow 0$, for a consistent finite difference scheme, then it is said to be a convergent scheme.

Accuracy:

Accuracy is tested by the ability of the finite difference method to reproduce the terms of

the differential equation without introducing extraneous terms which are large enough to affect the solutions. A stable finite difference method is not necessary an accurate one. There are three ways of investigating the accuracy of numerical methods:

- i) By determining the truncation error.
- ii) By analyzing the wave propagation and comparing the analytical and the numerical solutions.
- iii) By doing experiments with different numerical parameters (Δx , Δt etc.).

3.9 DIVAST Model

The numerical model DIVAST (Depth –Integrated Velocities and solute Transport), is a robust and reliable numerical model for solving 2D depth-integrated shallow water equations using a uniform rectangular mes grid. It has been widely used by many U.K and overseas consultants, Universities and research organizations for both industrial and research projects. DIVAST model was developed using the FORTRAN 77 programming language by Prof. Roger Falconer, Halcrow Professor of Environmental Water management and Dr. Binliang Lin, both of them from Cardiff School of Engineering, Cardiff University, UK. DIVAST is continually updated and improved by both Prof. Falconer’s team in Cardiff University and the MarCon staff.

DIVAST is a two dimensional, depth integrated, hydrodynamic and solute transport, time variant model which has been developed for estuarine and coastal modeling. It is suitable for water bodies that are dominated by horizontal, unsteady flow and do not display significant vertical stratification. The model simulates two dimensional distributions of currents, water surface elevations and various water quality parameters within a modeling domain as functions of time, taking into account the hydraulic characteristics governed by the bed topography and the boundary conditions.

The DIVAST model is based on the solution of the depth-integrated Navier-Stokes equations and includes the effects of local and advective accelerations, the earth’s rotation, free surface pressure gradients, wind action, bed resistance and a simple mixing length turbulence model. The differential equations are written in their pure differential form, thereby allowing momentum conservation in the finite-difference sense. Particular emphasis has been focused in the development of the model on the treatment of the

advective accelerations, a surface wind stress and the complex hydrodynamic phenomenon of flooding and drying.

The governing differential equations are solved using the finite difference technique and using a scheme based on the alternating direction implicit (ADI) formulation. The advective accelerations are written in a time centered by iteration. Whilst the model has no stability constraints, there is a Courant number restriction for accuracy in the hydrodynamic module. The finite difference equations are formulated on a space staggered grid scheme, with the water surface elevations and x- direction velocity components being initially solved for during the first half time step by using Gaussian elimination and back substitution (Falconer, 1992).

3.10 Governing Equation of Model

The DIVAST model has a number of modules for different purposes with different sets equations. In this study hydrodynamic module has been used. The numerical model used here is based on the solution of the depth –integrated Reynolds averaged Navier stokes equations. Full details of the derivation of these depth-integrated equation is given in Falconer and Chen (1996) but the final representations of the governing equations are cited herein for convenience with the conservation of mass equation in x and y directions.

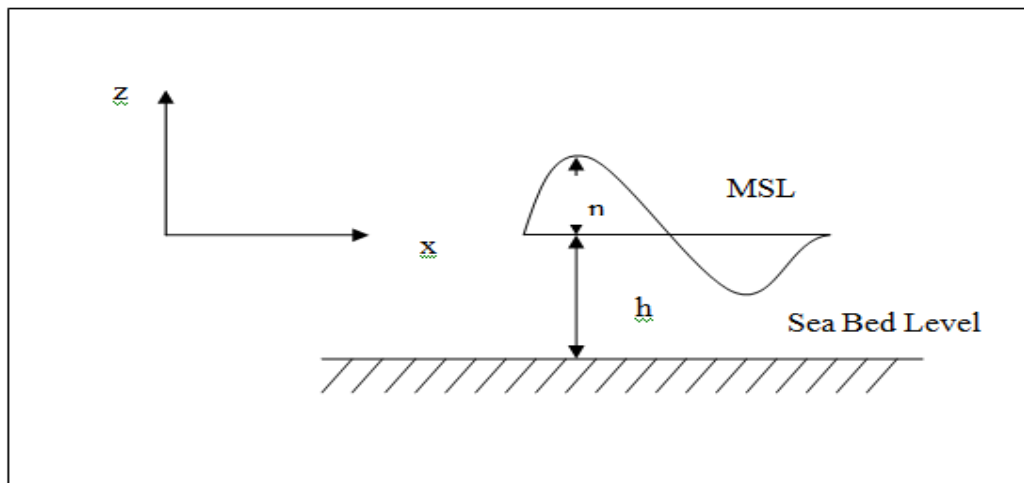


Figure 3.8: Definition sketch with notations and co-ordinates.

The depth integrated continuity equation:

$$\frac{\partial \eta}{\partial t} + \frac{\partial UH}{\partial x} + \frac{\partial VH}{\partial y} = 0 \quad 3.19$$

Where U, V are the depth-average velocity components in the x, y directions, η is water surface elevation due to wave from still water level, H is the total depth of flow (= h+ η).

The depth integrated momentum equation:

For x direction:

$$\frac{\partial UH}{\partial t} + \beta \left[\frac{\partial U^2H}{\partial x} + \frac{\partial UVH}{\partial y} \right] = fVH - gH \frac{\partial \eta}{\partial x} - \frac{H}{\rho} \frac{\partial Pa}{\partial x} + \frac{\tau_{xw}}{\rho} - \frac{\tau_{xb}}{\rho} + 2 \frac{\partial}{\partial x} \left[\epsilon \frac{\partial UH}{\partial x} \right] + \frac{\partial}{\partial y} \left[\epsilon \left(\frac{\partial UH}{\partial y} + \frac{\partial VH}{\partial x} \right) \right] \quad 3.20$$

For y direction:

$$\frac{\partial VH}{\partial t} + \beta \left[\frac{\partial UVH}{\partial x} + \frac{\partial V^2H}{\partial y} \right] = -fVH - gH \frac{\partial \eta}{\partial y} - \frac{H}{\rho} \frac{\partial Pa}{\partial y} + \frac{\tau_{yw}}{\rho} - \frac{\tau_{yb}}{\rho} + 2 \frac{\partial}{\partial y} \left[\epsilon \frac{\partial VH}{\partial y} \right] + \frac{\partial}{\partial x} \left[\epsilon \left(\frac{\partial UH}{\partial y} + \frac{\partial VH}{\partial x} \right) \right] \quad 3.21$$

Where, t is the time, x and y the horizontal coordinates toward east and north, U, V are the depth-averaged velocities in x, y direction, H is the total depth of flow (=h+ η), η , the water surface elevation due to the wave from the still water level, β is the momentum correction factor for non-uniform vertical velocity profile, Pa is the atmospheric pressure on the sea surface, ρ (= 1.03×10^3 kg/m³) is the seawater density, g is the gravitational acceleration and f is the Coriolis parameter ($2\omega \sin \psi$, where $\omega = 7.29 \times 10^{-5}$ rad/s is the angular speed of the rotation of the earth and ψ is the latitude of grid point). Here τ_{xw} , τ_{yw} = surface wind shear stress components in x, y direction, τ_{xb} , τ_{yb} = bed shear stress component in x,y direction and ϵ =depth-averaged eddy viscosity.

3.11 Methodology

Setting up Model for using Bathymetry data of Cox's Bazar of Bay of Bengal is summarized in the following sections:

3.11.1 Data Collection

To assess the hydrodynamic process along the coast of Cox's Bazar, necessary bathymetric data has been collected in two steps: 1) Primary Data and 2) Secondary Data.

All bathymetry data has been collected from Institute of Water Modeling (IWM), Bangladesh Water Development Board (BWDB) and Bangladesh Metrological Department (BMD) to set up the model. The primary data has been collected as Longitude, Latitude as

unit in degree and Depth in metre for setting up the bathymetry of the study area (Cox's Bazar). The Secondary data has been collected in BTM (Bangladesh Transverse Mercator) co-ordinate system. Then these data has been converted from BTM co-ordinate system to UTM (Universal Transverse Mercator) co-ordinate system and finally it has been converted into corresponding latitude-longitude for setting the bathymetry.

3.11.2 Bathymetry Data Organization for set up Model

At first, the bathymetry data (primary data) has been plotted in Google earth. When plotting the data in google earth we have been shown that after every 145 number data plot in the gogle earth then when next data plot it change it's direction toward the first point. By this, we have been specified the location of starting point in our study area. This point is the indicate the zero co-ordinate (91.421522 , 21.012718).From study area we can be shown that there are 145 point e. g 145 grid point in along X direction and 101grid point in along Y direction. By plotting the latitude-longitude co-ordinate in Google earth, we have been located our region of the study area that has been shown in figure 3.9.

Figure 3.9 presents the study area which is about 86400 x 60000 metre. In this map we can see that the model area consists of a two-way using a mesh of 144 x100 grid squares with a constant grid spacing of 600 m (metre). The model has three open boundaries: The northern boundary is the Fasiakhali and the southern boundary is in the near Chowdhury para and the western Boundary is in the open sea located bay of Bengal.

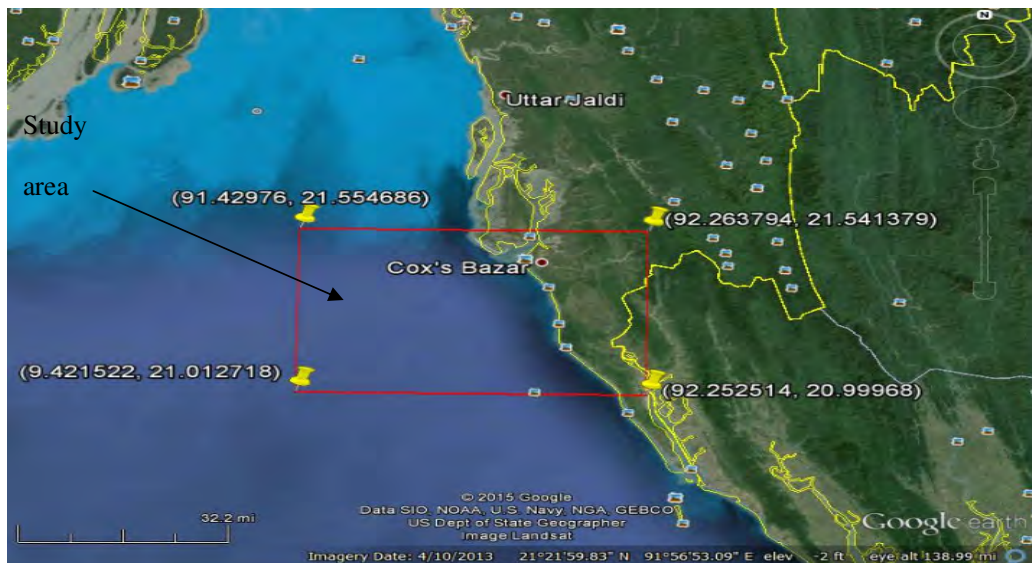


Figure 3.9: Satellite image for 2013(Source: Google Earth)

Secondly, the bathymetry data (secondary data) has been plotted in Google earth. There has been plotted sixteen (16) points, shown in Figure 3.10. These point indicates accordingly B1, B2, B3,.....B16. In figure 3.10, there has been seen that most of the point inside our study zone and rest of the points out sides of the area. All of these, there has been calculated the bathymetry data some of point such that B1, B4, B9, B11 (Figure 3.10). There has been showed that all wave height, peak wave period and wave period between 180 to 270 degree mean wave direction. For easily calculation mean wave direction divided into six quadrant e. g. every quadrant is 30 degree. Then, all data has been filtered according to every quadrant value. From these data, there has been calculated Significant wave height ($H_{1/3}$) and Significant period ($T_{1/3}$).

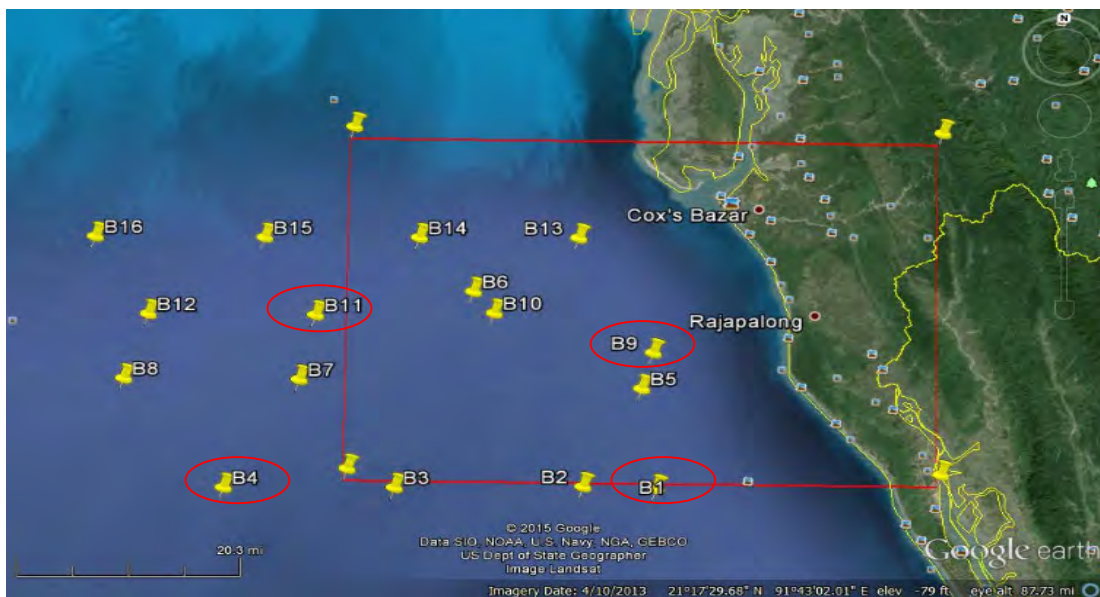


Figure 3.10: Satellite image for 2013(Source: Google Earth)

Thirdly, according to FORTRAN programme languages model the bathymetry (primary,e.g. latitude-longitude) data has been rearranged. According to rearranging latitude-longitude data the bathymetry depth data has been rearranged in Excel sheet and drawn contour map in Excel sheet for checking the orientation according to programme. Then Excel sheet data has been converted into notepad text as out grid file for suitable for run the programme.

Studies reveal that, with the influence of upper region (northern shallower areas) and the lower region (southern-western deep sea areas) of the Bay of Bengal the hydrodynamic behavior of this area has a great concern. Central part of the coastal zone can be described as the zone of transformation of the Meghna River into a wide, shallow shelf followed by a deeper basin. A number of large deltaic islands; Bhola, Hatia and Sandwip are located around the river mouth. The Meghna River falls into the Bay of Bengal through a number of channels: the Tetulia River, the Shahbazpur channel and the Hatia channel [Hossain, 2012, Azam et al., 2000]. The coast line of Bangladesh is characterized by a wide continental shelf, especially off the eastern part of Bangladesh. The triangular shape at the head of the Bay of Bengal helps to funnel the sea water pushed by the wind towards the coast and causes further amplification of the tidal levels [Hossain, 2012,].

The width of the continental shelf off the coast of Bangladesh varies considerably. It is less than 100 km off the south coast between Hiron Point and the Swatch of no ground and more than 250 Km off the coast of Cox's Bazar. Sediments are fine seaward and westward with the thickest accumulation of mud near the submarine canyon, the Swatch of no Ground. The shallow part (less than 20m) of the continental shelf off the coast of Chittagong and Teknaf is covered by sand and the intertidal areas show well-developed sandy beaches. The shallow part of southern continental shelf off the coast of the Sundarbans, Patuakhali and Noakhali is covered by silt and clay and extensive muddy tidal flats are developed along the shoreline [Hossain, 2012,].

Studies on the Bengal Deep Sea Fan suggest that the sandbars and ridges near the mouth of the Ganga-Brahmaputra delta pointing toward the Swatch of no Ground is the indication of sediments are tunneled through into the deeper part of the Bay of Bengal. Most of the sediment of the Bengal deep Sea Fan has been derived from the confluence of Ganges and Brahmaputra Rivers, which drain the south and north slopes of the Himalayan, respectively. It is concluded that low-density turbidity currents and sand cascading are perhaps dominating process of sediment transport from the shelf to the deep sea through the Swatch of no Ground under the present condition [Hossain, 2012,].

3.11.3 Setting up Model with boundary Condition

The Mathematical Model has been applied to along the nearshore of Cox's Bazar in Bay of Bengal with bathymetry data. The Model is based on FORTRAN 77 programming language [Navera, 2004]. The Model system has been developed for complex applications

with oceanographic, coastal and estuarine environments. The model simulates the water level variations and flows in response to a variety of forcing functions on flood plains, in lakes, estuaries and coastal areas. The model area is two-way nested using a mesh 144 x 100 grid squares with a constant grid spacing about 600 m. Three open boundaries such as the northern boundary is the Fasiakhali and the southern boundary is in the near Chowdhury para and the western Boundary is in the open sea located bay of Bengal.

In modeling the hydrodynamic features of along nearshore Cox’s Bazar of Bay of Bangal, it was necessary to introduce time-varying water level variations at the open seaward southern ,western boundary and also the northern boundary. The other Hydrodynamic input parameters of the model were used after trial and fine tuning, to calibrate and verify the model. The important input parameters used after trail and fine tuning for calibration and verification of model shown in table 3.1.

Table 3.1: Input Parameters used for calibration of Model

Model Input	Meaning of Parameter	Value
TIMESM	Time of simulation in hrs	0.50
HDT	Half time step in seconds	1.00
RUFFMM	Value of roughness length K(mm)	10.0
VISCMM	Kinematic viscosity of fluid (mm ² /sec)	1.31
REMIN	Minimum Reynolds number	1000
CODE	Eddy viscosity coefficient for non-uniform velocity distribution	1.0
WINDIS	Wind induced dispersion coefficient	1.4
WINDSPD	Absolute wind speed (m/s)	0
DENAIR	Density of air	1.25
DENWAT	Density of water	1026.0
DIAM50	Mean grain diameter in meters	0.0001

3.11.4 Solution technique by Finite Difference Schemes

To solve the governing differential equations for the hydrodynamic processes, the partial differential equations are replaced by finite difference equations on the computational mesh based upon Taylor's series approximation. There are three different ways to express the partial differential equation into finite difference representations such as forward, backward or centrally in space time-marching explicit solutions, where the unknown value can be calculated directly from known values without solving a matrix; and implicit solutions, where the unknown value is represented in terms of other neighboring unknowns.

There must be consistency between finite difference equation and the partial differential equation so that both equations describe the same physical phenomena. The finite difference scheme must be stable so that the cumulative effects of all round-off errors of a computer at any stage of computation are negligible and that the computed solutions only differ insignificantly from the exact solutions of the differential equation. The convergence condition relates the computed solution of the finite difference equation to the exact solution of the partial differential equation. The accuracy criterion defines the permissible magnitudes of the truncation error for a finite difference scheme.

Alternating direction implicit method a special type of finite difference scheme has been used in this model. This technique involves the sub-division of each time step into two half time steps. Thus a two-dimensional implicit scheme can be applied but considering only one dimension implicitly for each half time step without the solution of a full two-dimensional matrix. On the first half time step, the water elevation η , the U velocity component (or the unit width discharge) and the solute concentration are solved implicitly in the x-direction, whilst the other variables are represented explicitly. Similarly, for the second half time step, the water elevation η , the V velocity component (or the unit width of discharge) and the solute concentration are solved for implicitly in the y-direction, with other variables being represented explicitly. with the boundary conditions included, the resulting finite difference equations for each half time step are solved using the method of gauss elimination and back substitution.(geared and wheatly,1994)

A space staggered grid system is used, with the variables η (elevation) and S(concentration) being located at the grid Centre and with U and V at the Centre of the grid

sides as shown in the figure (3.11). The use of a staggered grid system prevents the appearance of oscillatory solutions which tend to occur in a non-staggered grid for space centered differences (fletcher, 1991). The depths are specified directly at the Centre of the grid sides so that twice as much bathymetry detail can be included as in the traditional way which gives depths at the corners.

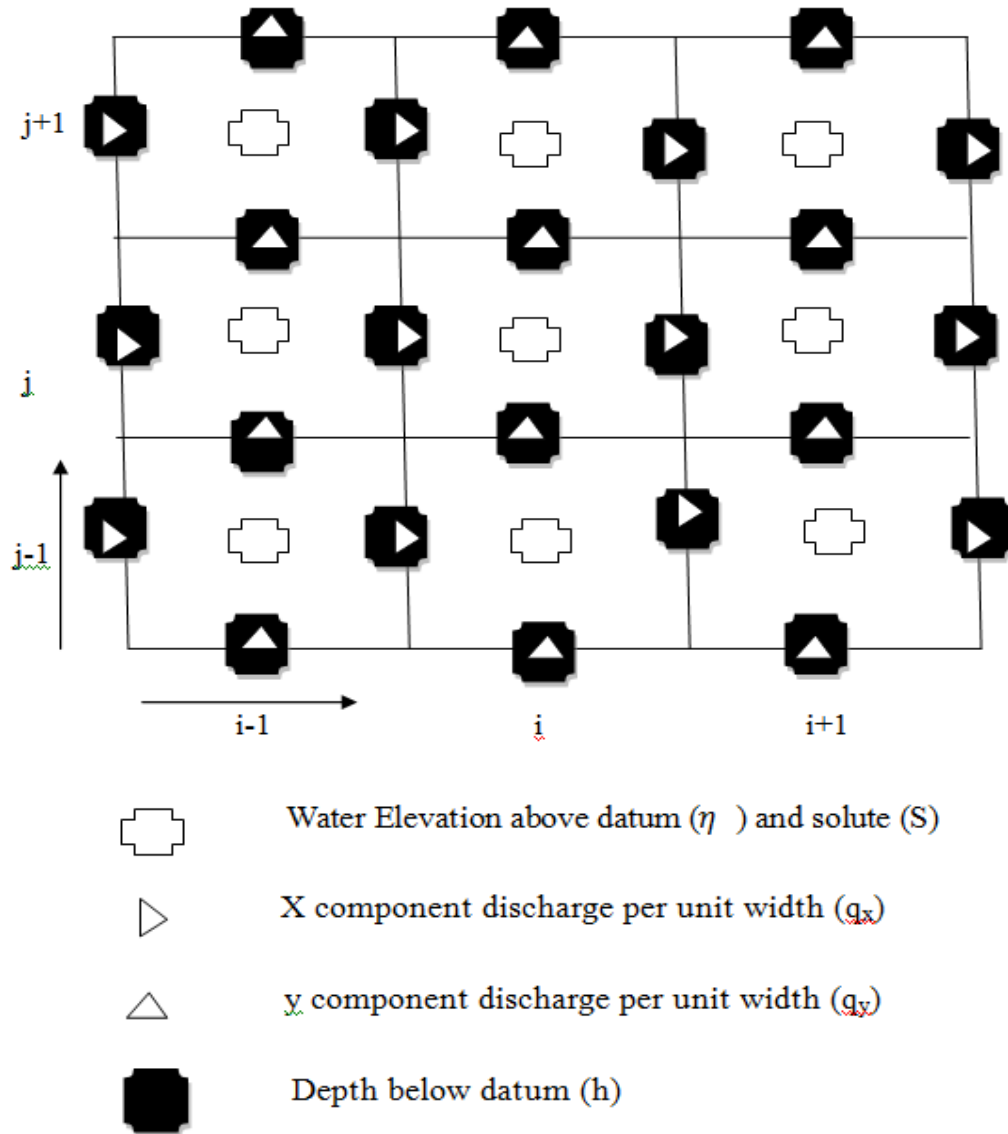


Figure 3.11: Computational space staggered grid system (Source: fletcher, 1991)

After discretization of the governing equations in time and space, a system of finite difference equations are obtained which have to be solved? however, when a three-point finite difference formula is used, the set of equations generate a tridiagonal structure for the coefficient matrix and there is a special algorithm, known as the Thomas algorithm or double sweep algorithm, or gauss elimination method for efficiently solving the set of equations which takes the advantage of the banded nature of the matrix.

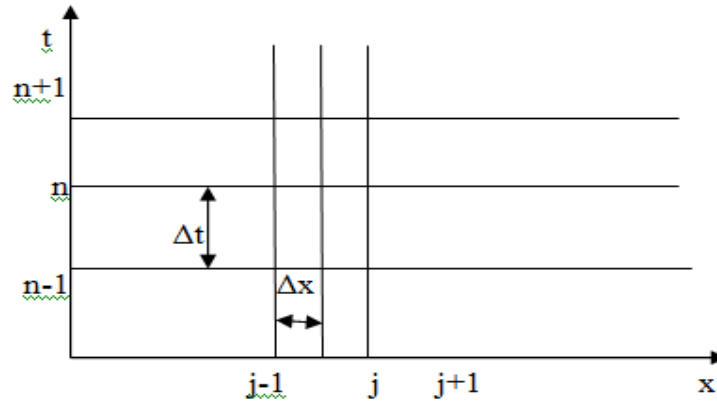


Figure 3.12: Finite difference computational grid in (x,t) plane.

For an example, considering the diffusion equation $\frac{\partial f}{\partial x} = D \frac{\partial^2 y}{\partial x^2}$ and using a three point implicit scheme to solve it. Then one will get the system of finite difference equations

$$a_j f_{j-1}^{n+1} + b_j f_j^{n+1} + c_j f_{j+1}^{n+1} = d_j \tag{3.22}$$

Where a_j, b_j, c_j and d_j ($j= 2,3,\dots,\dots, J-1$) are known and f_{j-1}^{n+1}, f_j^{n+1} and f_{j+1}^{n+1} are given as boundary conditions. For J computational points, there is a system of $(J-2)$ equations. With the two boundary conditions, the system of equations may be solved for any time step Δt . Equation (3.22),when repeated for every node, gives the matrix below

$$\begin{array}{|c|}
\hline
\begin{array}{cccc}
b_2 & c_2 & & \\
a_3 & b_3 & c_3 & \\
& a_4 & b_4 & c_4 \\
& & a_5 & b_5 & c_5 \\
& & & : & : \\
& & & : & : \\
& & & & a_{J-2} & b_{J-2} & c_{J-2} \\
& & & & & a_{J-1} & b_{J-1}
\end{array}
\end{array}
=
\begin{array}{|c|}
\hline
\begin{array}{c}
f_2^{n+1} \\
f_3^{n+1} \\
f_4^{n+1} \\
f_5^{n+1} \\
\vdots \\
f_{J-2}^{n+1} \\
f_{J-1}^{n+1}
\end{array}
\end{array}
=
\begin{array}{|c|}
\hline
\begin{array}{c}
d_2 - a_2 f_1^{n+1} \\
d_3 \\
d_4 \\
d_5 \\
\vdots \\
d_{J-1} - c_{J-1} f_J^{n+1}
\end{array}
\end{array}$$

Dropping the superscripts of the unknown quantities f, Eq. (3.22) may be written as

$$a_j f_{j-1} + b_j f_j + c_j f_{j+1} = d_j \quad 3.23$$

For j=2, Eq.(3.22) becomes,

$$a_2 f_1 + b_2 f_2 + c_2 f_3 = d_2 \quad 3.24$$

Which can be expressed as, $f_2 = \alpha_2 f_3 + \beta_2$ 3.25

$$\alpha_2 = -\frac{c_2}{b_2} \quad 3.26$$

$$\beta_2 = \frac{d_2 - a_2 f_1}{b_2} \quad 3.27$$

For j=3 Eq.(3.22) becomes,

$$a_3 f_2 + b_3 f_3 + c_3 f_4 = d_3 \quad 3.28$$

Writing similar equations for grids j= 4,5,.....,J-1, a general equation

$$f_j = \alpha_j f_{j+1} + \beta_j \quad 3.29$$

Where the recurrence relationships are defined by

$$\alpha_j = -\frac{c_j}{b_j + a_j \alpha_{j-1}} \quad 3.30$$

$$\beta_j = \frac{d_j - a_j \beta_{j-1}}{b_j + a_j \alpha_{j-1}} \quad 3.31$$

Since f_j is known from the given boundary condition, Eq(3.29) may be used successively for $j= J-1, J-2, \dots, 4, 3, 2$ to compute the values of f at the grid points. Thus, the double sweep or tridiagonal matrix algorithm for solving Eq(3.22) consists of two steps. In the first step, called the forward sweep, the coefficients α_j and β_j ($j= 2, 3, 4, \dots, J-2, J-1$) are calculated using Eqs (3.26), (3.27), (3.30) and (3.31).

In the second step, called the return or backward sweep, the values of f_j ($j= J-1, J-2, \dots, 4, 3, 2$) at the advance time level $(n+1)$ are calculated using (3.29) starting from f_j^{n+1} by back substitution.

3.11.4 Model Input Data

Reliable data are prerequisite to carry out model study. The bathymetry data has been collected from IWM. Model input data has been given below:

- Computational square mesh and bathymetry
- Boundary condition.
- Simulation of time.
- Offshore wave angle to north (Wton).
- X-axis of local grid system to north (Xton).
- Angle of latitude for domain (ANGLAT).
- Wave Height
- Wave period
- Wave angle.

3.11.5 Model Development stages

The mathematical model is a long , tedious and iterative procedure. The important steps of different modeling activities could be grouped are schematically shown in figure below.

Although the steps in figure are shown in a sequentially, in practice a number those steps may have to be conducted simultaneously. Following are the main stages:

1. Conceptualization
2. Data collection
3. Calibration
4. Validation

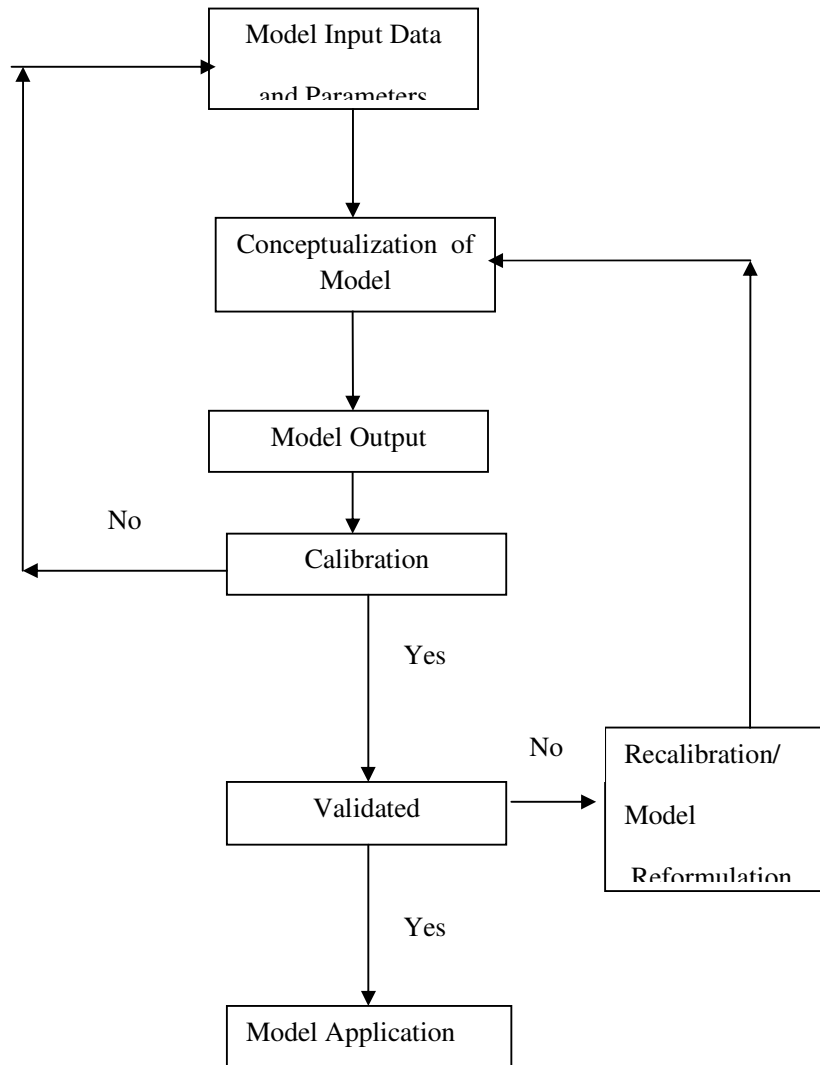


Figure 3.13: Schematic diagram of Model development stages.

3.12 Summary

The wave theories and related hydrodynamics equations required for wave height and wave period simulation have been described in this chapter. A short description has been discussed of DIVAST Model including the solution technique by finite difference scheme forming tridiagonal coefficient matrix and solution by double sweep method have also been described for study. The bathymetry of the Model of square grid size (600 m) has been generated. The model input and output including the development stages of model are also outlined for the study.

CHAPTER 4

RESULTS AND DISCUSSIONS

4.1 General

Since wave is a continuous process in the sea. But the difficulty in generating wave oscillation in a model lies with its variability in amplitude and phase. Since different constituents of wave interact among themselves. A mathematical model has been set up and applied to assessing wave velocity at several locations in the offshore and nearshore of the Cox's Bazar of Bay of Bengal. In view of that, these locations in Cox's Bazar have been chosen such as point B1 (longitude is $91^{\circ}59.209'$ and latitude $20^{\circ}58.793'$), point B4 (longitude is $91^{\circ}14.895'$ and latitude $20^{\circ}59.071'$), point B9 (longitude is $91^{\circ}51.053'$ and latitude $21^{\circ}15.303'$), and point B11 (longitude is $91^{\circ}22.571'$ and latitude $21^{\circ}15.290'$) which has been located out of study zone. The set of bathymetry data has been split into two parts. The one part is used for calibration and other part is used for verification of the model. The detail of the data analysis and results of the model is discussed in the following sections.

4.2 Study Area

The coastal areas of Bangladesh are different from rest of the country because of its unique geo-physical characteristics and vulnerability to several natural disasters like cyclone, storm-surges, erosion and accretion etc. Natural hazards are increasing with frequency and intensity along the coast of Bangladesh with the changes of global climate. These extreme natural events are termed as disasters when they adversely affect the whole environment including human beings, their shelters or the resources essential for their livelihoods [Hossain, 2012].

Wave in Bangladesh coast originates in India Ocean. It enters the Bay of Bengal through the two submarine canyons, the 'Swatch of No Ground' and the 'Burma Trench' and thus arrives very near to the 10 fathom contour line at Hiron Point and Cox's Bazar respectively at about the same

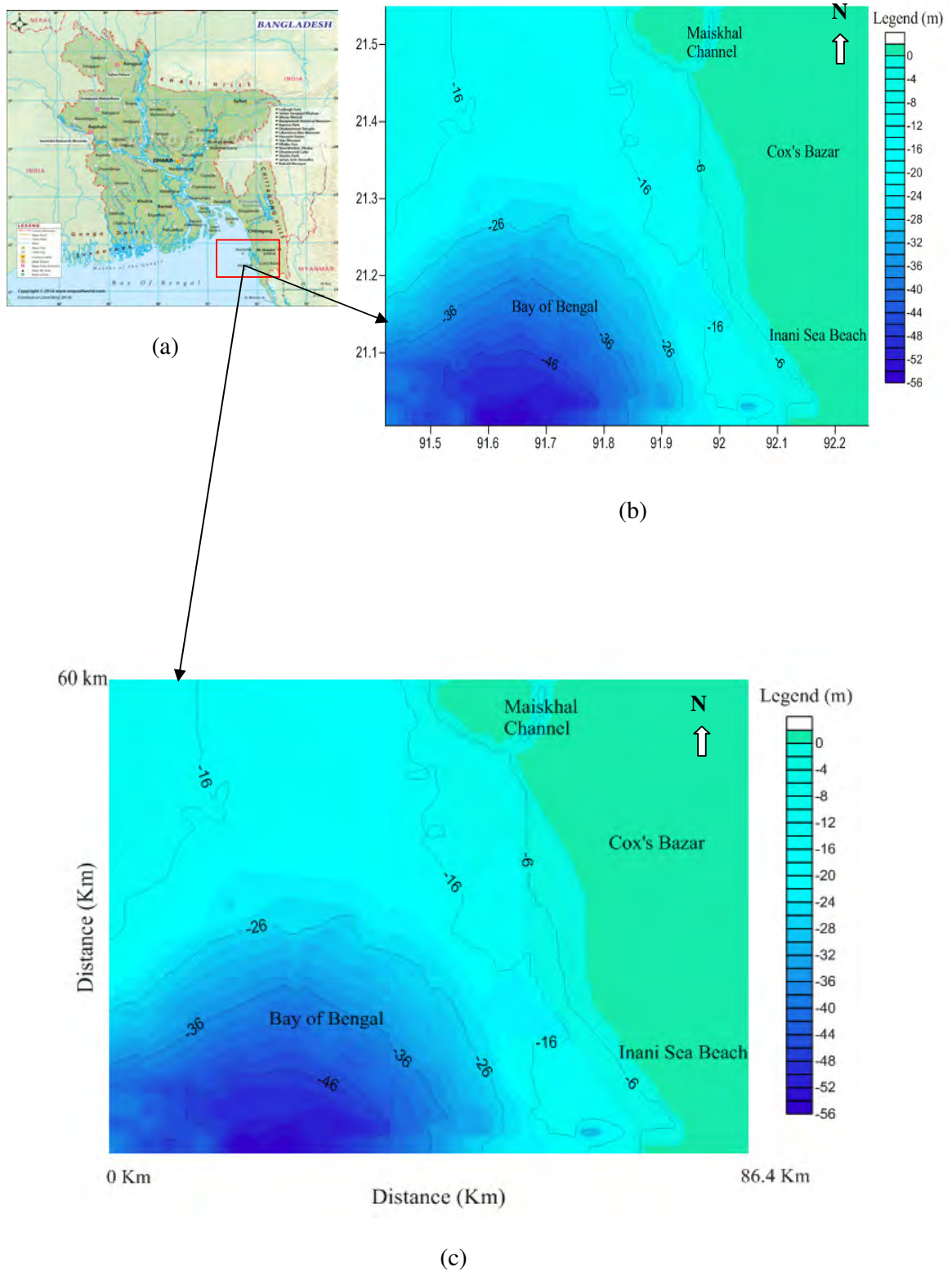


Figure 4.1: (a) Study area in localation in Bangladesh (source: mapsofworld, 2015);
 (b) study area in Latitude & longitude (c) study area in Kilometers.

The study area which has been located in the bay of Bengal near the Cox,s Bazar. The study area has been set up based on data of Cox’s bazar from Maishkhal channel to Inani Sea beach of Bay of Bengal. In Figure 4.1 has been shown the study area.

A wave has been travelling from deep water to shallow water due to gradients (spatial differences in surface level) in the water surface. As water always flows to the lowest point, these gradients are the cause of wave or tidal flows. Just like tidal wave, this flow is periodical and changes from flood when the flow is directed upstream towards land to ebb when the flow is directed back towards the sea.

4.3 Selection of Different Hydrodynamic Condition

The secondary bathymetry data (wave height, Peak wave period, wave period and wave direction) has been collected for location at sixteen points. These data has been collected from IWM, BWDB and BMD. The data has been collected from 01/01/2004 to 31/08/2013. From these data there has been selected two points. At first the data has been generated according to wave direction. The bathymetry data has been arranged according to wave direction range 0 to 90 degree, 90 to 180 degree, 180 to 270 degree, 270 to 360 degree. Then the data again rearrange according to range 180 to 210 degree, 210 to 240degree, 240 to 270 degree, 270 to 300 degree. There has been taken the wave direction range 210 to 240 degree, 240 to 270 degree and 270 to 300 degree. For every point there has been calculated mean wave height, mean wave period, maximum wave height, maximum wave period, significant wave height and significant wave period for different range of wave direction.

Case 1: Boundary condition generated with the data within study area

In this case point B1 has been selected. Its location is at latitude: 20°58.793´ and Longitude: 91°59.209´. It is located in the study area Shown in Figure 4.2.The model has been run different condition such as different wave direction, significant height and significant wave period. Table 4.1 is shown the total condition for run the program.

Table 4.1: The total condition for run the program for case 1

Wave Direction With North (degree)	Significant Wave Height, H_s (m)	Wave Period, T_s (sec)
230	2.09	13.7
240	1.19	14.2
250	1.19	14.2
260	1.19	14.2
270	1.28	13.8
280	1.28	13.8
290	1.28	13.8

Case 2: Boundary condition generated with the data from deep sea

In this case point B11 has been selected. Its location is at latitude: $21^{\circ}15.290'$ and Longitude: $91^{\circ}22.571'$. It is located out of the study area Shown in Figure 4.2. The model has been run different condition such as different wave direction, significant height and significant wave period. Table 4.2 is shown the total condition for run the program.

Table 4.2: The total condition for run the program for case 2

Wave Direction With North (degree)	Significant Wave Height, H_s (m)	Wave Period, T_s (sec)
230	1	11.9
240	1.59	11.7
250	1.59	11.7
260	1.59	11.7
270	1.13	14.1
280	1.13	14.1
290	1.13	14.1

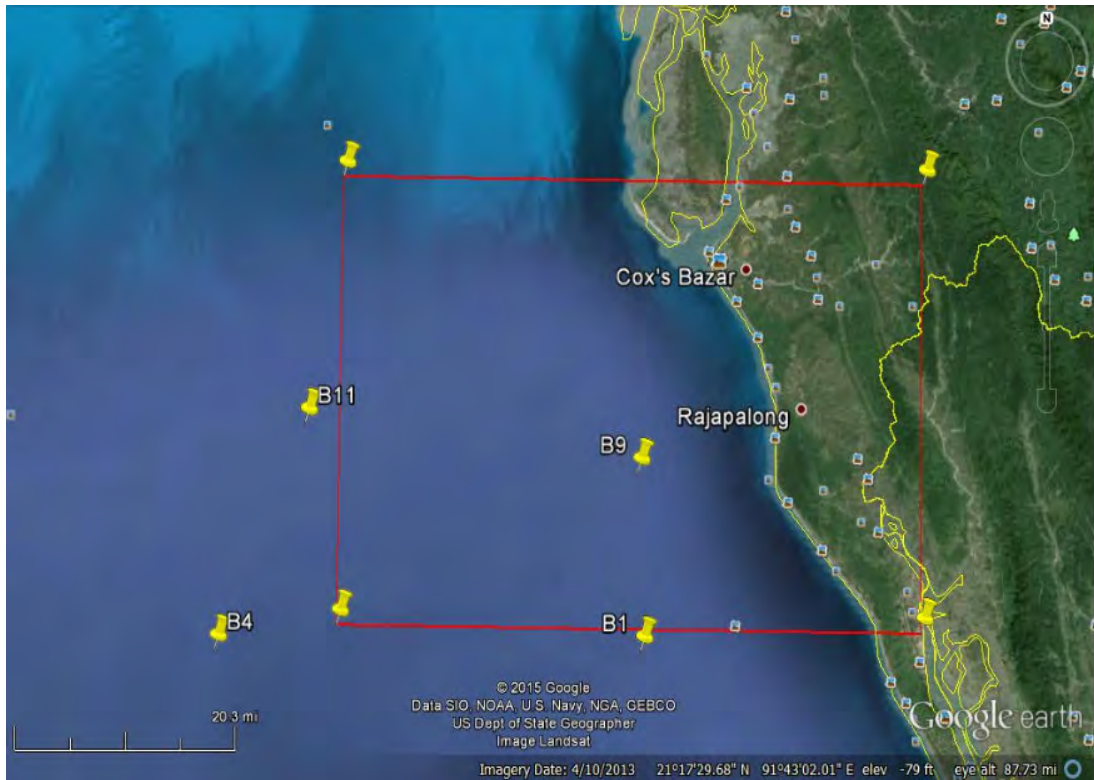


Figure 4.2: The satellite image for 2013 [Source: Google earth].

4.4 Calibration

Model parameters require adjustment due to a number of reasons. Due to insufficient data and in reality it may not be possible to directly measure the data. The model calibration has been accomplished using maximum wave height data for every month i.e. twelve months of the year 2011 for location point B4 at Bay of Bengal. The wave height data for 2011 has been collected from IWM. All maximum wave height for every month is given below the table.

Table 4.3: The maximum wave height for Year 2011

Location Point	Month	Maximum Wave Height, (m)
B4 (long:91°14.895' and lat: 20°59.071')	January	1.69118
	February	1.74796
	March	1.92816
	April	2.0116
	May	2.78699
	June	6.11651
	July	4.05767
	August	4.43043
	September	3.44166
	October	4.04875
	November	1.48766
	December	2.05247

The model is capable to generate the wave height for wave where each wave height is taken every 2 hrs. So the time of simulation of the model is set up for every month of the year 2011. The time step of 60 seconds is considered to ensure the stability of the numerical scheme. The model has attained stability by maintaining the Courant number ($g^{1/2}h^{1/2}\Delta t/\Delta s$) less than or equal to 1, in which Δt is the computational time step (=60 s) and Δs is the grid spacing of 600 m. Hydrodynamic model calibration has been done by fine tuning the important variable input parameters of higher sensitivity like: Minimum Reynolds number (=1000), water temperature in degree centigrade (=10), wind speed (=0 m/s).

As the model area is considerably big and model has the option of selecting only one type grid size for simulating the wave height so that each grid size of model is considered as 600 m based on coarse grid size of bathymetry data from IWM. Again the problems in

taking small grid size over the whole area are (i) the number of grid points increases tremendously and thus increases the computer overhead and (ii) smaller grid size requires smaller time steps to ensure the Courant-Friedrichs-Lewy (CEL) stability criterion.

4.4.1 Calibration Results

Hydrodynamic model calibration has been accomplished against wave height at location point B4 but date and time are different according to the availability of measured wave height data. The output wave height for 12 month of the year 2011 of the model are compared with the measured maximum wave height at the location and is shown in Figure 4.3. From Table 4.3 and Figure 4.3 it is found that maximum wave height measurement starts at every month of the year. Both the measured and output maximum wave height of this time period at the location is very close and similar in wave height pattern with each other and have insignificant percentage of deviation. Analyzing the above mentioned graph it is found that, the output maximum wave height for every month and corresponding measured maximum wave height for every month which is very similar and close. The graphical representation of both output and measured maximum wave height at Figure 4.3 shows excellent result.

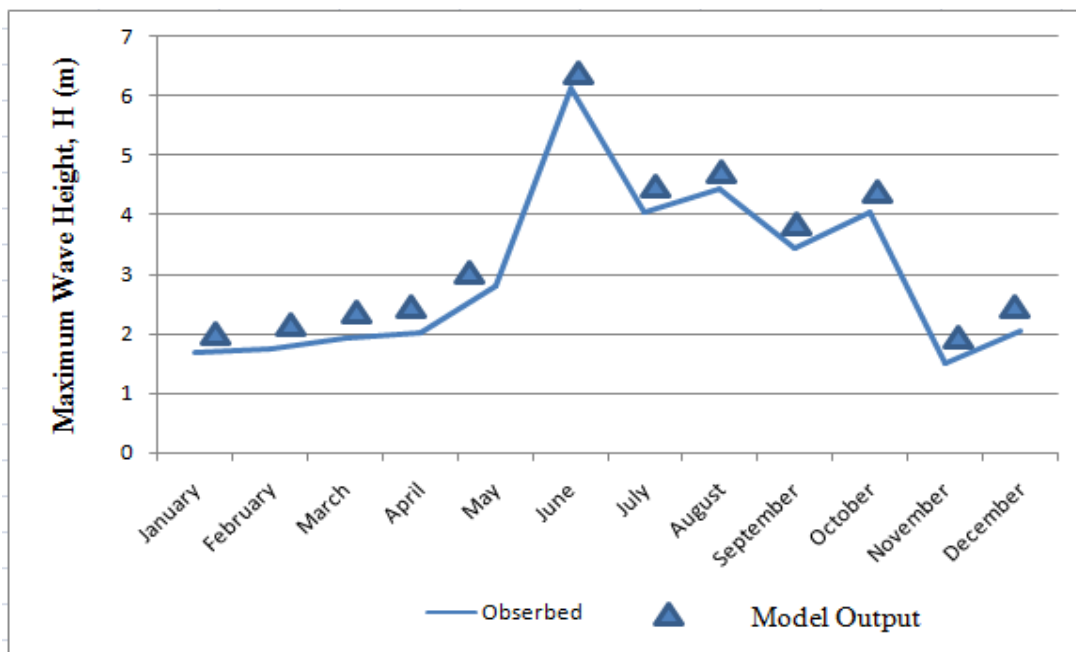


Figure 4.3: The maximum wave height for every month of the year 2011 Calibration at location point B4.

4.5 Verification

The model verification has been accomplished maximum wave height data for every month i. e twelve month of year 2012 for location at point B9 in Bay of Bengal. The wave height data for 2012 has been collected from IWM. All measured maximum wave height for every month is given below the table. The model is capable to generate the wave height for wave where each wave height is taken every 2 hrs. So the time of simulation of the model is set up for every month of the year 2012.

For the purpose of verification and analysis the output result of maximum wave height is compared with the measured measured maximum wave height at the location and has been discussed with the figure.

Table 4.4: The maximum wave height for Year 2012

Location Point	Month	Maximum Wave Height, (m)
B9 (long:91°51.053' and lat: 21°15.303')	January	1.74234
	February	1.58497
	March	3.03338
	April	2.32519
	May	2.0558
	June	3.97288
	July	3.29691
	August	2.85047
	September	3.46621
	October	2.68346
	November	1.53691
	December	1.35894

4.5.1 Verification Results

Hydrodynamic model verification has been accomplished against wave height at location point B4 but date and time are different according to the availability of measured wave height data. The output wave height for 12 month of the year 2012 of the model are compared with the measured maximum wave height at the location and is shown in Figure 4.4. From Table 4.4 and Figure 4.4 it is found that maximum wave height measurement

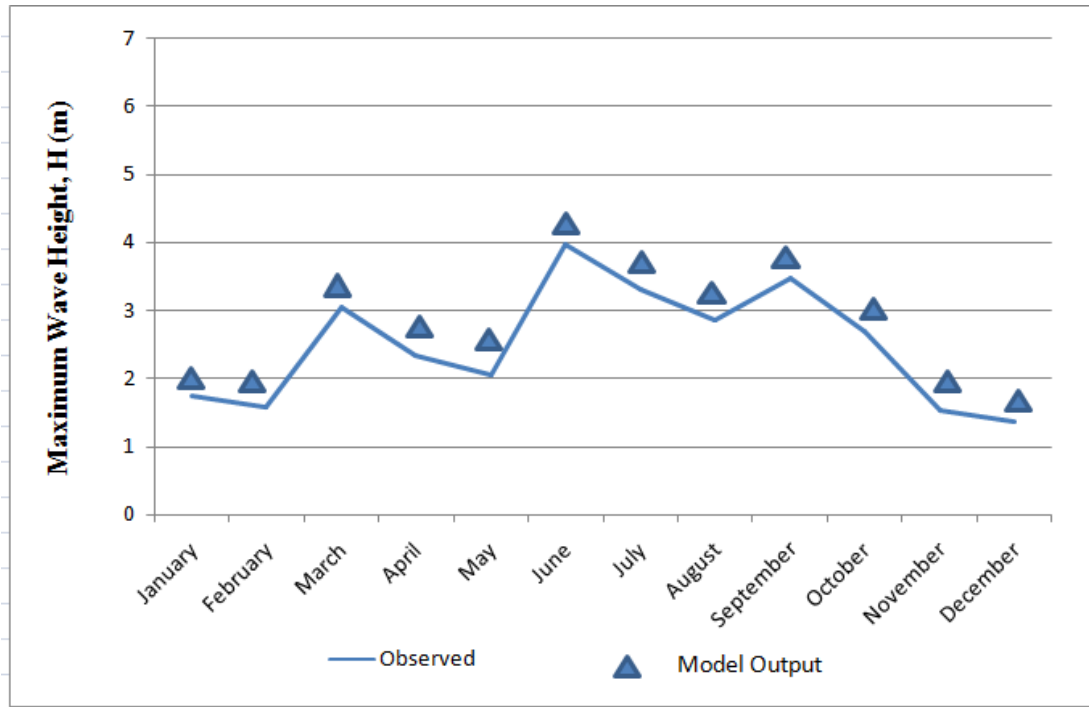


Figure 4.4: The maximum wave height for every month of the year 2012 Calibration at location point B9.

starts at every month of the year. Both the measured and output maximum wave height of this time period at the location is very close and similar in wave height pattern with each other and have insignificant percentage of deviation. Analyzing the above mentioned graph it is found that, the output maximum wave height for every month and corresponding measured maximum wave height for every month which is very similar and close. The graphical representation of both output and measured maximum wave height shows at Figure 4.4.

4.5 Results

A wave travelling from deep sea through the nearshore causes gradients (spatial differences in surface level) in the water surface. As water flows to the lowest point, these gradients are the cause of wave velocity flows observed in the coast. The sediment distribution in the nearshore is mainly governed by the magnitude and net flow direction of the wave flow. Erosion and accretion along the banks and shorelines of coast are very much related to the flow velocities dominated by wave.

The velocity profile for Case 1:

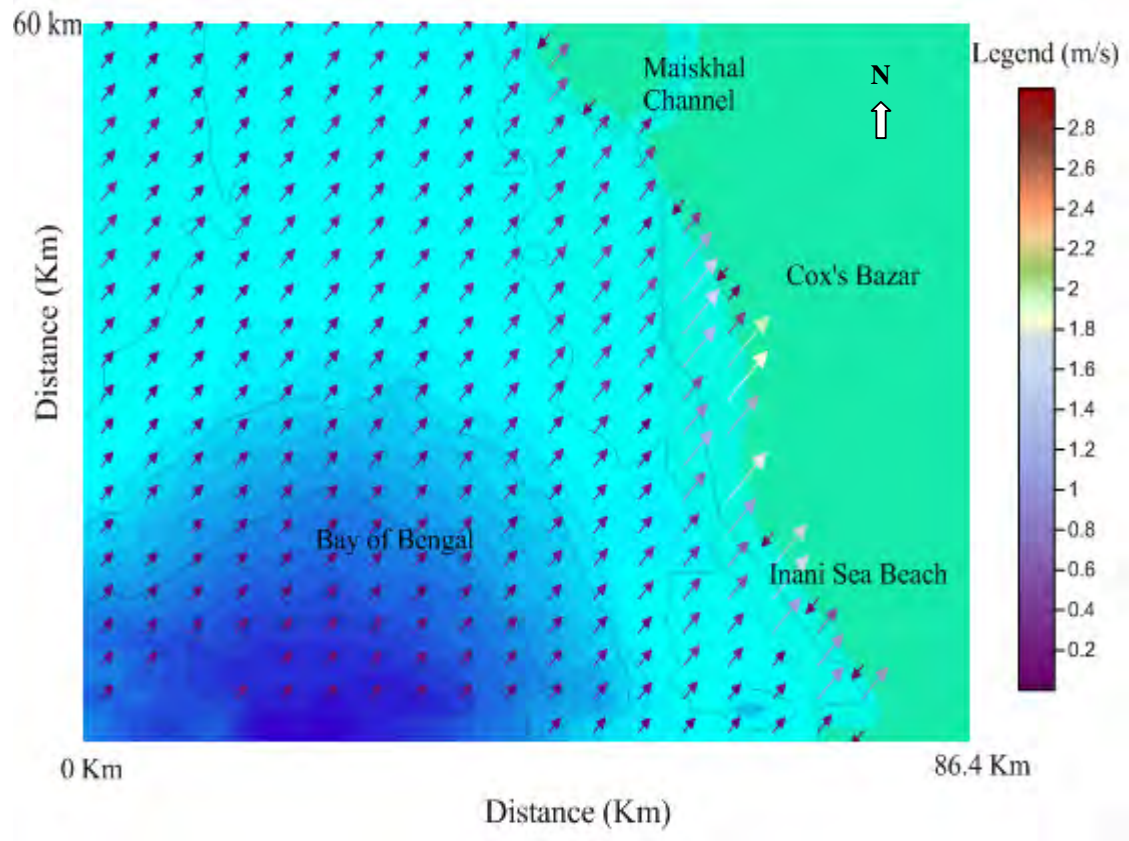


Figure 4.5: Velocity profile for incoming wave angle 230° with North

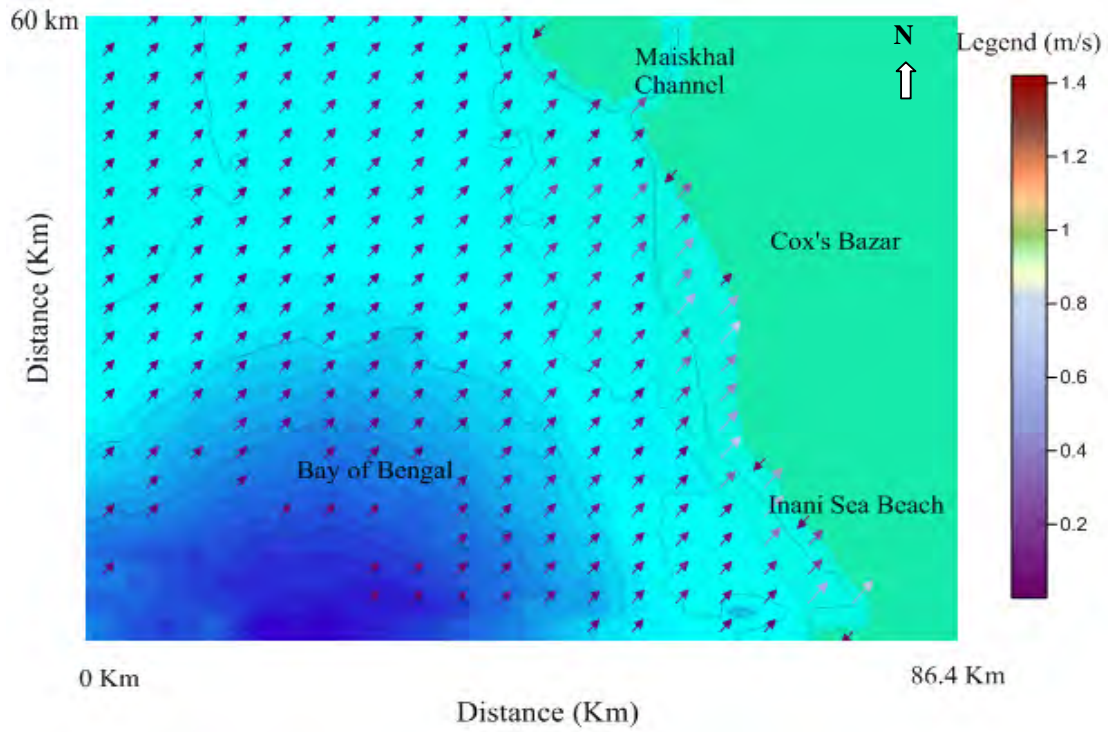


Figure 4.6: Velocity profile for incoming wave angle 240° with North

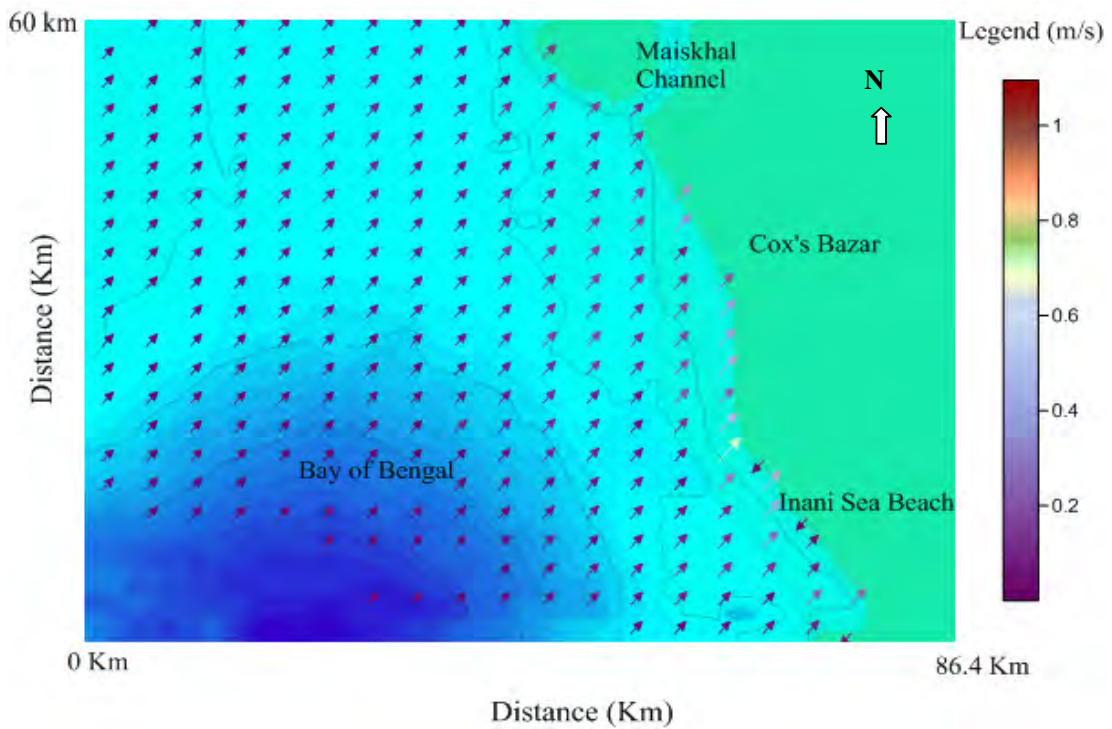


Figure 4.7: Velocity profile for incoming wave angle 250° with North

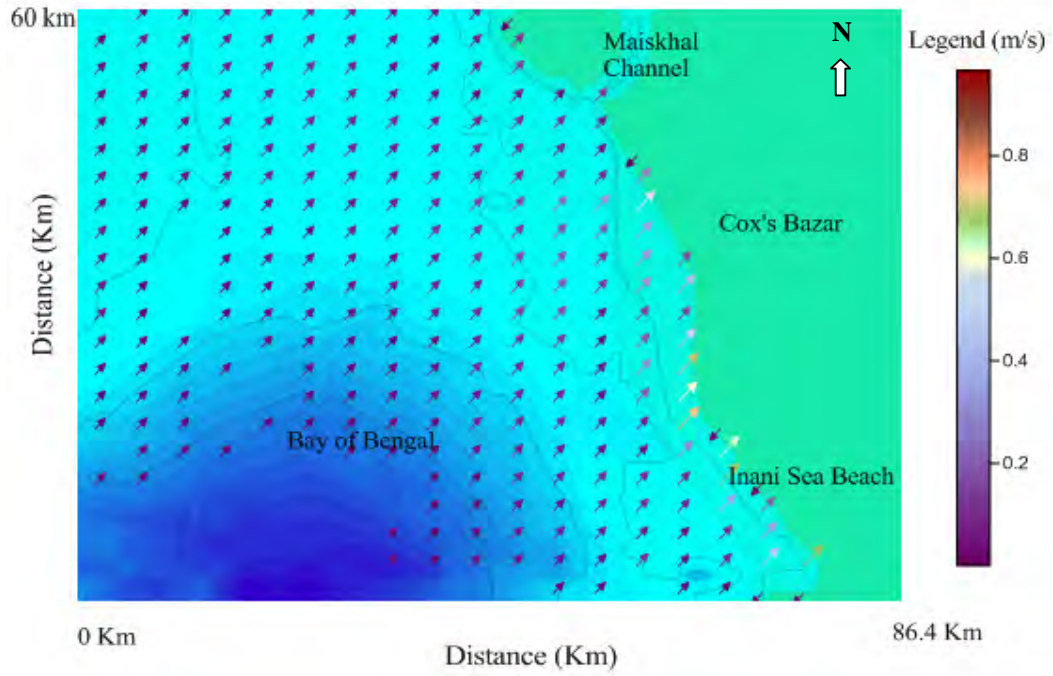


Figure 4.8: Velocity profile for incoming wave angle 260° with North

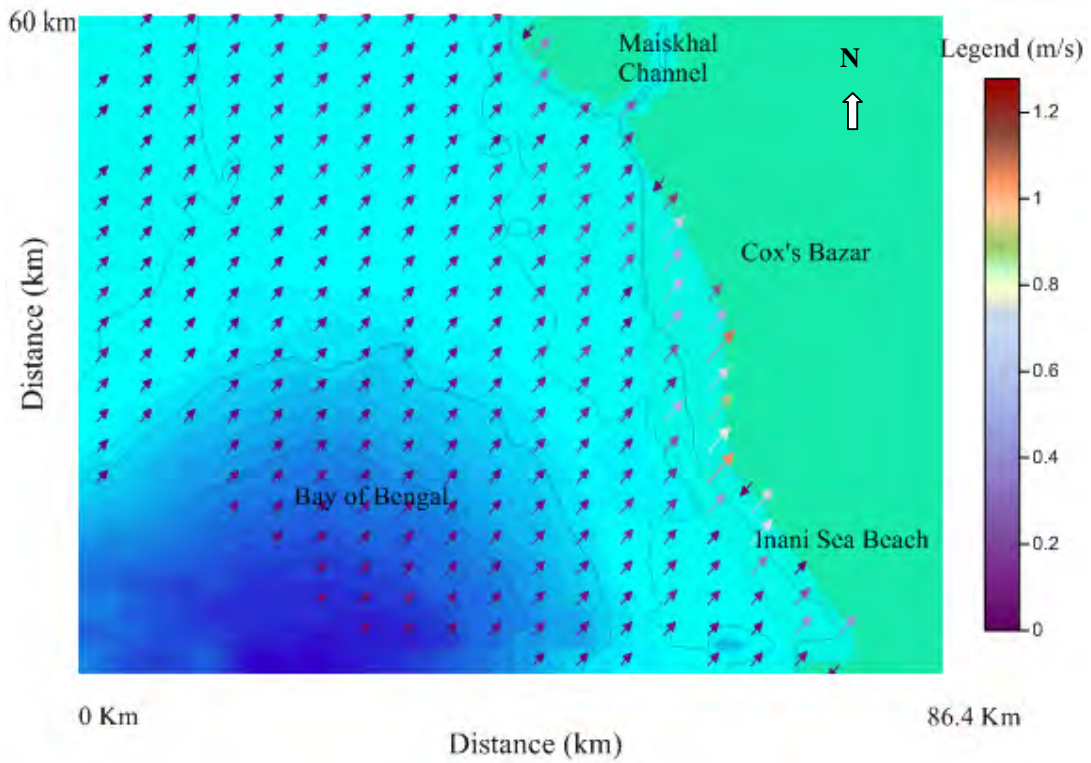


Figure 4.9: Velocity profile for incoming wave angle 270° with North

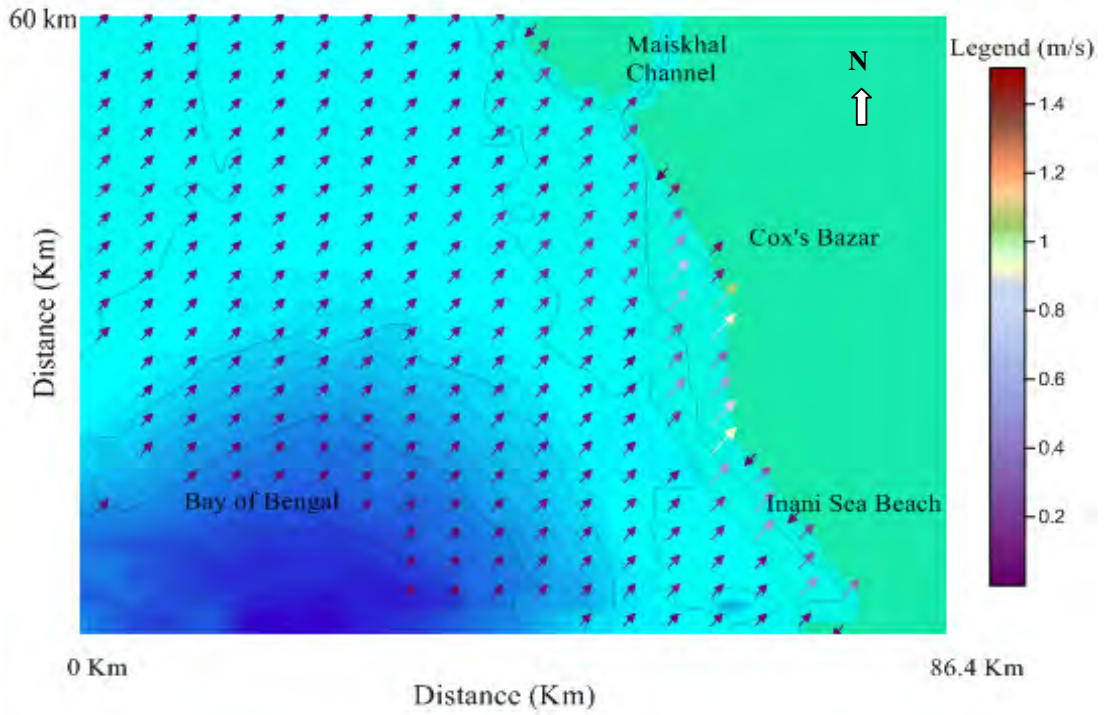


Figure 4.10: Velocity profile for incoming wave angle 280° with North

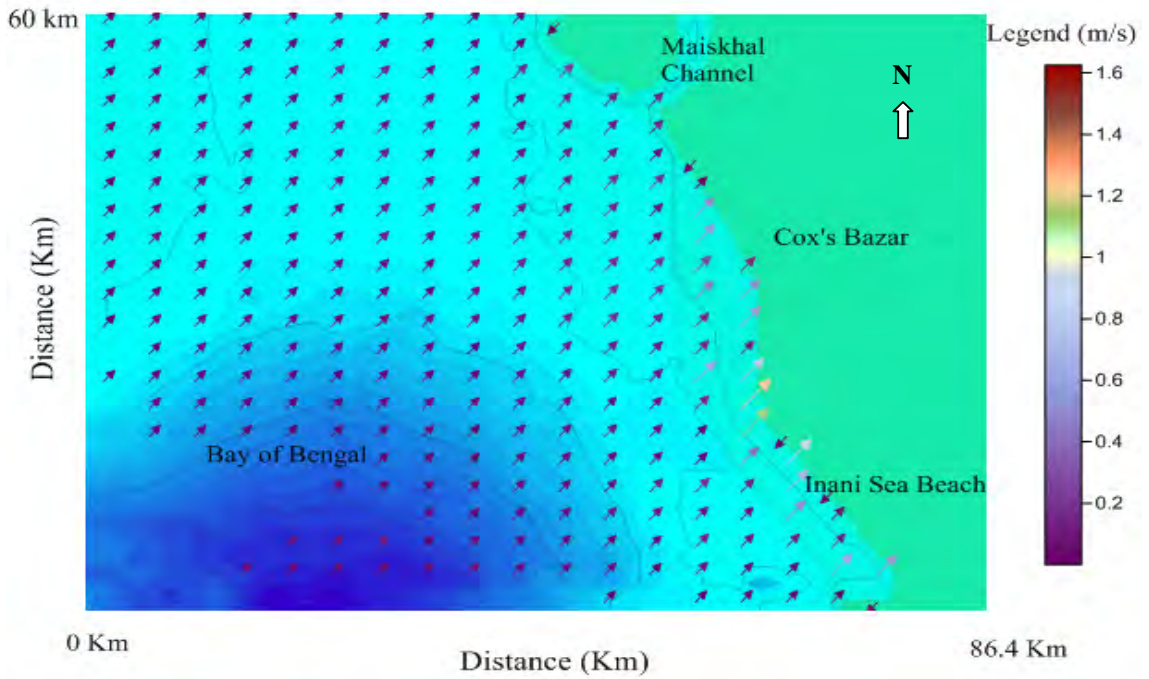


Figure 4.11: Velocity profile for incoming wave angle 290° with North

The velocity profile for Case 2 :

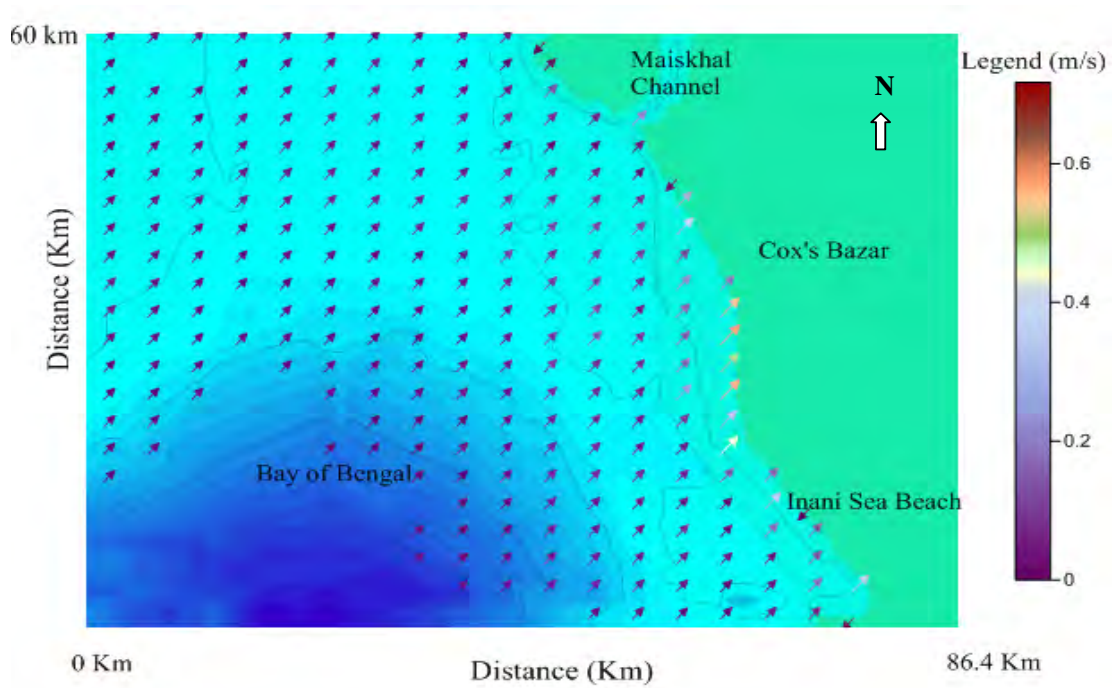


Figure 4.12: Velocity profile for incoming wave angle 230° with North

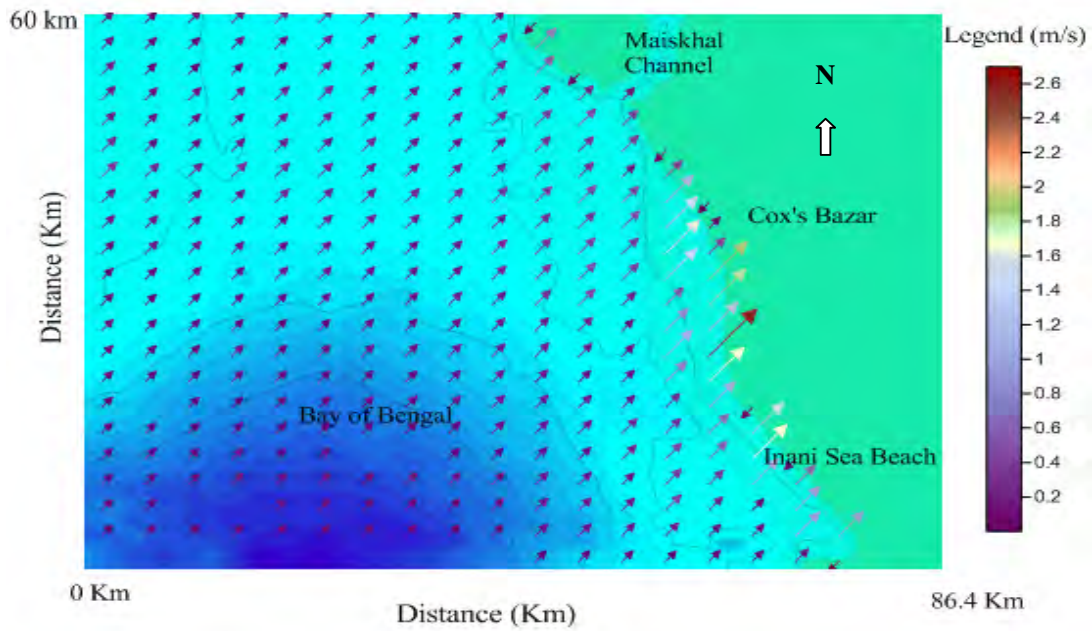


Figure 4.13: Velocity profile for incoming wave angle 240° with North

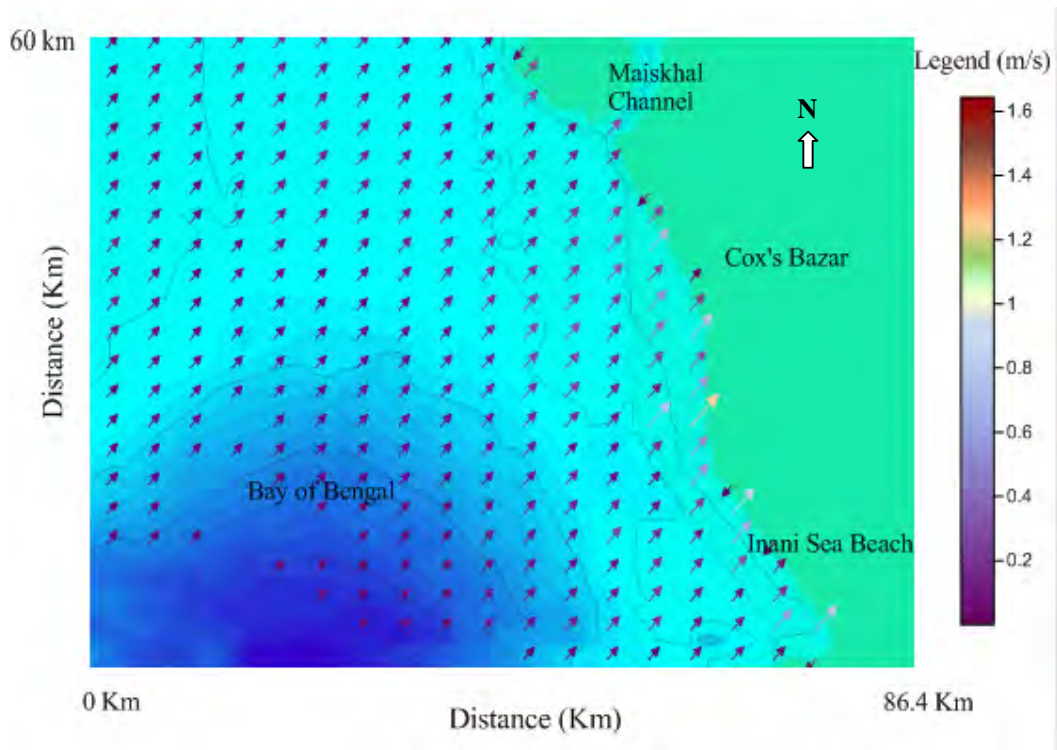


Figure 4.14: Velocity profile for incoming wave angle 250° with North

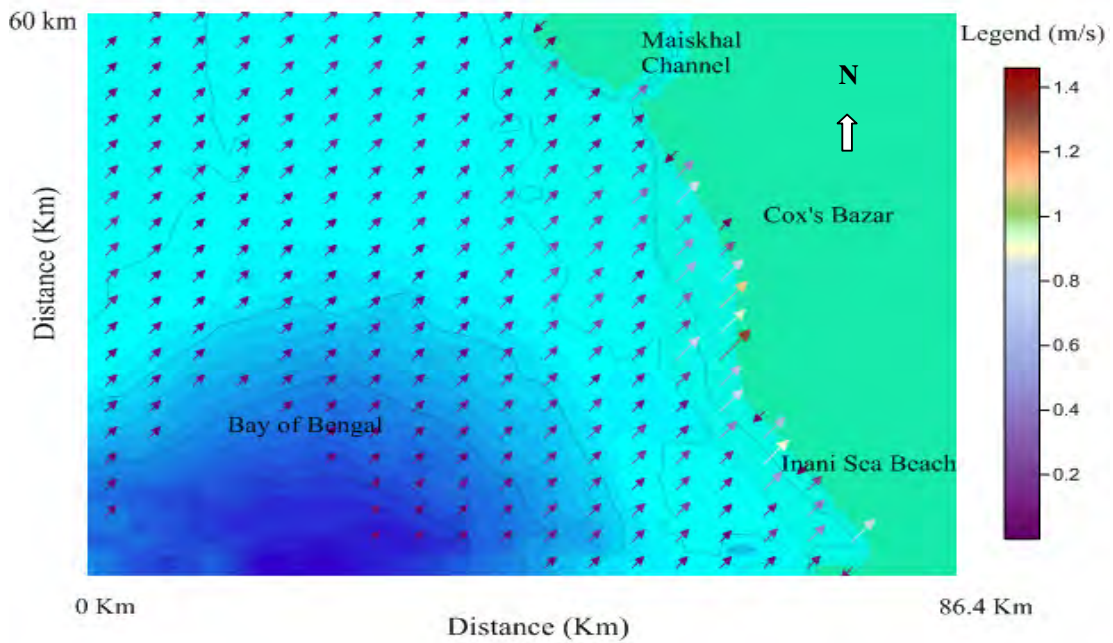


Figure 4.15: Velocity profile for incoming wave angle 260° with North

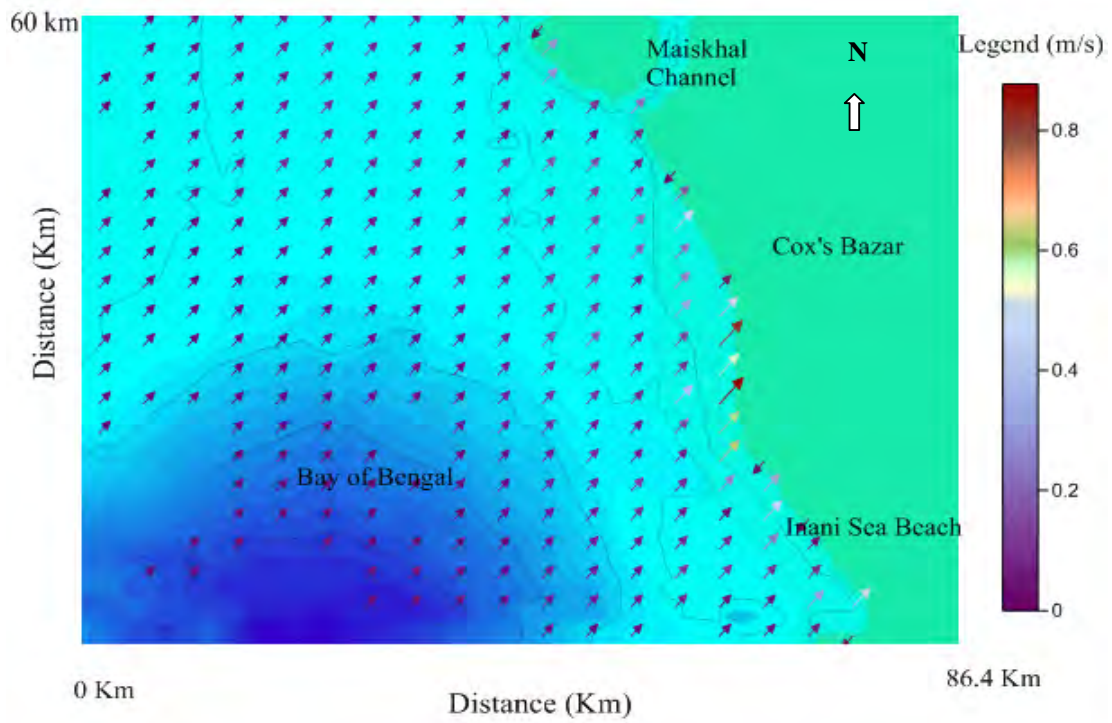


Figure 4.16: Velocity profile for incoming wave angle 270° with North

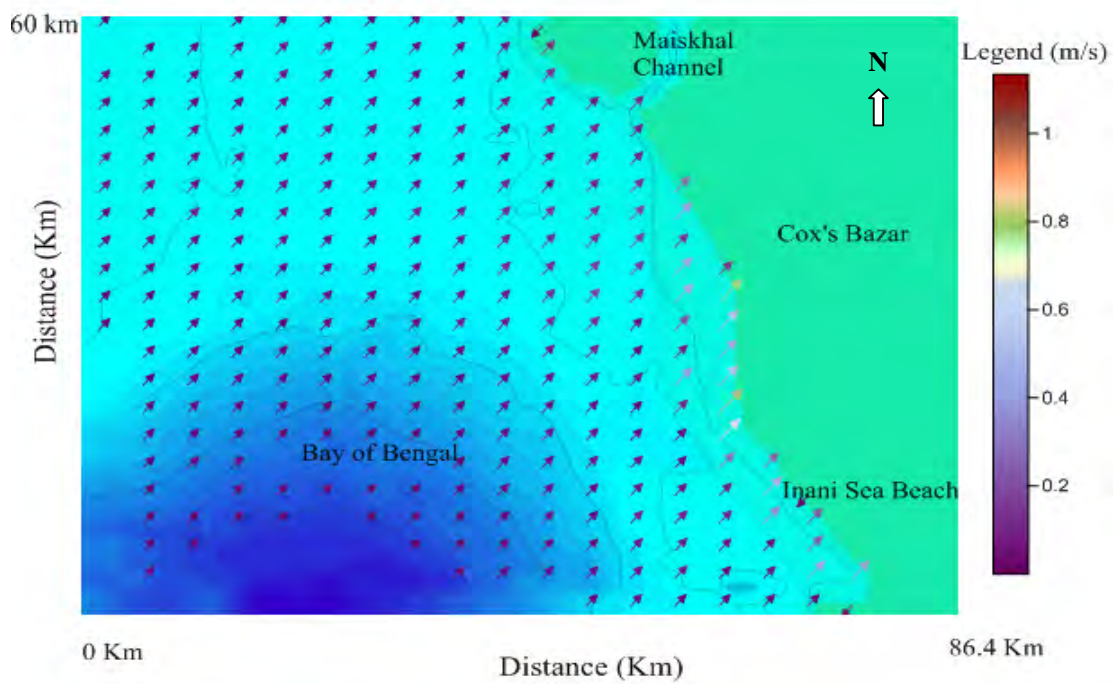


Figure 4.17: Velocity profile for incoming wave angle 280° with North

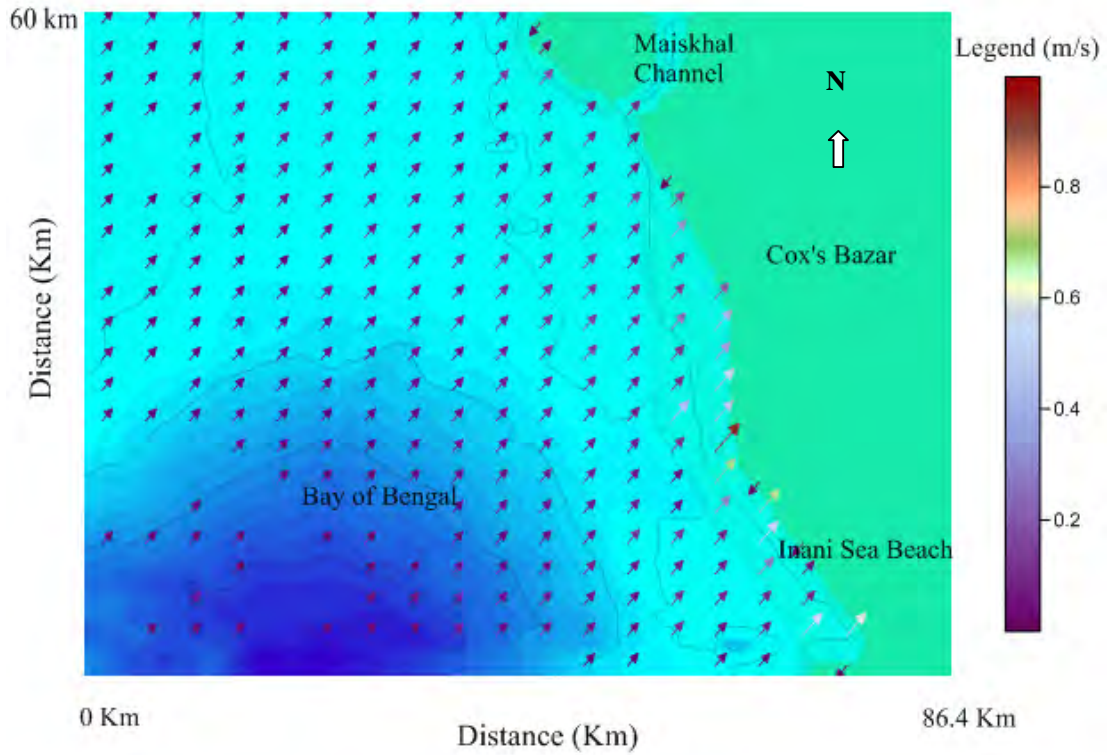


Figure 4.18: Velocity profile for incoming wave angle 290° with North.

The velocity profile over the model domain for different wave direction for different cases generated by DIVAST model are shown from Figure 4.5 to 4.18 respectively. It is observed from the velocity profile that for different wave direction the change the magnitude of the maximum velocity. It also shown that for different wave angle but same significant wave height and significant wave period the magnitude of maximum velocity shows different.

The celerity (C) and group velocity (Cg) profile for Case 1 :

Figure 4.19 has been shown the section A-A.

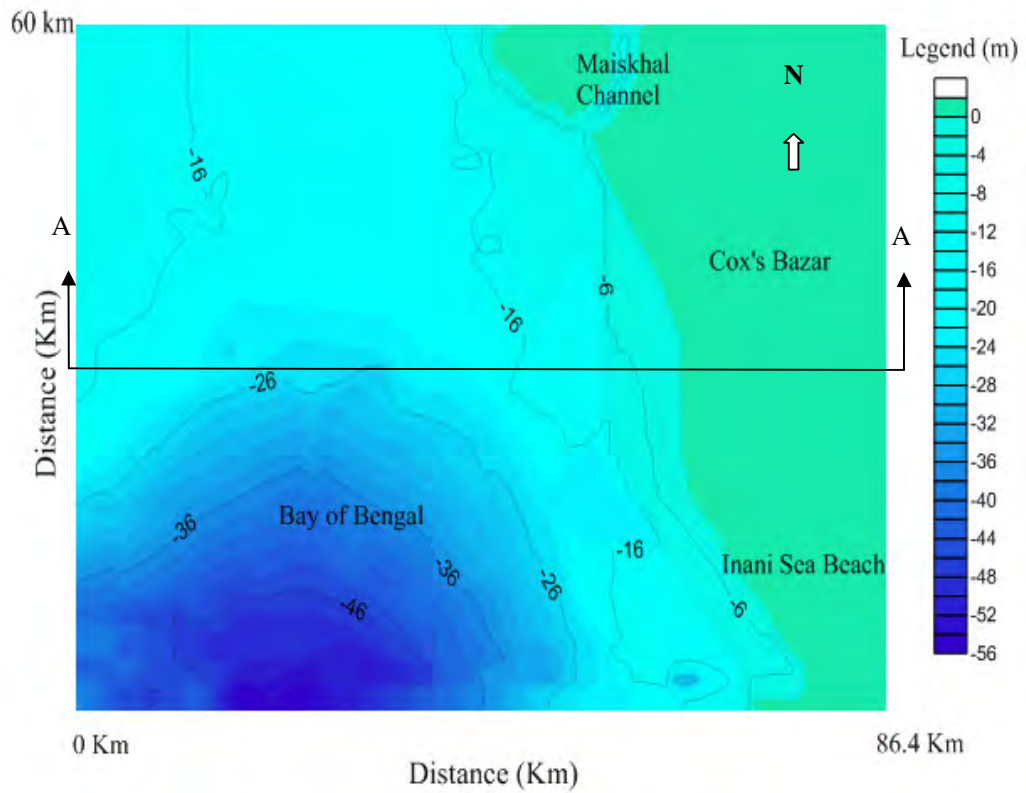


Figure 4.19: Study area with section A-A.

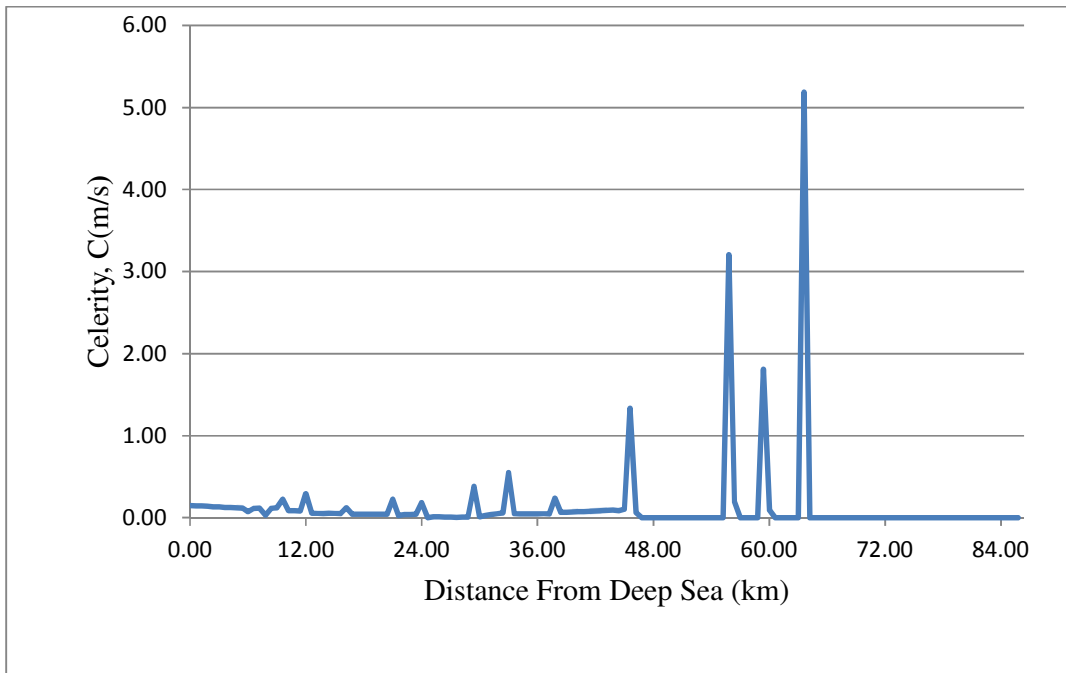


Figure 4.20: Celerity (C) for incoming wave angle 230° with north for section A-A

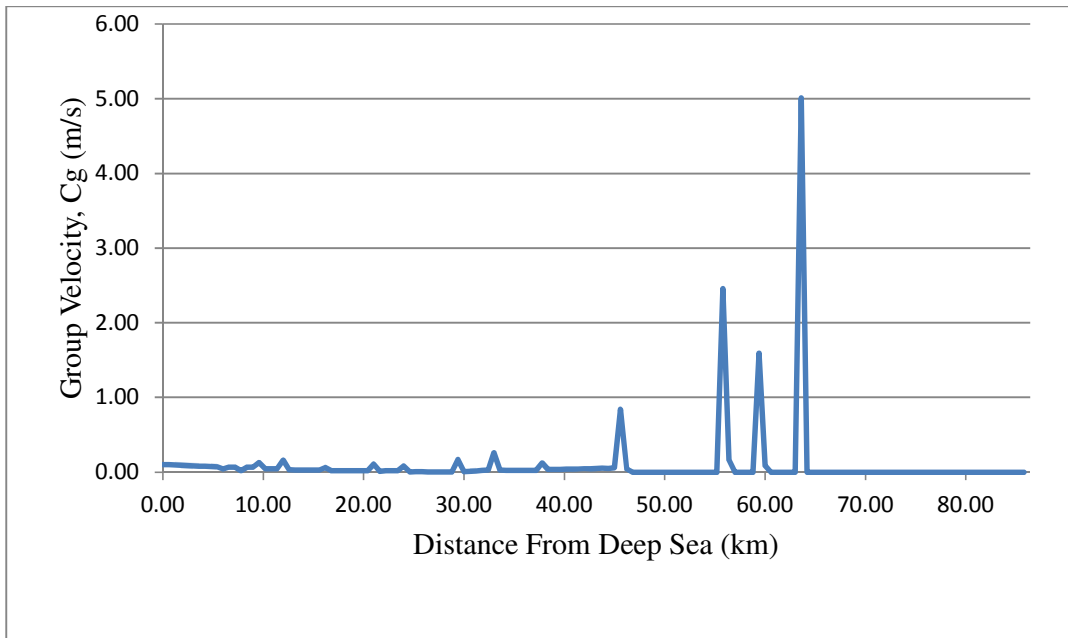


Figure 4.21: Group velocity (C_g) for incoming wave angle 230° with north for section A-A

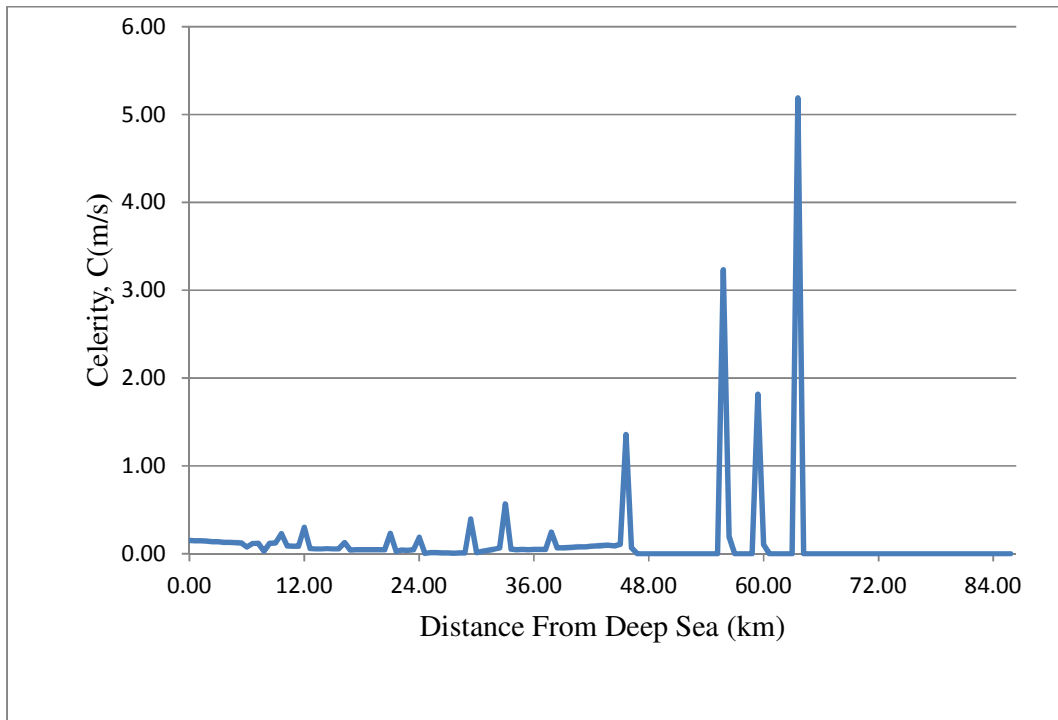


Figure 4.22: Celerity (C) for incoming wave angle 240° with north for section A-A

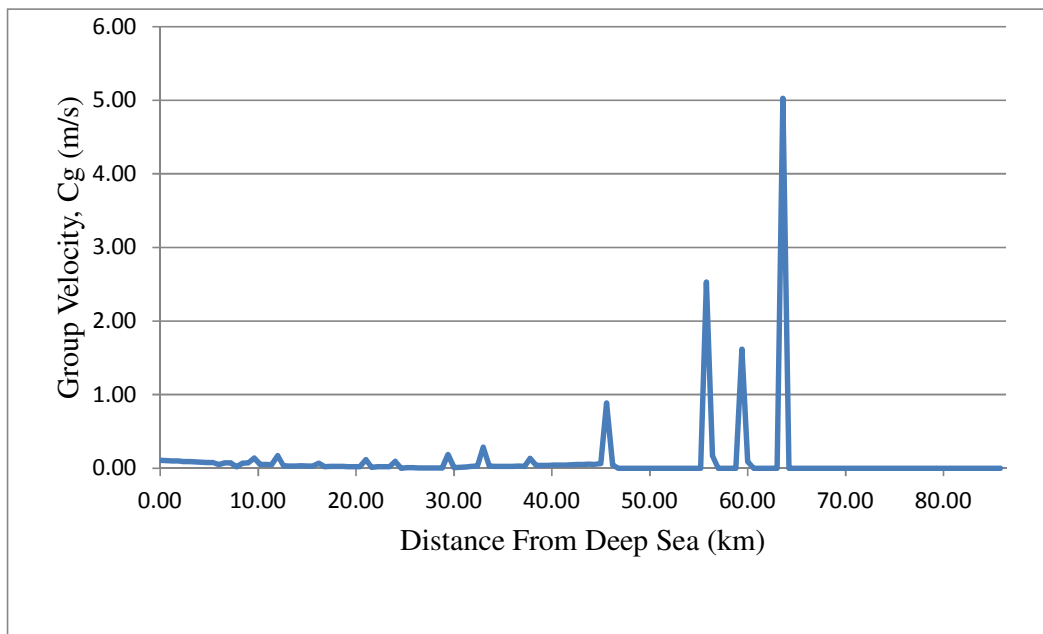


Figure 4.23: Group velocity (Cg) for incoming wave angle 240° with north for section A-A

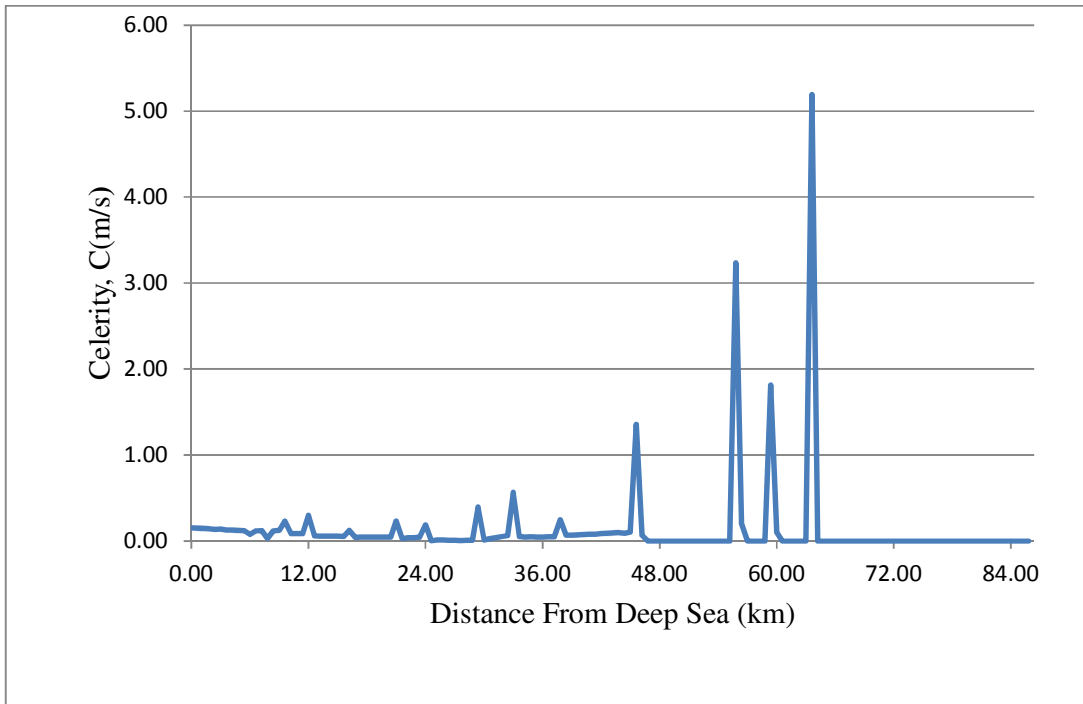


Figure 4.24: Celerity (C) for incoming wave angle 250° with north for section A-A

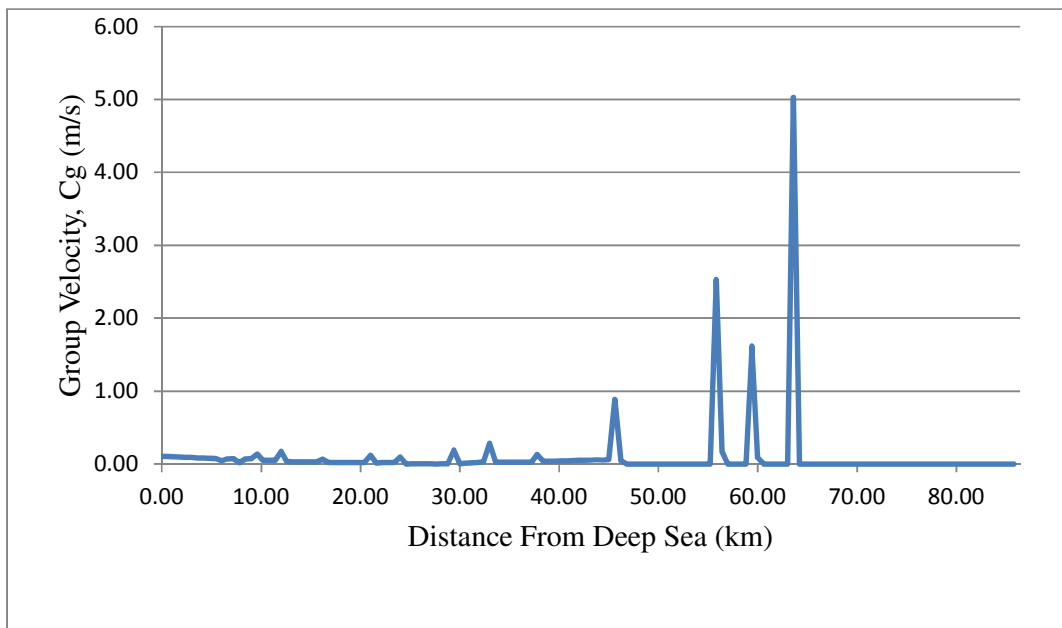


Figure 4.25: Group velocity (Cg) for incoming wave angle 250° with north for section A-A

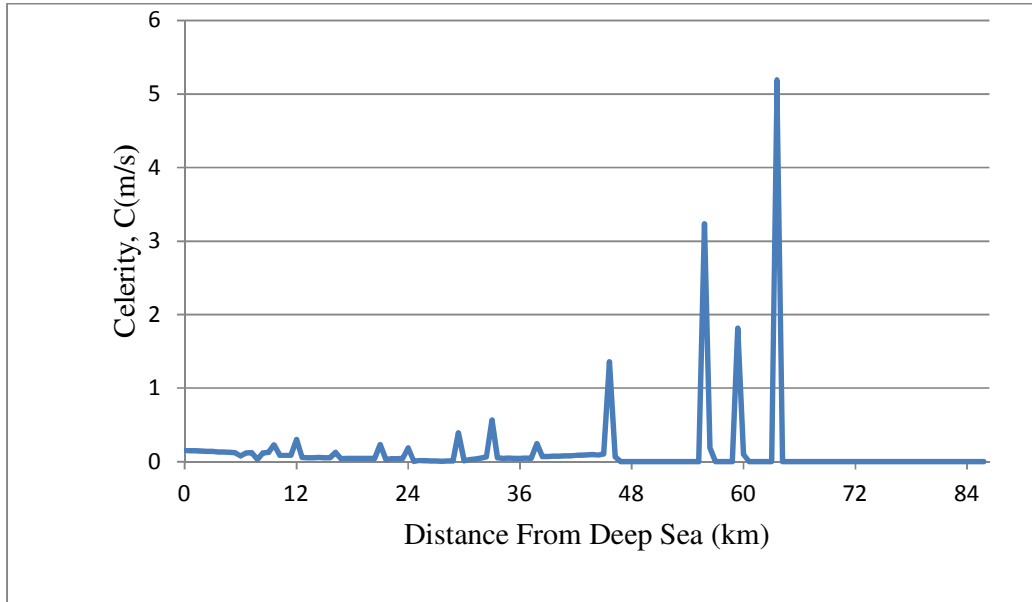


Figure 4.26: Celerity (C) for incoming wave angle 260° with north for section A-A

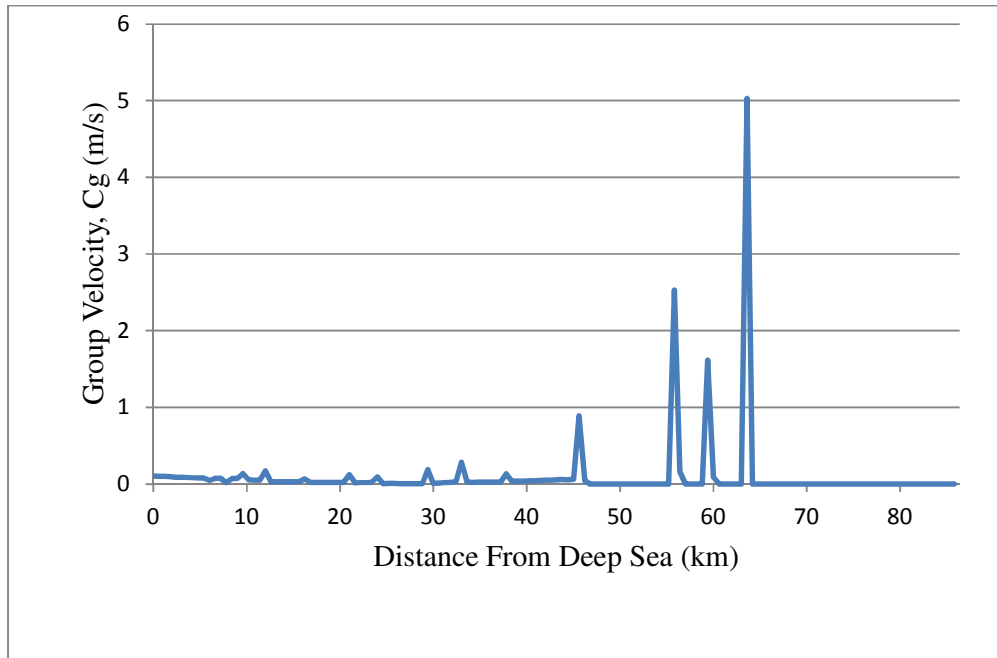


Figure 4.27: Group velocity (Cg) for incoming wave angle 260° with north for section A-A.

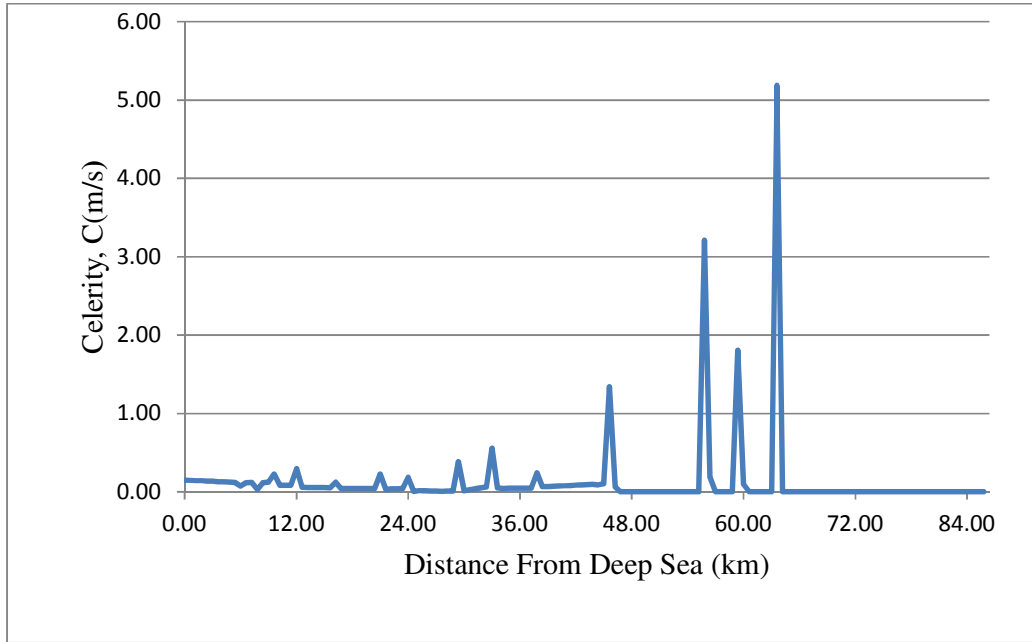


Figure 4.28: Celerity (C) for incoming wave angle 270° with north for section A-A

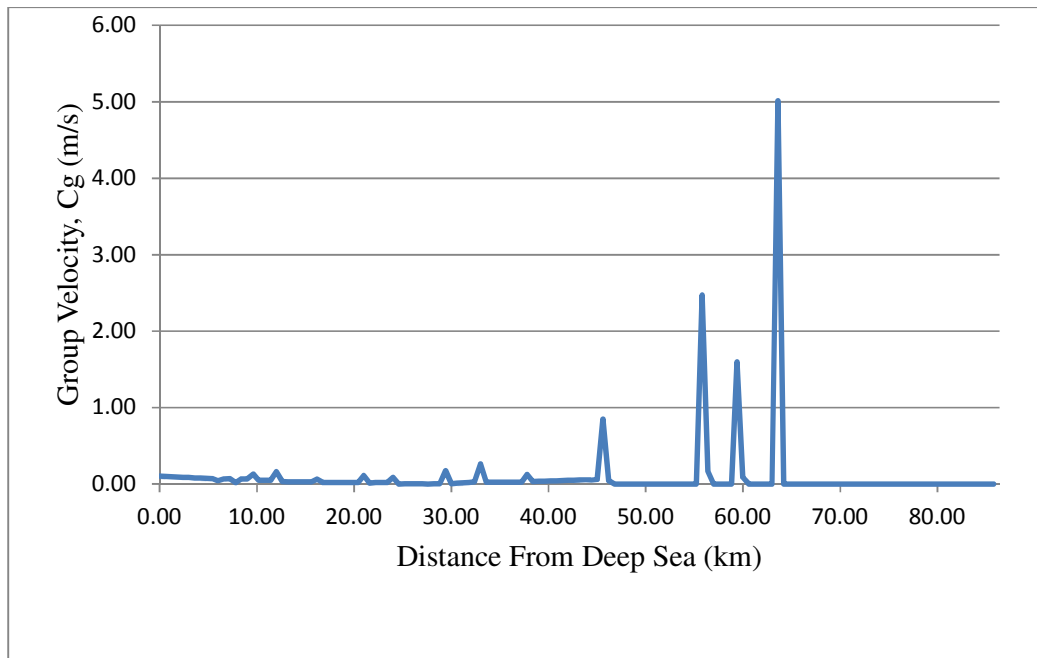


Figure 4.29: Group velocity (C_g) for incoming wave angle 270° with north for section A-A.

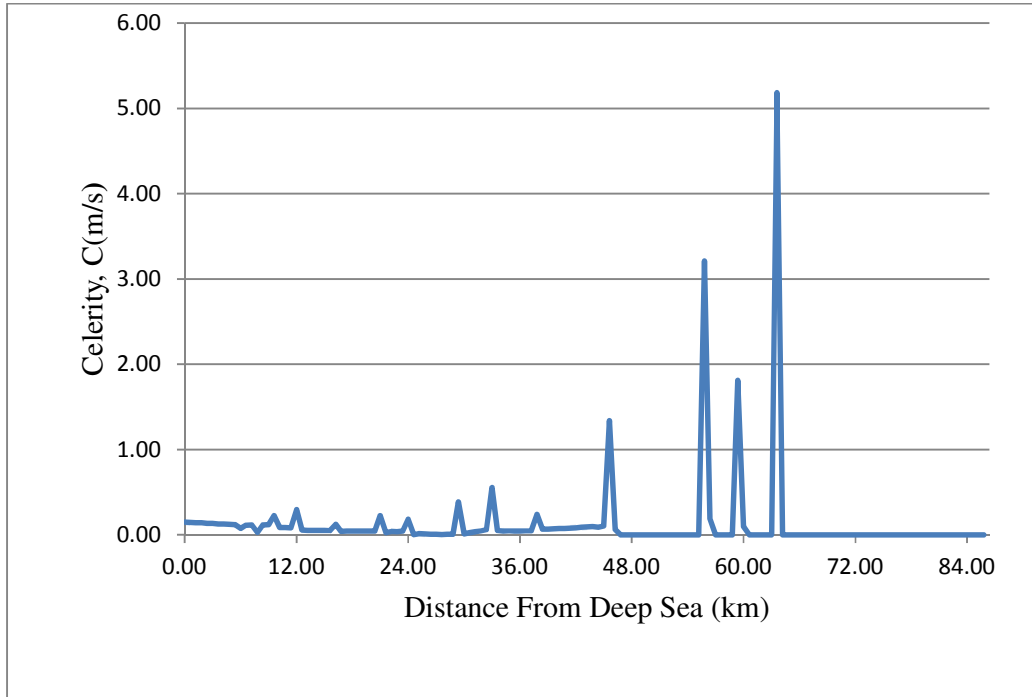


Figure 4.30: Celerity (C) for incoming wave angle 280° with north for section A-A

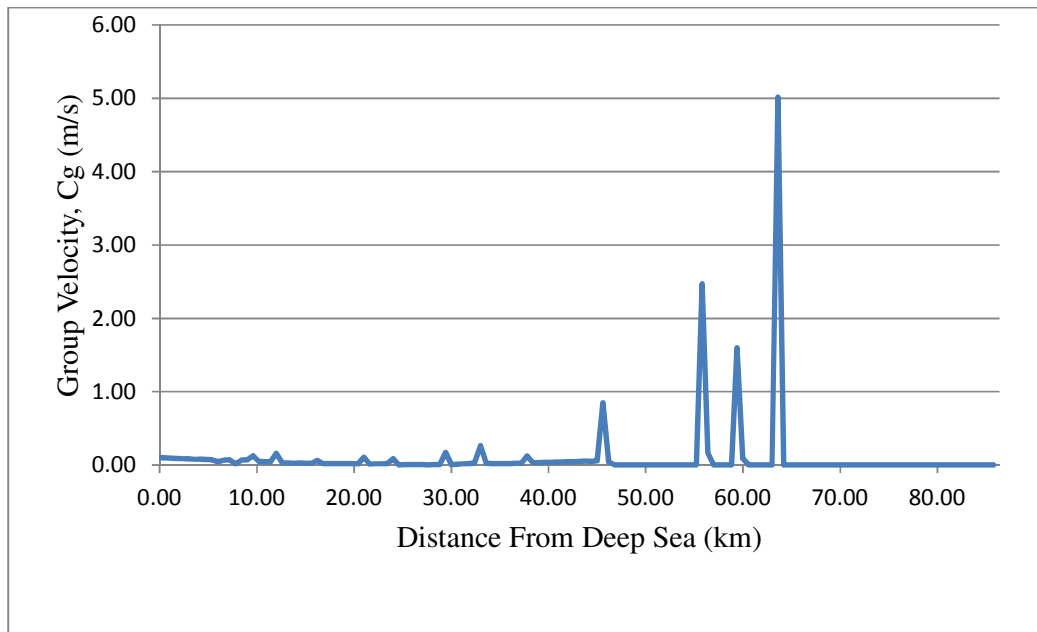


Figure 4.31: Group velocity (C_g) for incoming wave angle 280° with north for section A-A

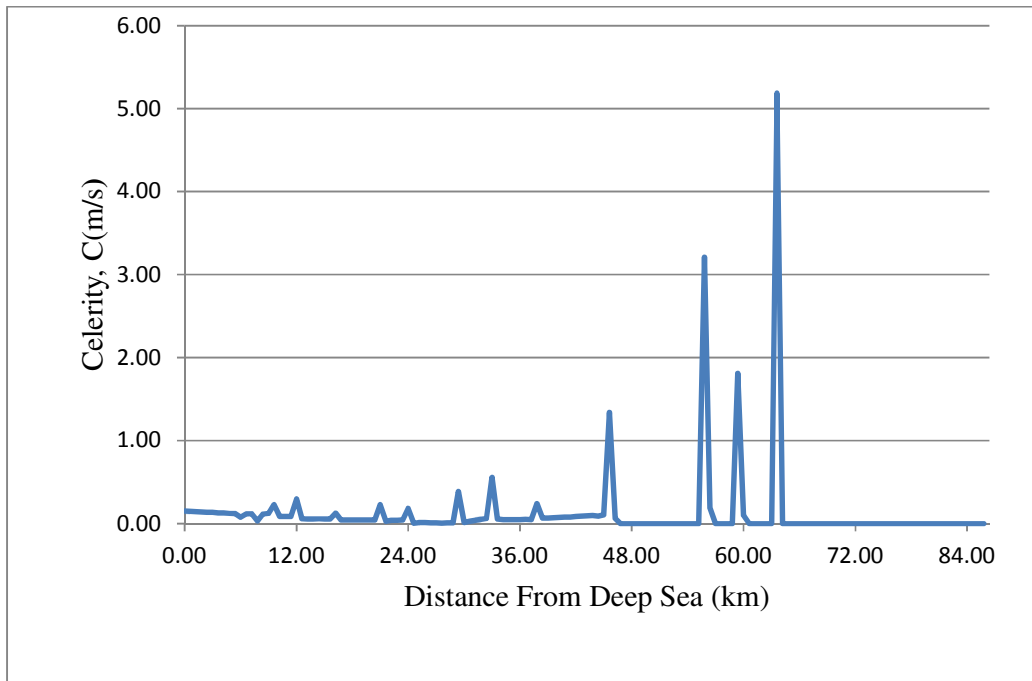


Figure 4.32: Celerity (C) for incoming wave angle 290° with north for section A-A

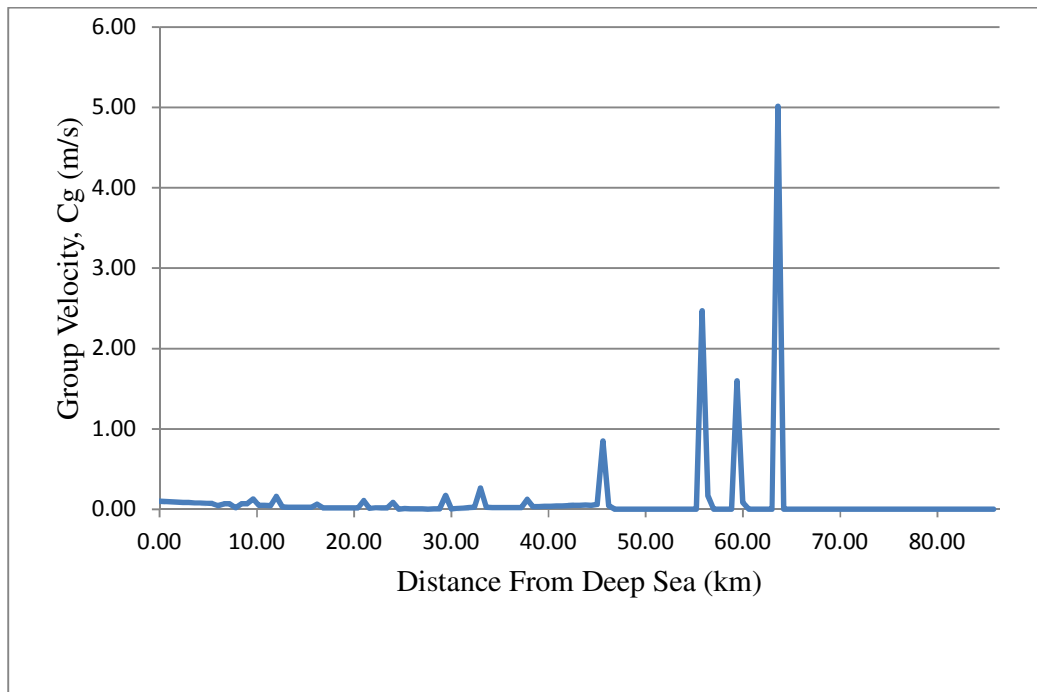


Figure 4.33: Group velocity (C_g) for incoming wave angle 290° with north for section A-A

The celerity (C) and group velocity (Cg) profile for Case 2 :

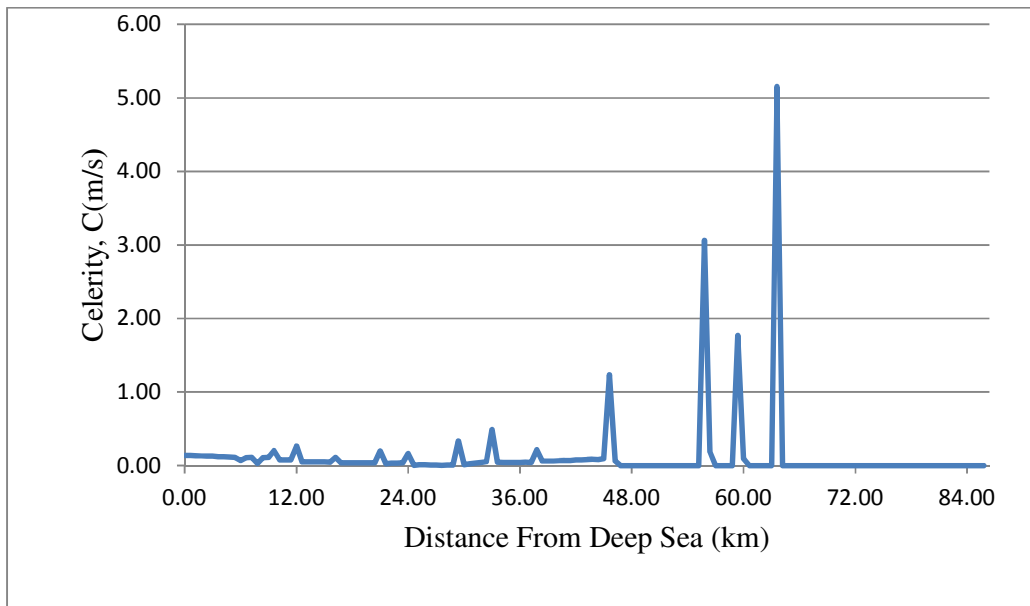


Figure 4.34: Celerity (C) for incoming wave angle 230° with north for section A-A

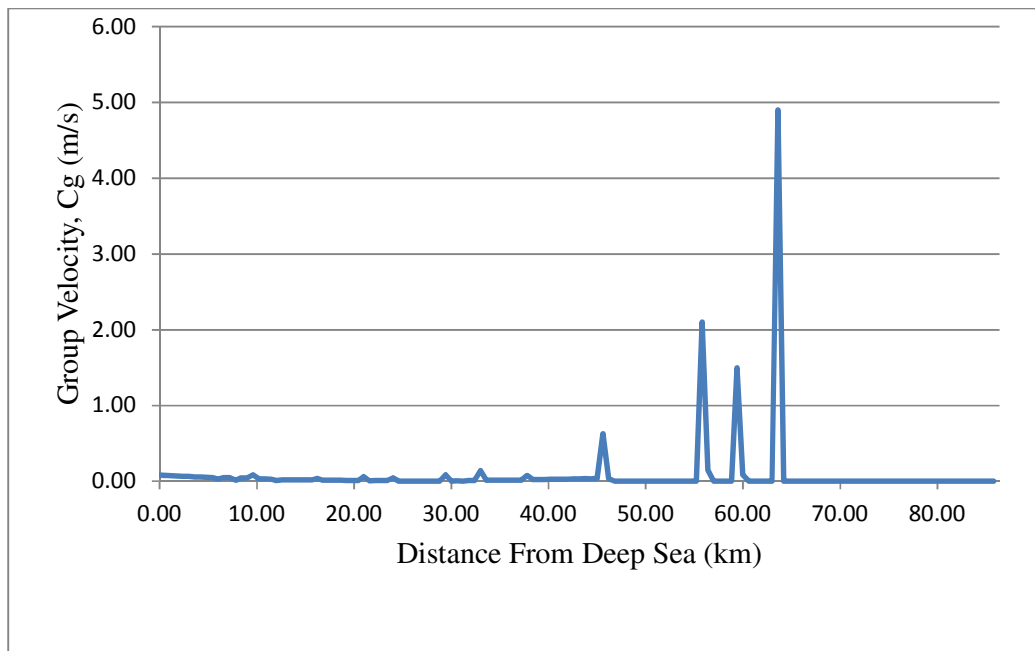


Figure 4.35: Group velocity (Cg) for incoming wave angle 230° with north for section A-A

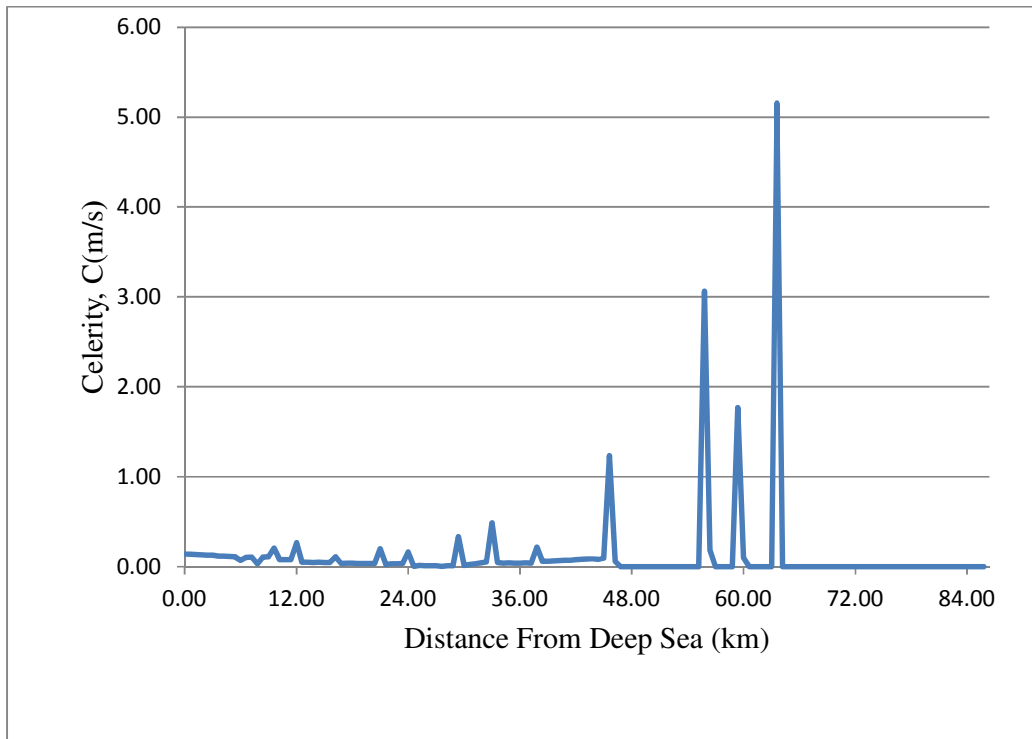


Figure 4.36: Celerity (C) for incoming wave angle 240° with north for section A-A

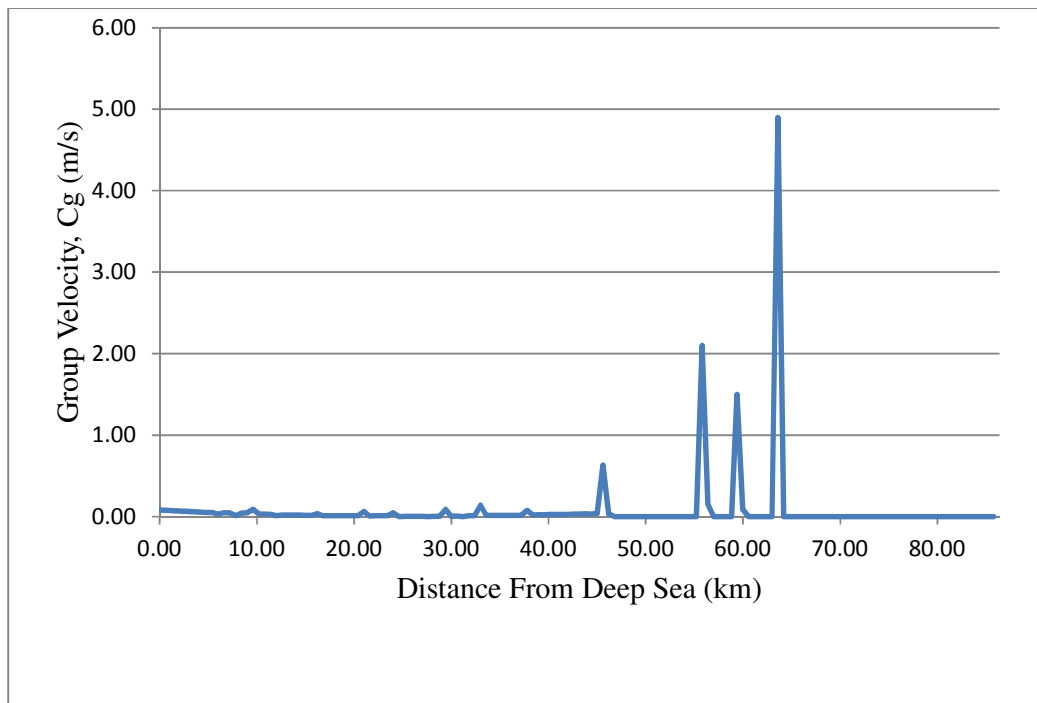


Figure 4.37: Group velocity (C_g) for incoming wave angle 240° with north for section A-A

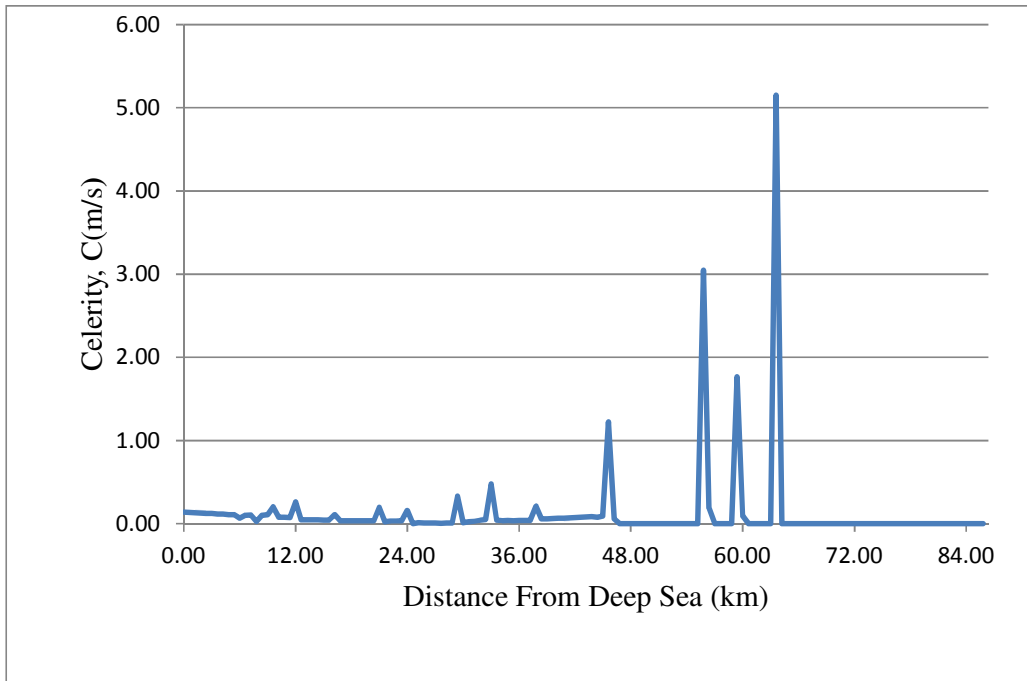


Figure 4.38: Celerity (C) for incoming wave angle 250° with north for section A-A

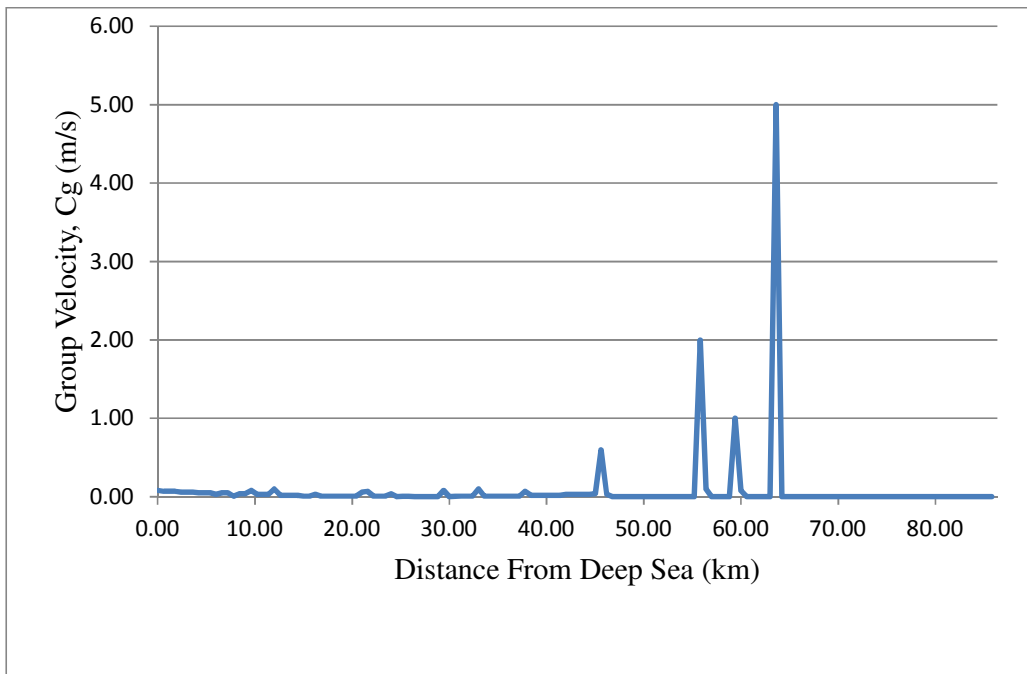


Figure 4.39: Group velocity (Cg) for incoming wave angle 250° with north for section A-A

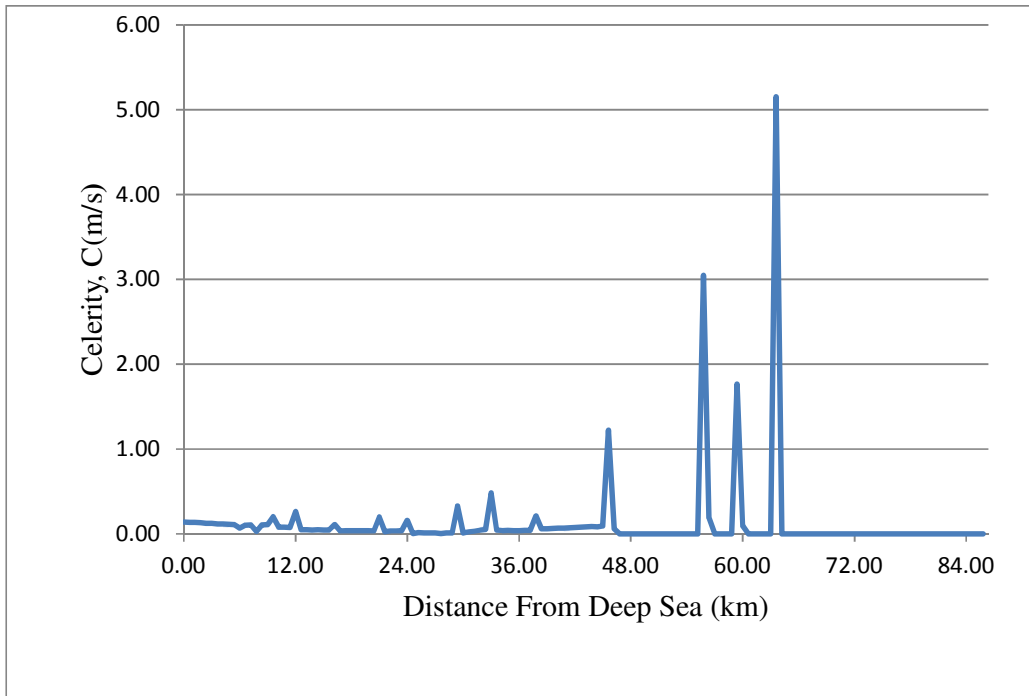


Figure 4.40: Celerity (C) for incoming wave angle 260° with north for section A-A

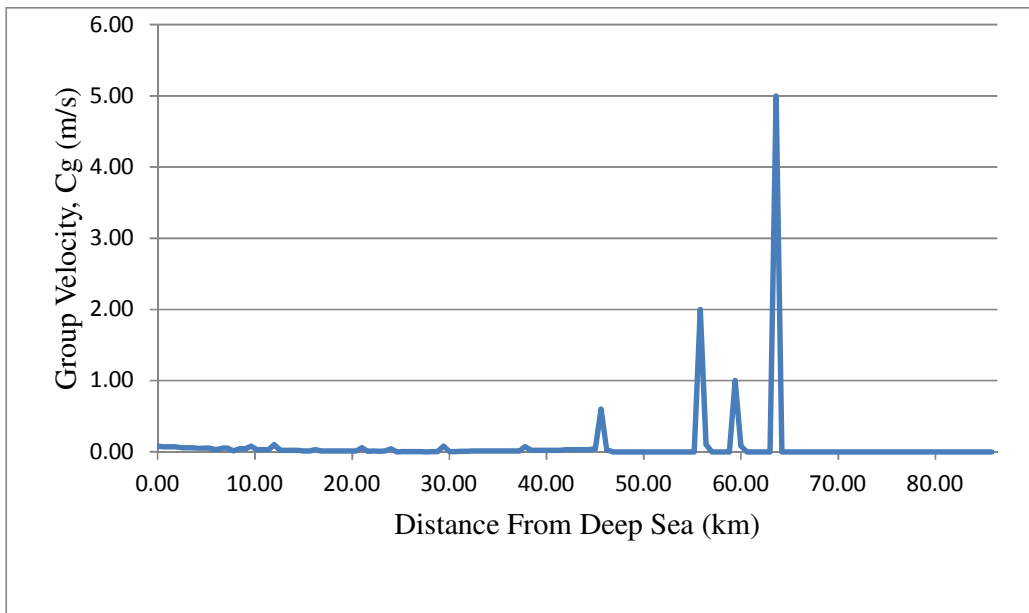


Figure 4.41: Group velocity (Cg) for incoming wave angle 260° with north for section A-A

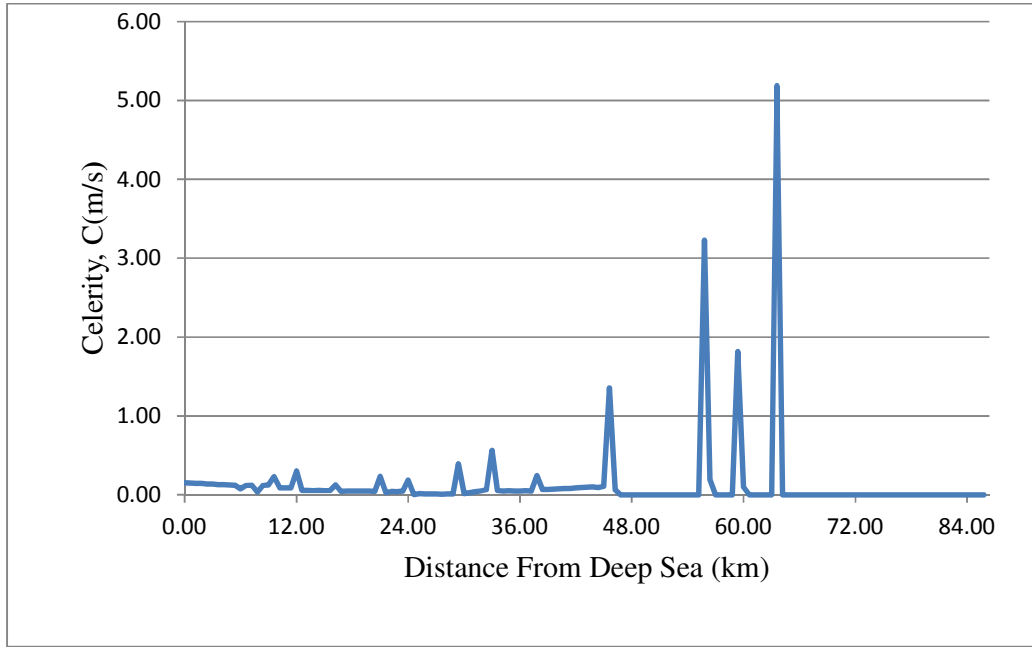


Figure 4.42: Celerity (C) for incoming wave angle 270° with north for section A-A

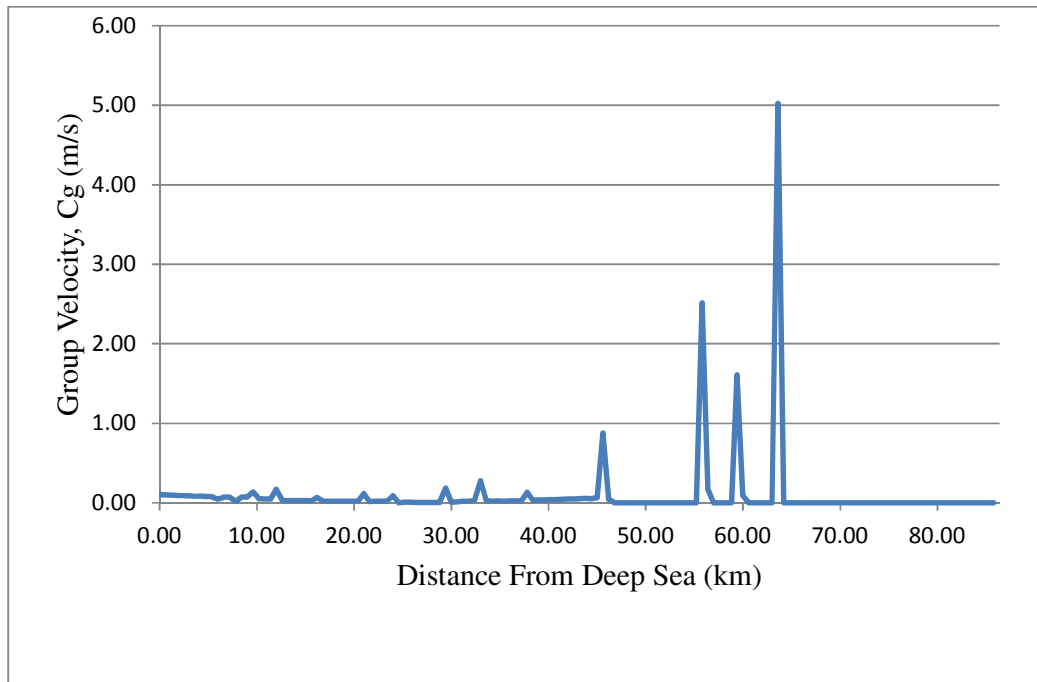


Figure 4.43: Group velocity (Cg) for incoming wave angle 270° with north for section A-A

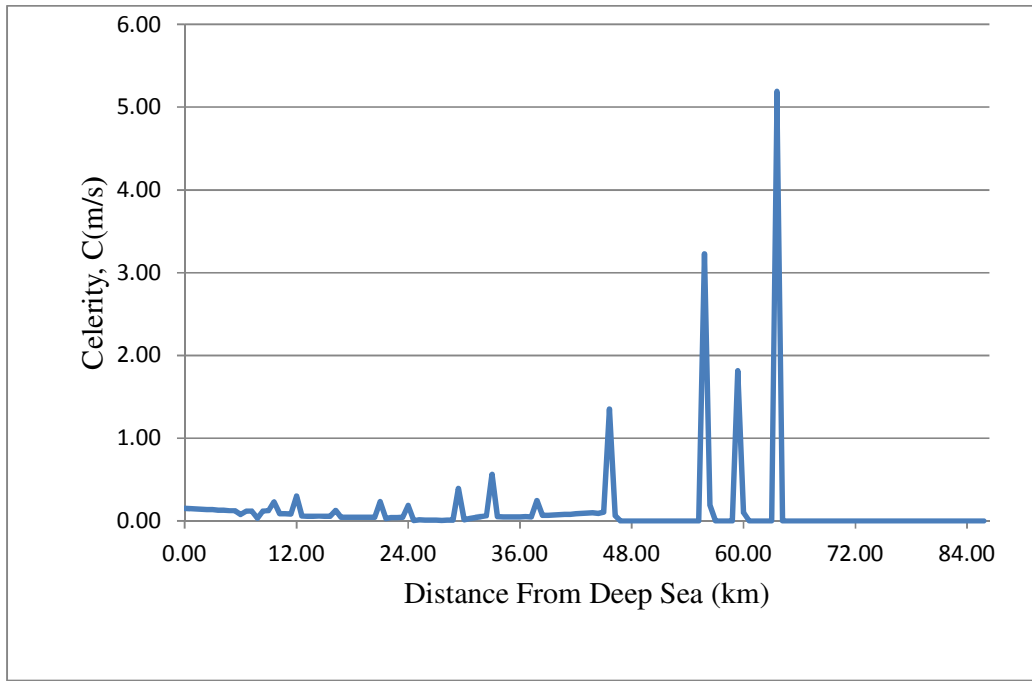


Figure 4.44: Celerity (C) for incoming wave angle 280° with north for section A-A

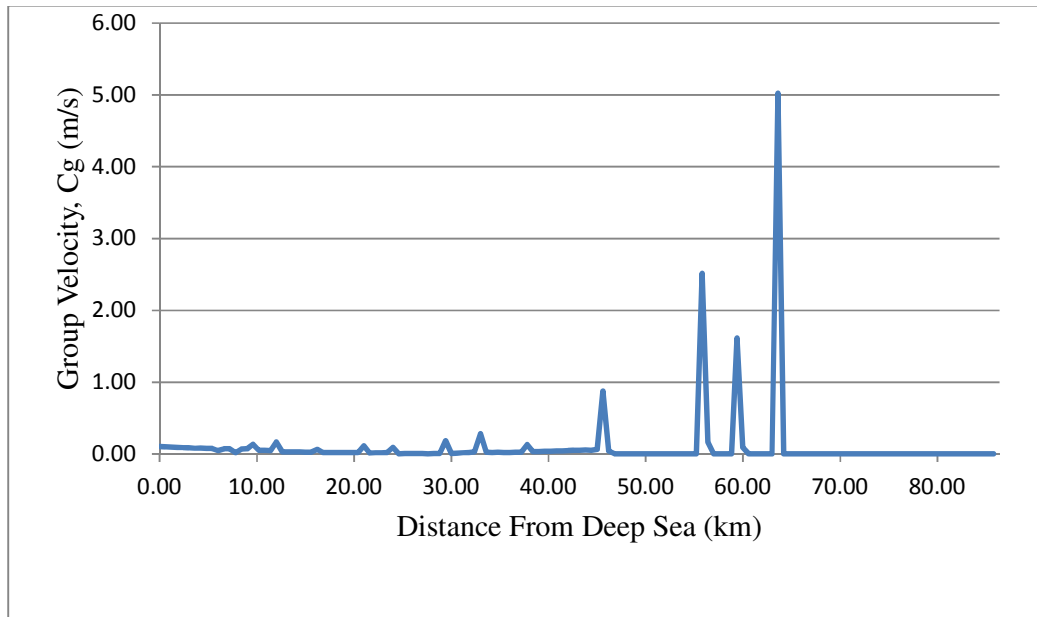


Figure 4.45: Group velocity (Cg) for incoming wave angle 280° with north for section A-A.

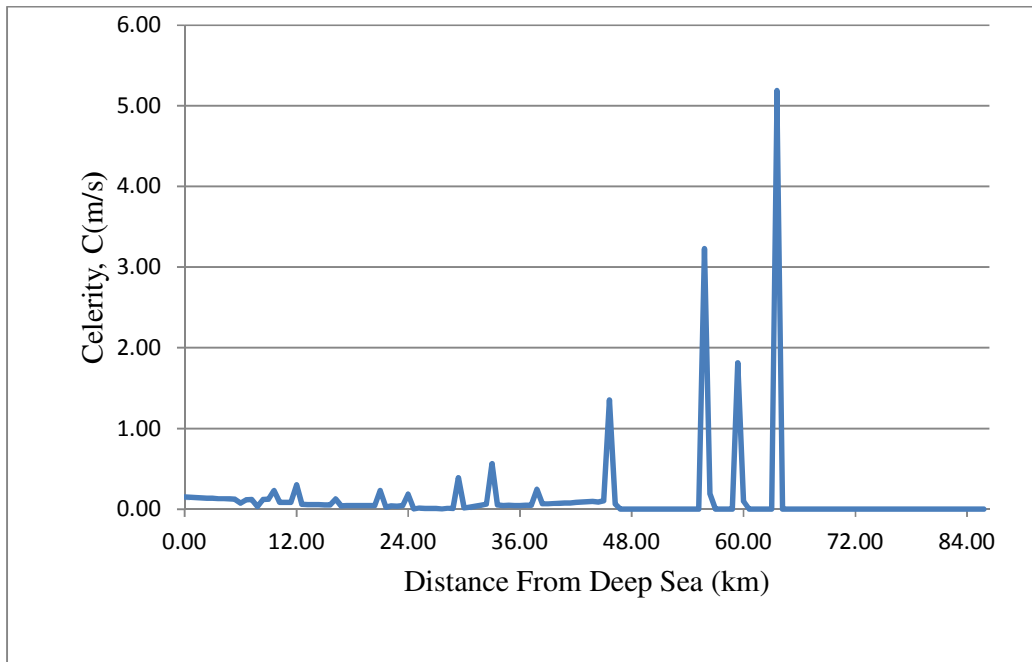


Figure 4.46: Celerity (C) for incoming wave angle 290° with north for section A-A

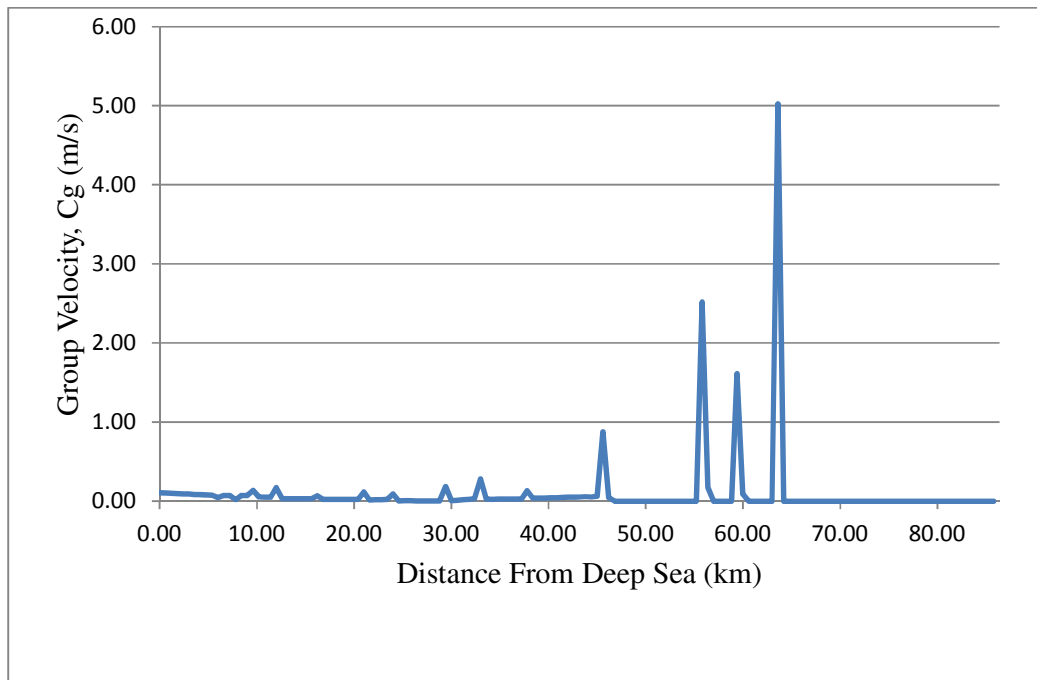


Figure 4.47: Group velocity (Cg) for incoming wave angle 290° with north for section A-A

The wave height profile for Case 1:

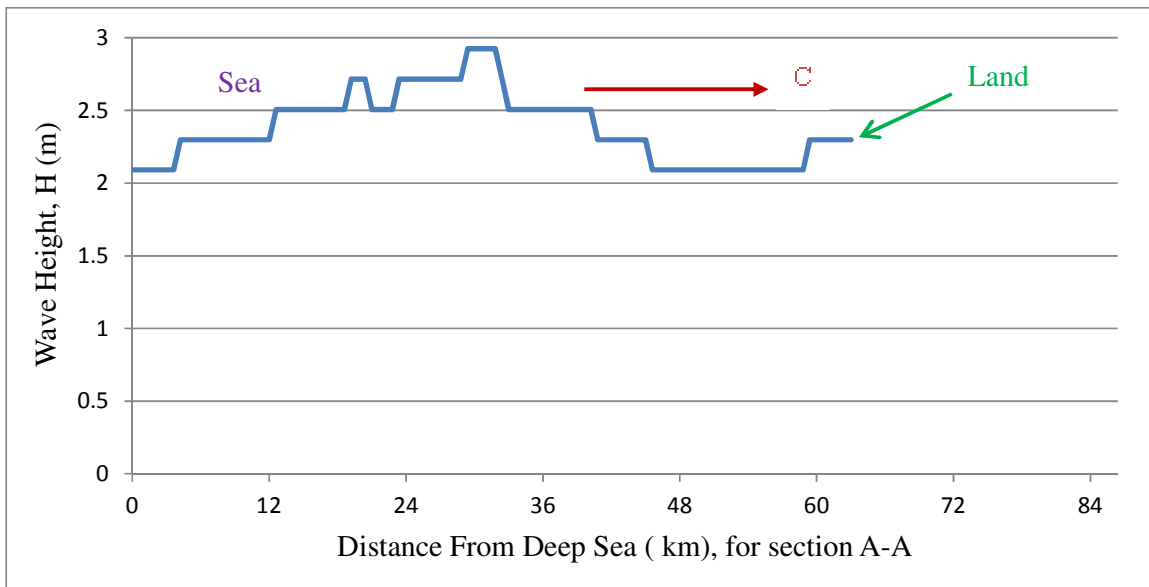


Figure 4.48: Wave Height for incoming wave angle 230° with north for section A-A

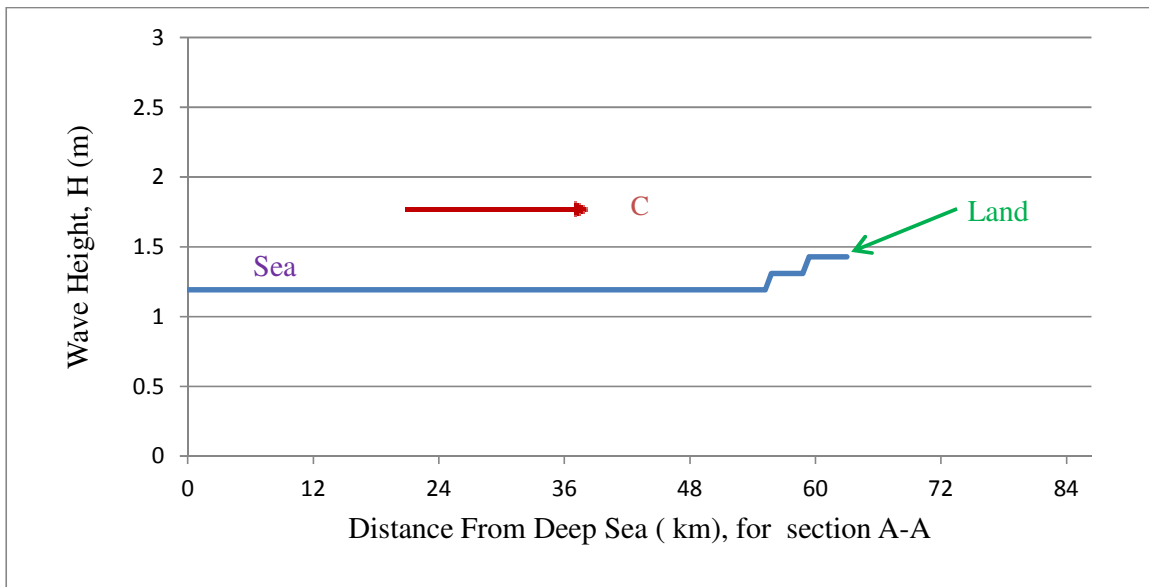


Figure 4.49: Wave Height for incoming wave angle 240° with north for section A-A

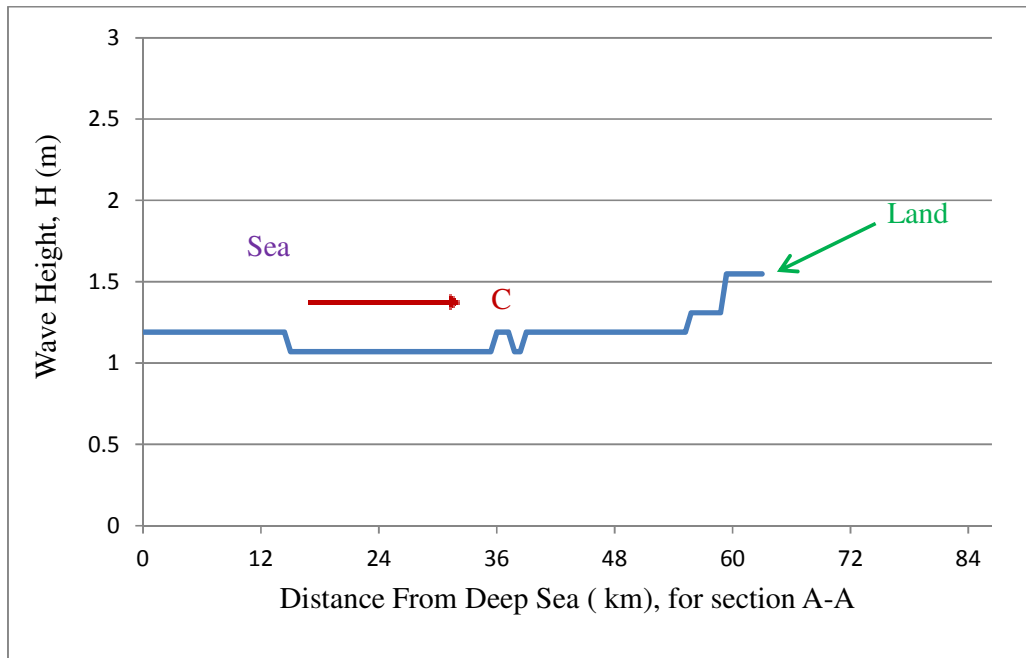


Figure 4.50: Wave Height for incoming wave angle 250° with north for section A-A

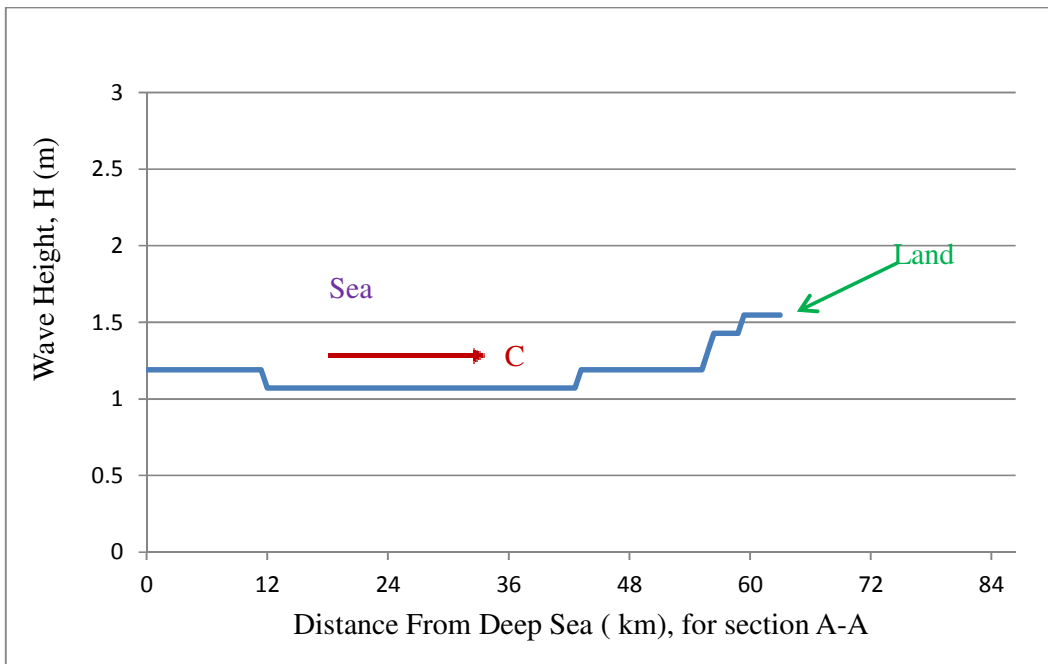


Figure 4.51: Wave Height for incoming wave angle 260° with north for section A-A

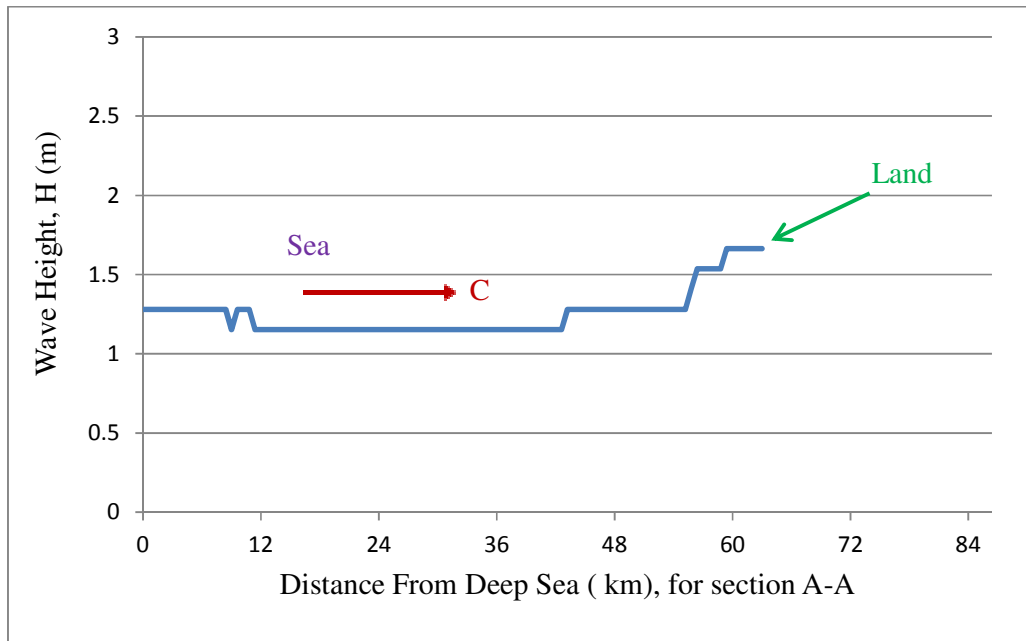


Figure 4.52: Wave Height for incoming wave angle 270° with north for section A-A

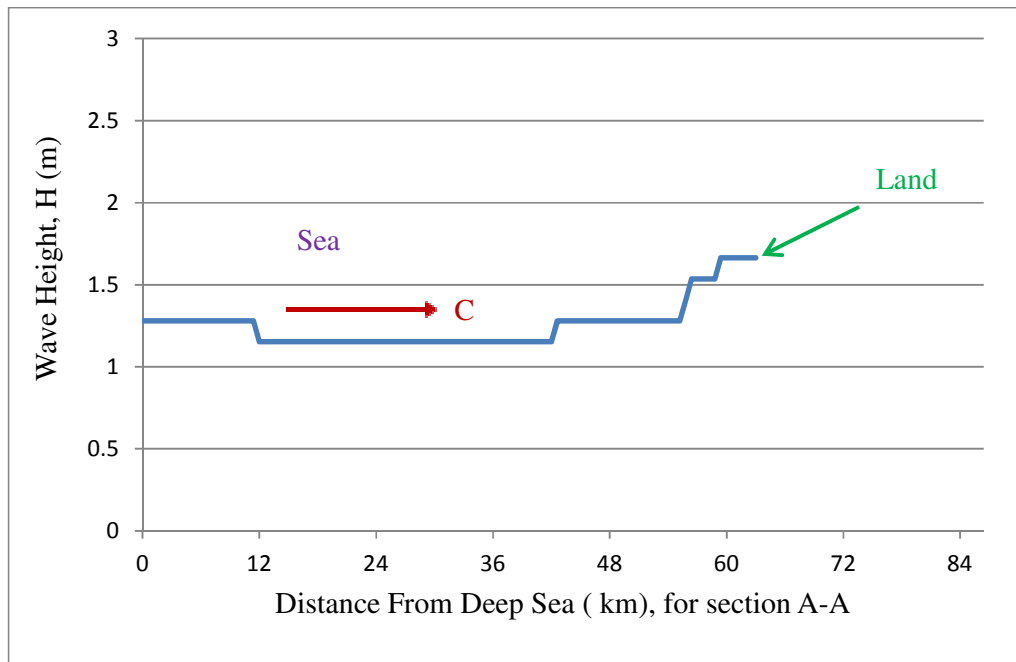


Figure 4.53: Wave Height for incoming wave angle 280° with north for section A-A

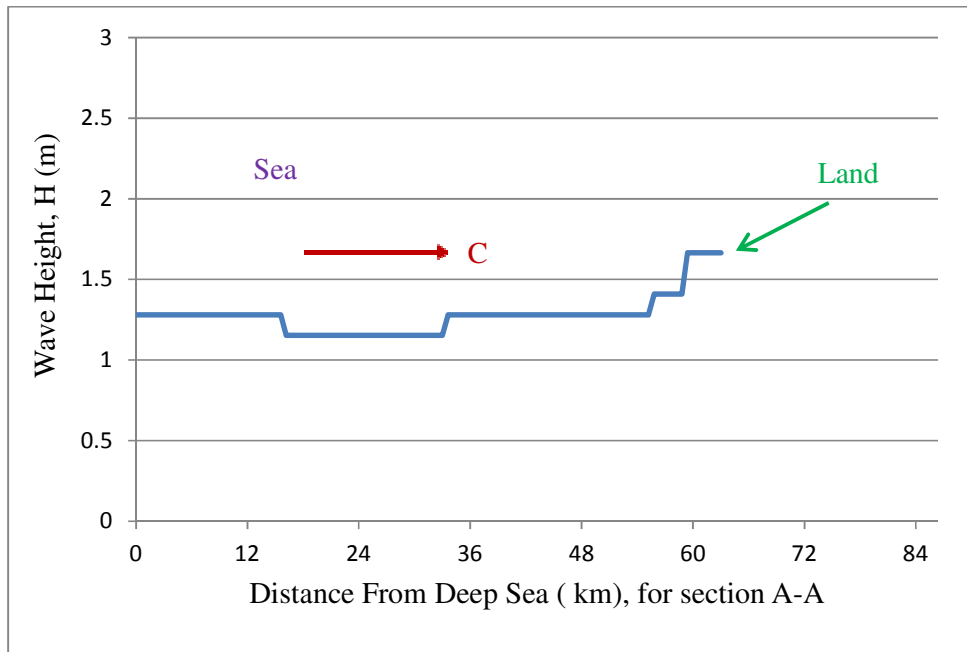


Figure 4.54: Wave Height for incoming wave angle 290° with north for section A-A.

The wave height profile for Case 2:

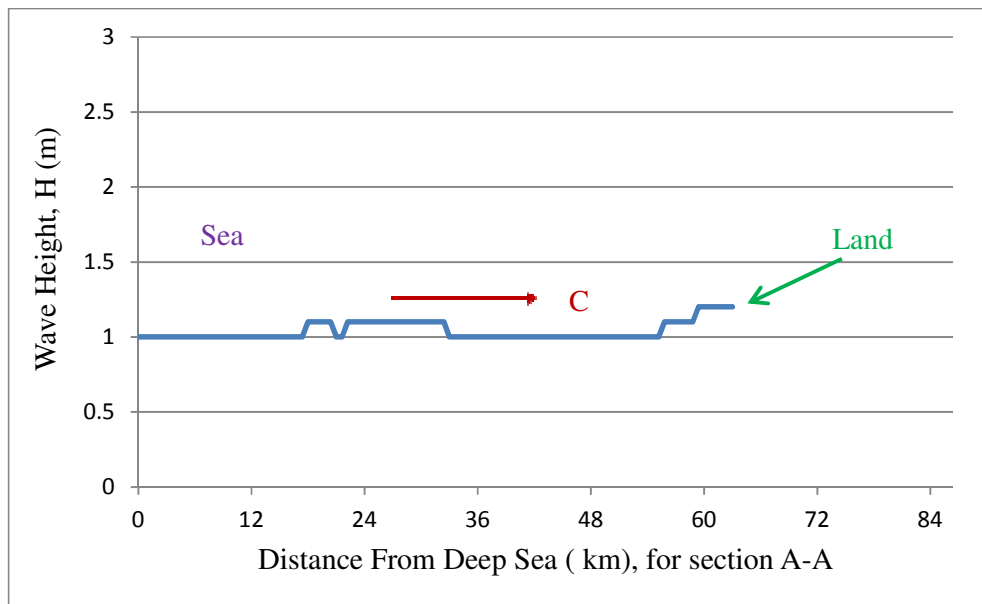


Figure 4.55: Wave Height for incoming wave angle 230° with north for section A-A

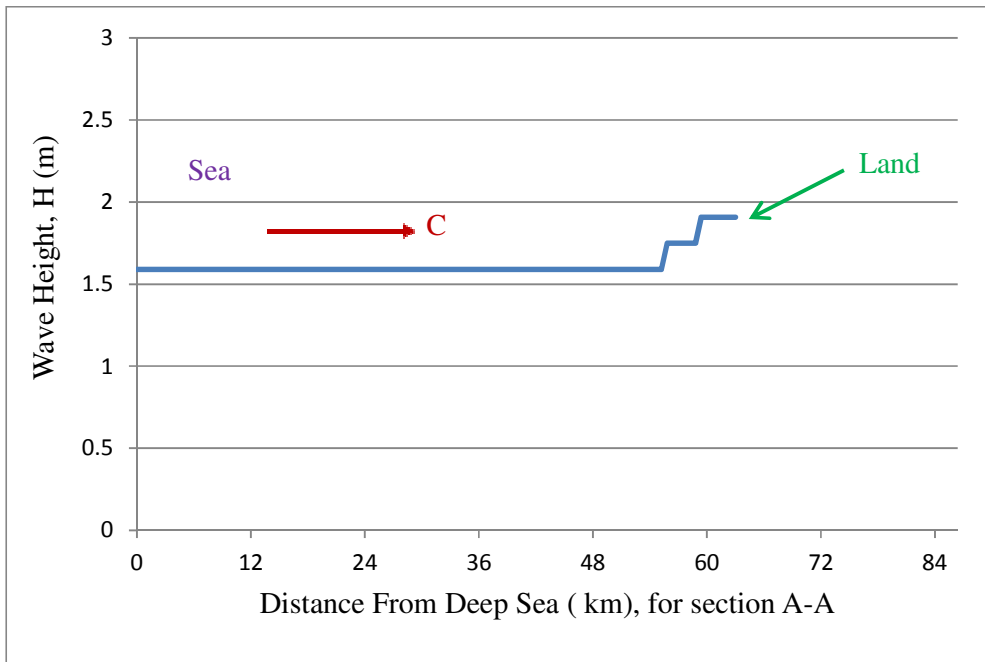


Figure 4.56: Wave Height for incoming wave angle 240° with north for section A-A

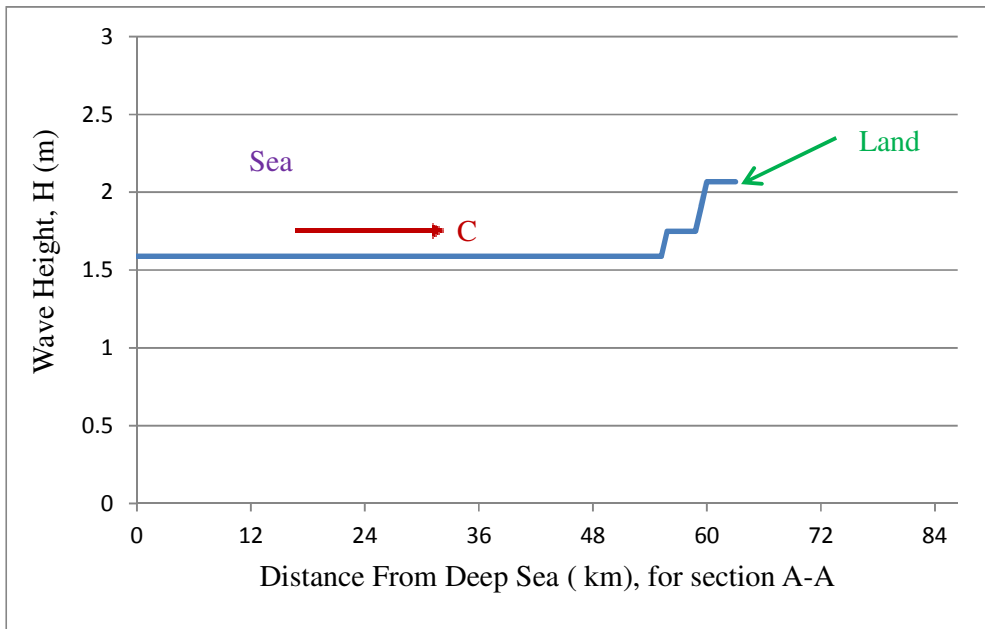


Figure 4.57: Wave Height for incoming wave angle 250° with north for section A-A

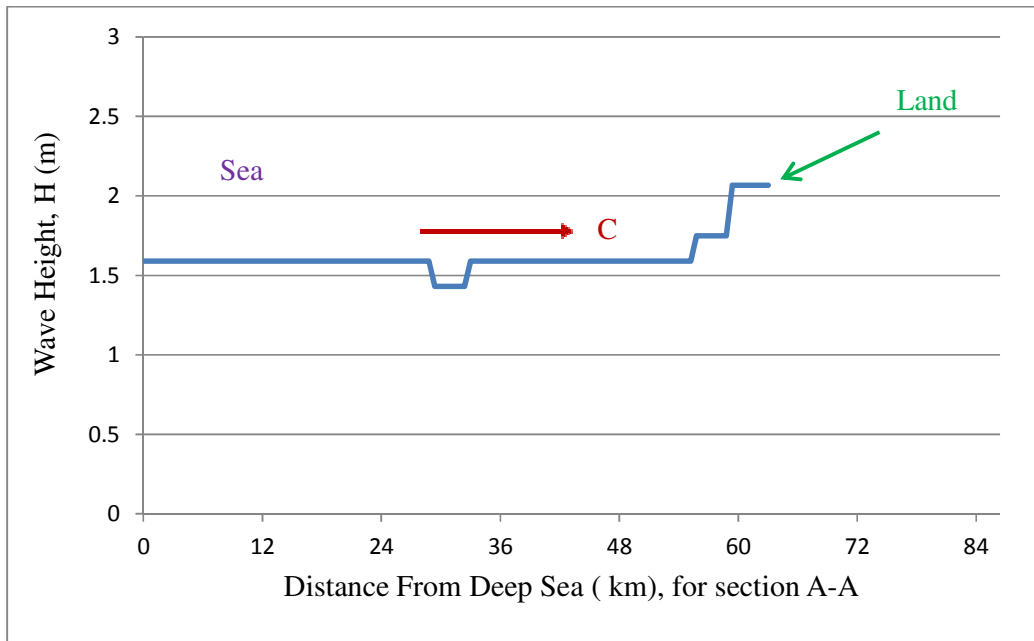


Figure 4.58: Wave Height for incoming wave angle 260° with north for section A-A

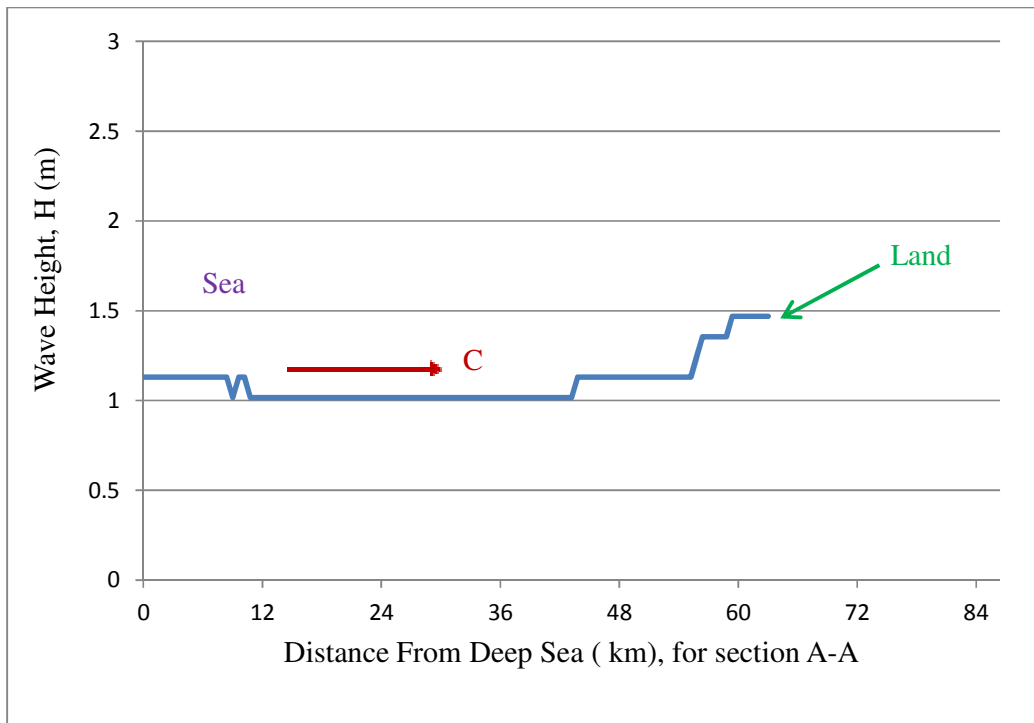


Figure 4.59: Wave Height for incoming wave angle 270° with north for section A-A

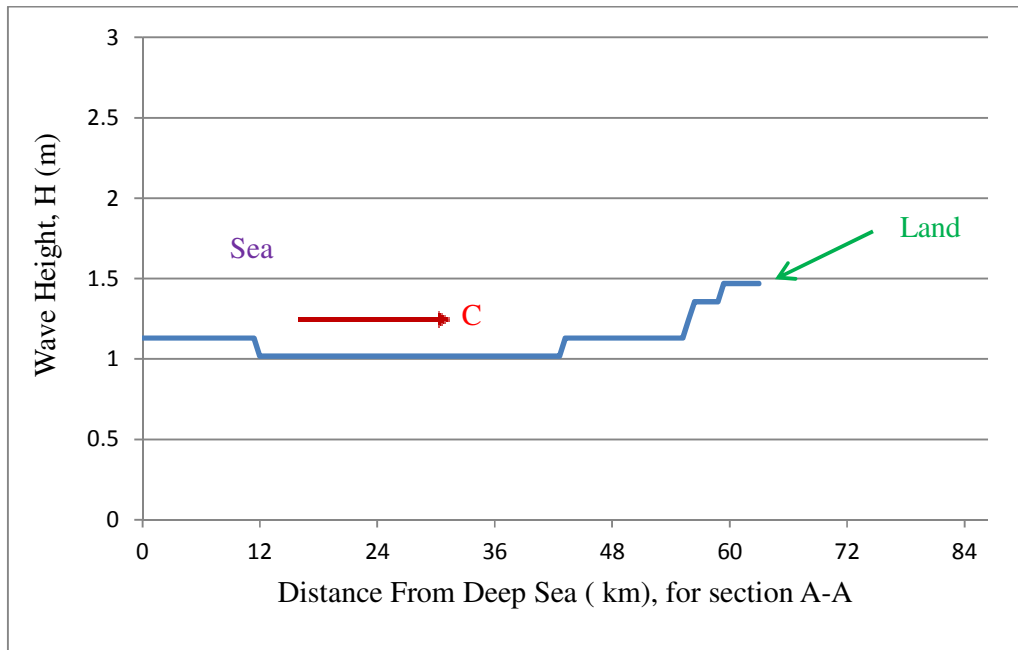


Figure 4.60: Wave Height for incoming wave angle 280° with north for section A-A

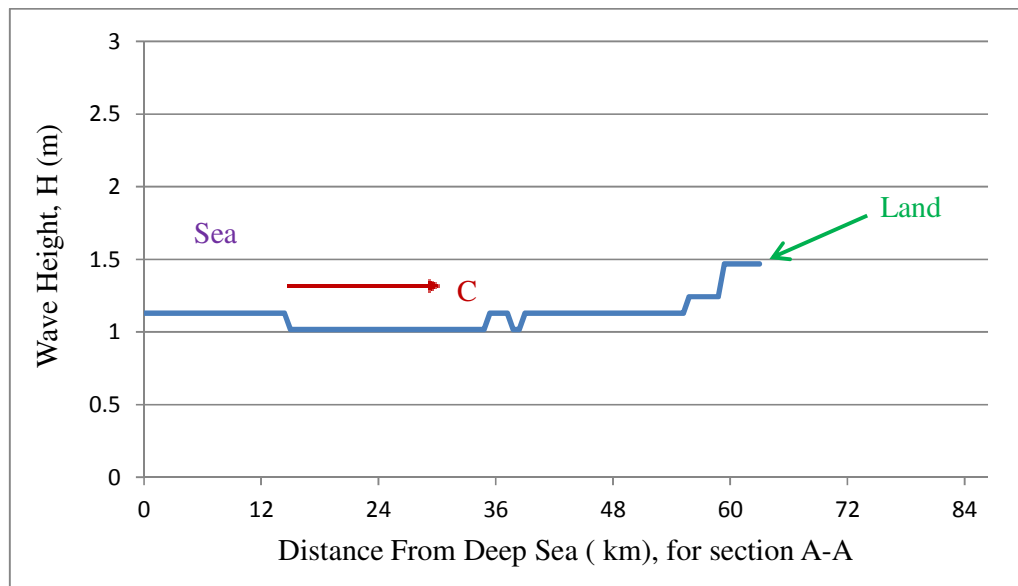


Figure 4.61: Wave Height for incoming wave angle 290° with north for section A-A

The celerity and group velocity profiles over the model domain for different wave direction for different cases generated by DIVAST model are shown from Figure 4.20 to 4.47 respectively. It is observed from the velocity profile that for different wave direction the

change the magnitude of the celerity and group velocity almost same. It also shown that for different wave angle but same significant wave height and significant wave period the magnitude of celerity and group velocity shows almost same.

The wave height profile over the model domain for different wave direction for different cases generated by DIVAST model has been shown from Figure 4.48 to 4.61 respectively. It is observed from the wave height profile that for different wave direction the change the magnitude of the maximum velocity. It also shown that for different wave angle but same significant wave height and significant wave period the magnitude of wave height shows different.

4.6 Wave Climate:

Nearshore wave climate will be assessed based on the change in wave height due to change in different deep water wave angle. For different angle and different position the wave climate observed which has been given below the figures

For Case 1:

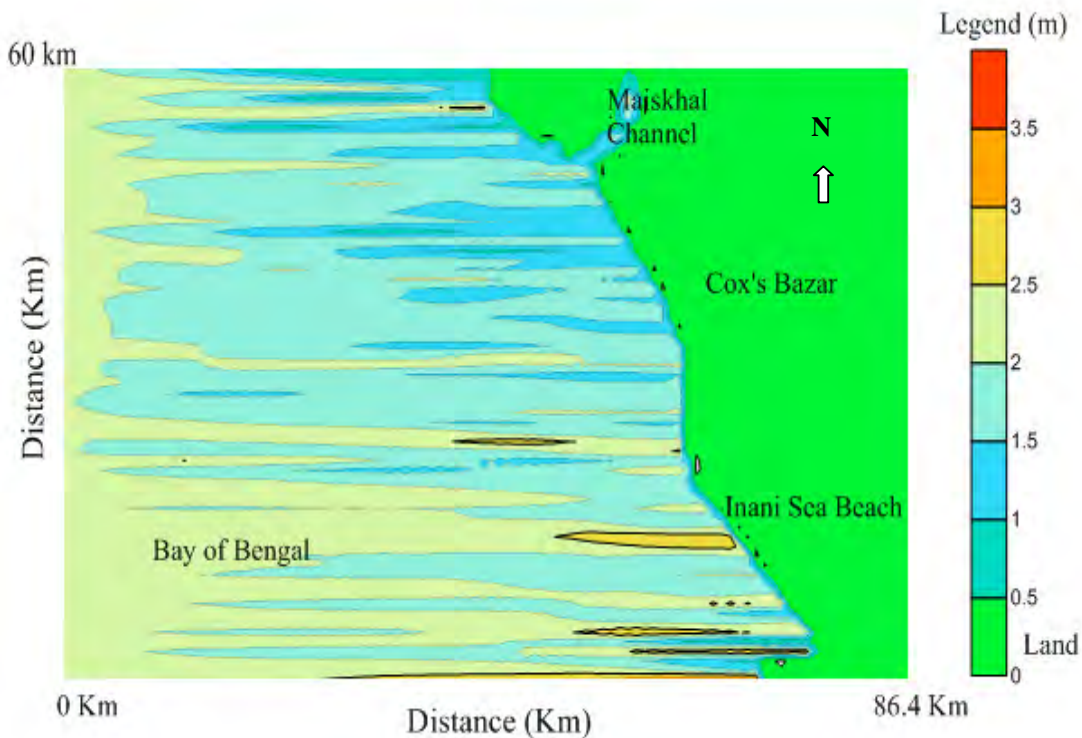


Figure 4.62: Wave Climate profile for incoming wave angle 230° with north

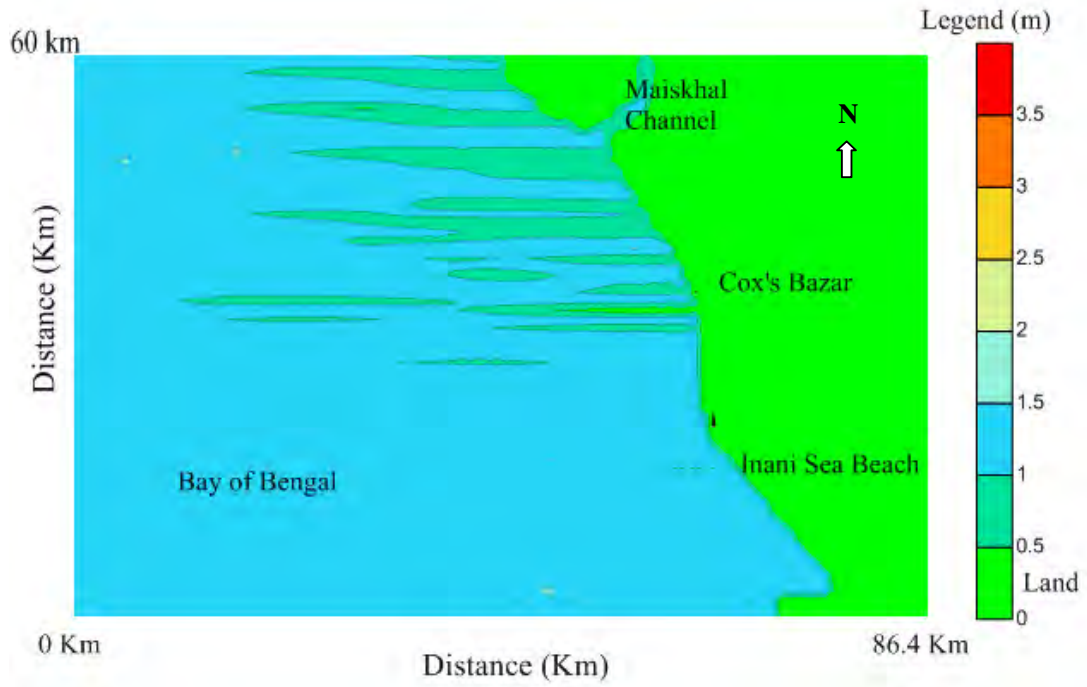


Figure 4.63: Wave Climate profile for incoming wave angle 270° with north

For Case 2:

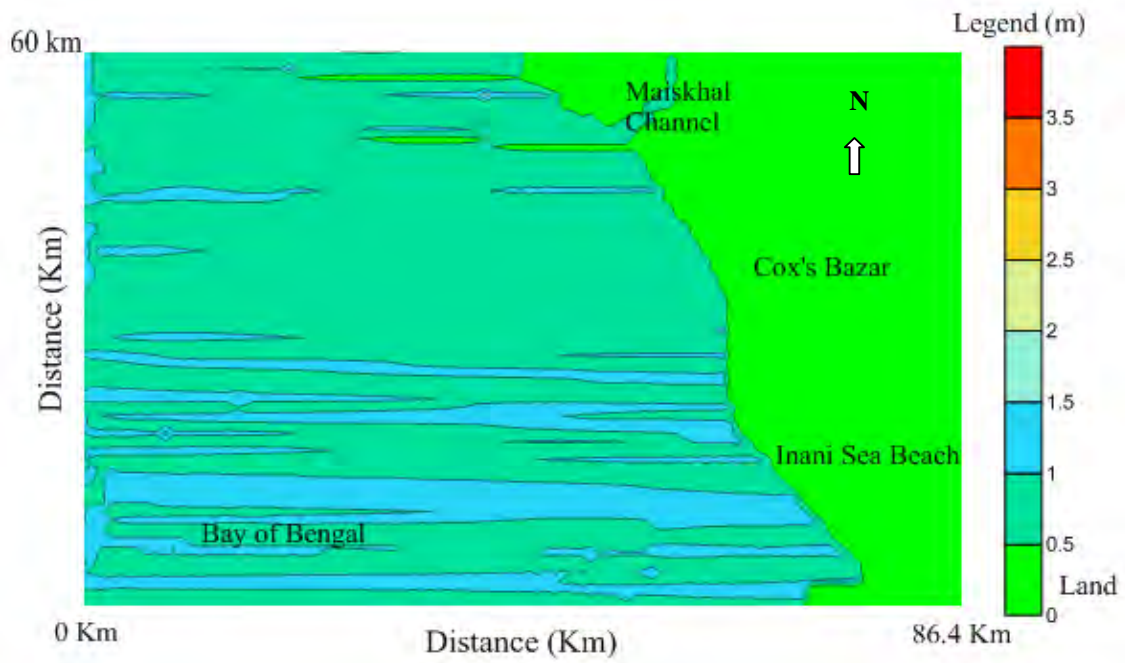


Figure 4.64: Wave Climate profile for incoming wave angle 230° with north

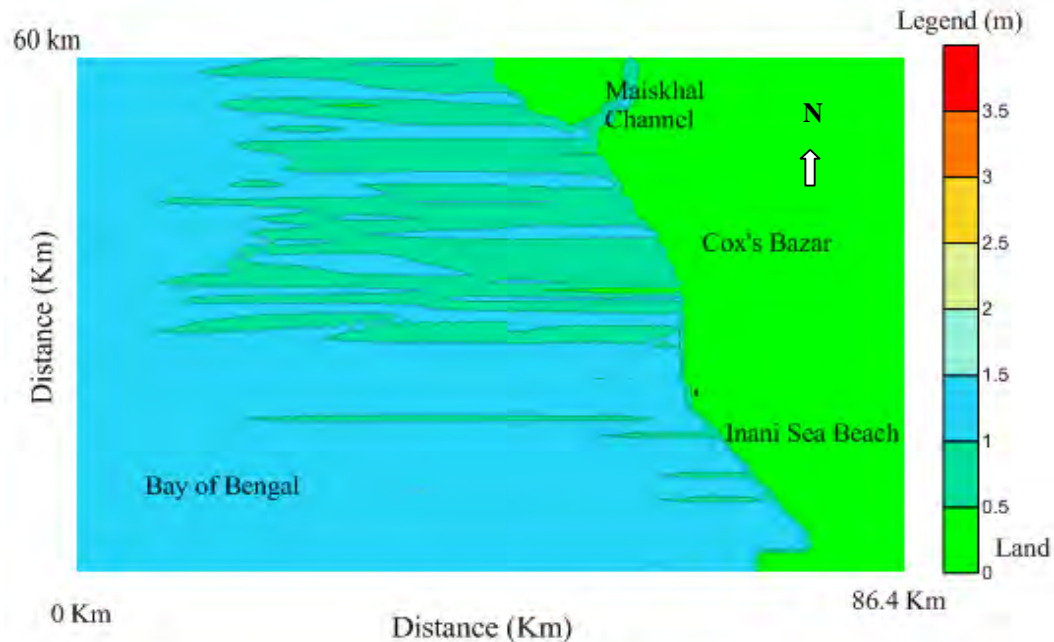


Figure 4.65: Wave Climate profile for incoming wave angle 270° with north

The wave climate over the model domain for different wave direction for different cases generated by DIVAST model has been shown from Figure 4.62 to 4.65 respectively. In this figure there has been seen that the maximum wave height generated nearshore in the Sea.

4.7 Summary

In this chapter the calibration and verification of model has been done against measured maximum wave height with output maximum wave height at different locations of coastal areas in different month and year. DIVAST model generated velocity profile for different range of wave direction for different cases are shown and their features have also been interpreted and discussed in this chapter. Celerity, group velocity and wave height profile also discussed and velocity profile of different location has been measured by the mathematical model with help of the 'Surfer' In this chapter. From the result shown here it appears that the maximum wave velocity in onshore line along the coast and minimum wave velocity in the offshore or deep sea. When wave coming from deep water towards the shallow water, the velocity accordingly increasing toward the shallow water. Hence it is can be concluded that DIVAST model shows an encouraging and good performance in study area.

CHAPTER 5

CONCLUSIONS AND RECOMEDATIONS

5.1 General

The coastal areas of Bangladesh are different from other parts of the country due to its unique geo-physical characteristics and vulnerability to several natural disasters like cyclones, storm surges, erosion and accretion, SLR ect.

The bathymetry data has been generated based on Model using DIVAST model. The model area of Bay of Bengal consists of 144 x 100 grid square with a constant grid spacing 600 m. The model has three open boundaries : The northern boundary is the Fasiakhali and the southern boundary is in the near Chowdhury para and the western Boundary is in the open sea located bay of Bengal. The coastline of Bangladesh is characterized by a wide continental shelf, especially off the eastern part of Bangladesh. The triangular shape at the head of the Bay of Bengal helps to funnel the sea water pushed by the wind towards the coast and causes amplification of the wave levels at the exposed low lying coastal areas. This is basically occurs in the amplification of wave or tidal levels on Bangladesh coast.

In this study a two dimensional hydrodynamic model DIVAST (Depth Integrated Velocity and Solute Transport) has been used considering the different parameters like co-efficient of eddy viscosity, Manning roughness, advective and diffusion coefficient etc. of Bay of Bengal. The model is set up on a combination of specific information as input of the model area i. e. bathymetry, topography, wind and water density. The model is based on FORTRAN PROGRAMING. The model has been used simulate the maximum wave height, wave velocity, celerity and group velocity as output along the selected important locations of coastal region of Cox's Bazar of Bay of Bengal.

5.2 Conclusions of the study

The hydrodynamics of the selected area of Bay of Bengal is simulated by solving two-dimensional governing equations numerically with finite difference (ADI-Scheme) method. Consequently the water elevation η and the respective velocity components U, V in the x and y directions are calculated across the selected locations of coastal domain for prescribed set of initial and boundary conditions. Simulated maximum wave height has been verified at selected locations of coastal area with the measured field data.

The following conclusions can be made viewing over all discussion and summarizing this work:

1. The hydrodynamic model has been set up at nearshore coastal water of Cox's Bazar which results in good agreement with the field data.
2. The model has been calibrated with the measured data at location such as location point B4 (Latitude: $20^{\circ}58.955'$, Longitude: $91^{\circ}29.071'$) and location point B9 (Latitude: $21^{\circ}15.303'$, Longitude: $91^{\circ}51.053'$) of the Bay of Bengal. Calibration result of this work shows good agreement between the measured and model output of maximum wave height of nearshore areas of Cox's Bazar.
3. The model has been validated with the measured data at location such as location point B9 (Latitude: $21^{\circ}15.303'$, Longitude: $91^{\circ}51.053'$) in the Bay of Bengal. Validation results of this work shows a good agreement between the measured and model output of maximum wave height of nearshore areas of Cox's Bazar.
4. The model output results like celerity and group velocity has been found out at location point B1 and B11 in Cox's Bazar of Bangladesh. From the group velocity profile there has been shown that maximum group velocity developed in the nearshore area.
5. The maximum wave velocity has been observed which was developed in the nearshore area.
6. The nearshore wave climate has been observed from the wave height fluctuation.

5.3 Recommendations for future study

The following recommendations can be made based on the present study and that may produce better results for future study.

1. This model study has been carried out for simulation of maximum wave height. Further studies may be carried out such as a comparison of two models in terms of data requirements, CPU time, simulation of salinity concentration, sediment concentration, environmental impact assessment etc.
2. Further study may be done with comparatively smaller grid size to define clearly all coastal zone i.e. all islands and chars in the Bay of Bengal to get improved simulated results.
3. Bathymetry data from 2004 to 2013, has been used in this research work. Inclusion of more recent and up to date bathymetry will improve the reliability of the model results of the research work.

References

Azam, M. H., Jakobsen, F., Kabir, M. and Hye, J. M. A., 2000, "Sensitivity of the Tidal Signal Around the Meghna Estuary to the Changes in River Discharge: A Model Study", The 12th International APD-IAHR Conference, Bangkok.

Ali, A., 2007, Sediment Dynamics in the Meghna Estuary, Bangladesh, cedb.asce.org/cgi/WWWdisplay

"Bay of Bengal," Banglapedia, http://www.banglapedia.org/HT/B_0406.htm

Barua, D. K. and Kana, T. W., 1995, "Deep Water Wave Hindcasting, Wave Refraction Modeling, and Wind and Wave Induced Motions in the East Ganges-Brahmaputra Delta Coast", Journal of Coastal Research, Vol. 11, No. 3, pp. 834-848.

CDS, 2006, "Coastal development Strategy", Ministry of Water Resources, Government of the People's Republic of Bangladesh, Dhaka.

Chowdhury, J. U., "Issues in Coastal Zone Management in Bangladesh", Institute of Water and Flood Management (IWFM), Bangladesh University of Engineering and Technology (BUET).

Crossland, C. J., Baird, D., Ducrotoy, J. P., Lindeboom, H., Buddemeier, R.W., Dennison, W. C., Maxwell, B. A., Smith, S. V. and Swaney, D.P., 2005, "The Coastal Zone – a Domain of Global Interactions", Coastal Fluxes in the Anthropocene Global Change-The IGBP Series, Chapter1, pp.1-37.

CZPo, 2005, "Coastal Zone Policy", Ministry of Water Resources, Government of the People's Republic of Bangladesh, Dhaka.

Directional Waves Along North Tamilnadu Coast, India", Journal of Coastal Research, Vol.17, No(2), pp. 322-327.

Ebersole, B. A. and Dalrymple, R. A., 1980, "Numerical Modelling of Nearshore Circulation", Coastal Engineering Proceedings, 1(17).

Enemark, S., 2007, "Coastal Areas and Land Administration – Building the Capacity", Strategic Integration of Surveying Services, 6th FIG Regional Conference 2007, San José, Costa Rica, 12-15 November, 2007.

- Falconer, R. A., 1992, "Flow and Water Quality Modeling in coastal and inland Waters", *Journal of Hydrology*, Vol.-124, pp. 59-79.
- Falnes, J., 2007, "A review of Wave-energy Extraction", *Marine Structures*, Vol. 20, pp. 185–201.
- Fedra, K. and Feoli, E., 1988, "GIS technology and spatial analysis in coastal zone Management", *EEZ Technology*, Ed. 3, pp.171-179.
- Folley, M., 2009, "Analysis of the nearshore wave energy resource", *Renewable Energy*, 34 (2009), pp.1709–1715.
- Halim, M. A., and Faisal, I. M., 1995, "Mathematical Modeling", Department of Water Resources Engineering , BUET, Dhaka.
- Herbich, J. B., 1990, " Handbook of coastal and ocean engineering" , (Vol. 1). Houston, TX: Gulf publishing company.
- Hiles, C. E., On the Use of Computational Models for Wave Climate Assessment in Support of the Wave Energy Industry, B.Eng., University of Victoria, 2007. [35]
- Holmes, P., 2001, "Coastal Processes: Waves", *Coastal Defense Systems 1*, CDCM Professional Training Programme, 2001.
- Hossain, M. D., 2012, Application of 2D Mathematical Model for Verification of Water Velocity at Coastal Area of Bangladesh, M. Sc. Thesis, Water Resource Engineering Department, Bangladesh University of Engineering and Technology, 2012.
- Hossain, M. S., 2001, "Biological aspects of the coastal and marine environment of Bangladesh", *Ocean & Coastal Management*. Vol. 44, pp. 261-282.
- <http://www.mapsofworld.com/bangladesh/#>, last accessed (31.03.2015).
- Inman, D. L. and Brush, B. M., 1973, "The Coastal Challenge", *Science*, New Series, Vol. 181, No. 4094 (Jul. 6, 1973), pp. 20-32.

- Islam, K. S., Xue, X. Z. and Rahman, M. M. 2009, “Successful Integrated coastal Zone Management (ICZM) Program model of a Developing Country (Xiamen, China) – Implementation in Bangladesh Perspective”, *Journal of Wetlands Ecology*, vol. 2, pp 35-41.
- Islam, M. R., 2004, “ Where Land Meets the Sea: A Profile of the Coastal Zone of Bangladesh”, The University Press Limited, Dhaka.
- Ito, Y. and Tanimoto, K., 1972, “A Method of Numerical Analysis of Wave Propagation-Application to Wave Diffraction and refraction”, *Coastal Engineering Proceedings* 1.13 (1972).
- Jackobsen, F., Azam, M. H. and Kabir, M. M. U., 2002, “ Residual Flow in the Meghna Estuary on the Coastline of Bangladesh”, *Journal of Estuarine, Coastal and Shelf Science*, Vol. 55, pp. 587-597.
- Jain, I., Rao, A. D., Jitendra, V. and Dube, S. K., 2010, “ Computation of Expected Total Water Levels along the East Coast of India”, *Journal of Coastal Research*, Vol. 26, No. 4, pp. 681-687.
- Jena, B.K., Chandramohan, P., and Kumar, V .S., 2001, “Longshore Transport Based on Directional Waves Along North Tamilnadu Coast, India”, *Journal of Coastal Research*, Vol.17, No(2), pp. 322-327.
- Kamphuis, J. W., 2012, “ Coastal Engineering Education And Coastal Models,” Emeritus Professor of Civil Engineering, Queen’s University, Kingston, ON, Canada, K7L 2R4.
- Kamphuis, J. W., 2012, “Coastal Engineering Education and Coastal Models”, *Coastal Engineering Proceedings*, 1(33), management-30.
- Khanom, S. and Salehin M., 2012, “Salinity Constraints To Different Water Uses In Coastal Area Of Bangladesh”, *Bangladesh J. Sci., Res* 25 (1), pp 33 – 42.
- Komol, M. K., 2011, “Numerical Simulation of Tidal Level at Selected Coastal Area of Bangladesh”, M. Sc.Thesis, Water Resource Engineering Department, Bangladesh University of Engineering and Technology.
- Lee, J. L. and Wang, H., 1992, “Evaluation of Numerical Models on Wave-Current Interactions”, *Coastal Engineering Proceedings*, 1(23).

Leont'yev, I. O., 1999, "Modeling of morphological changes due to coastal structure", Russian Academy of Sciences, P.P. Shirshol Institute of Oceanology, Nakhimol Prospect, 36, 117851 Moscow, Russia.

Lewis, M., Bates, P., Horsburgh, K., Neal, J. and Schumann, G., 20013, " A storm surge inundation model of the northern Bay of Bengal using publicly available data" ,Quarterly Journal of the Royal Meteorological Society, Vol.139, pp. 358-369.

Lewis, M., Horsburgh, K. and Bates, P., 2014, "Bay of Bengal Cyclone Extreme Water Level Estimate Uncertainty", Journal of Natural Hazards, Vol.72, No.2, pp.983-996.

Mahodadhi, 2013, "Bay of Bengal," http://en.wikipedia.org/wiki/Bay_of_Bengal.

Meadows, G. A. and Wood, W. L., 2003, "Coastal Engineering", CRC Press LLC.

Navera, U. K., Developement of a Model for Predicting Wave Current Interactions and Sediment Transport Processes in nearshore Coastal Waters, Ph. D Thesis, University of Wales, Cardiff, Wales, United kingdom, 2004.

Nicholls, R. J. and Wong, P. P., 2007, "Coastal systems and low-lying Areas", Climate change 2007: impacts, adaptation and vulnerability. Contribution of Working Group II to the Fourth. Assessment Report of the Intergovernmental Panel on Climate Change, M.L. Parry, O.F. Canziani, J.P. Palutikof, P.J. van der Linden and C.E. Hanson, Eds., Cambridge University Press, Cambridge, UK, 315-356.

Nielsen, P., 1983, "Analytical Determination of Neareshore Wave Height Variation Due to Refraction shoaling and Friction", Coastal Engineering, 7(1983), pp. 233-235.

Noda, E. K., 1974, "Wave Induced Nearshore Circulation", 27 Journal of Geophysical Research, Vol. 79, No. September 20, 1974.

Nwogu, B. O., 1993, "Alternative Form of Boussinesq Equation for Nearshore Wave Propagation", Journal of Waterway, Port, Coastal, Ocean Engineering, Vol.119, pp 618-638.

Ozyurt, G. and Ergin, A., 2010, "Improving Coastal Vulnerability Assessments to Sea-Level Rise: A New Indicator-Based Methodology for Decision Makers", Journal of Coastal Research, Vol. 26, No. 2, pp. 265-273.

- Rahman, D. M. A., 2010, “Coastal zone Management in Bangladesh”, Presented in the International Geosphere Biosphere Programme (IGBP) SIE LDCs Workshop at Maputo, Mozambique Held on September 20-22, 2010.
- Ris, R. C., Holthuijsen, L. H. and Booij, N., 1999, “ A Third- Generation Wave Model For Coastal Regions”, journal of Geophysical Research , Vol. 104, No. C4, pp. 7667-7681. [28]
- Sarwar, M. G. M., 2005, “Impacts of Sea Level Rise on the Coastal Zone of Bangladesh”,Masters Thesis, Lund University, Sweden, 21 november,2005.
- Syvitski, J. P. M., Harvey, N. and Wolanski, E. 2005, “Dynamics of the Coastal Zone”, Global change- The IGBP Series, 2005, pp. 39-94.
- Uddin, A. M. K. and Kaudstaal, R., 2003, “ Delineation of The Coastal Zone”, Working Paper WP005.
- Valk, C. F., 1999, “ Estimation of 3-D current fields near the Rhine Outflow from HF Radar Surface Current Data”, ARGOSS, PO Box 61, 8325 ZH Vollenhole, Netherlands Coastal Engineering, Vol. 37, pp. 487-511.
- Wei, B. G. and Kirby, J. T., 1995, “Time Dependent Numerical Code for Extended Boussinesq Equations”, Journal of Waterway, Port, Coastal and Ocean Engineering, 1995. pp. 251.
- Weide, J. V. D., 1993, “A Systems View of Integrated Coastal Management”, Ocean & Coastal Management, 21(129-148).
- Wolf, J. and Prandle, D., 1999, “Some Observations of Wave–current Interaction”, Journal of Coastal Engineering , Vol. 37, pp. 471–485.
- Wolf, J., 2009, “Coastal flooding: impacts of coupled wave–surge–tide models”, Natural Hazards (2009) , Vol. 49, pp. 241-260.
- Yoo, D. and O’Connor , B. A.,1986, “Mathematical Modelling Of Wave-Induced Nearshore Circulation”, Coastal Engineering Proceedings, 1(20).